Fall 2014

Current steering and electrode spanning with partial tripolar stimulation mode in cochlear implants

Ching-Chih Wu
Purdue University

Graduate School ETD Form 9
(Revised 12/07)

PURDUE UNIVERSITY
GRADUATE SCHOOL
Thesis/Dissertation Acceptance

This is to certify that the thesis/dissertation prepared

By Ching-Chih Wu

Entitled

Current Steering and Electrode Spanning with Partial Tripolar Stimulation Mode in Cochlear Implants

For the degree of Doctor of Philosophy

Is approved by the final examining committee:

THOMAS M. TALAVAGE
Chair

XIN LUO

MICHAEL D. ZOLTOWSKI

MICHAEL G. HEINZ

To the best of my knowledge and as understood by the student in the *Research Integrity and Copyright Disclaimer (Graduate School Form 20)*, this thesis/dissertation adheres to the provisions of Purdue University's "Policy on Integrity in Research" and the use of copyrighted material.

Approved by Major Professor(s): THOMAS M. TALAVAGE

Approved by: M. R. Melloch 10-15-2014
Head of the Graduate Program Date

CURRENT STEERING AND ELECTRODE SPANNING WITH PARTIAL TRIPOLAR STIMULATION MODE IN COCHLEAR IMPLANTS

A Dissertation

Submitted to the Faculty

of

Purdue University

by

Ching-Chih Wu

In Partial Fulfillment of the

Requirements for the Degree

of

Doctor of Philosophy

December 2014

Purdue University

West Lafayette, Indiana

For my parents.

ACKNOWLEDGMENTS

During my years at Purdue, I am very grateful to have the opportunity to work as a research assistant for Dr. Xin Luo, an intelligent, supportive, and patient person and a great mentor! I would not have completed this dissertation if not for his help and guidance. I also appreciate the suggestion and feedback from Dr. Talavage, Dr. Heinz, and Dr. Zoltowski for this dissertation.

TABLE OF CONTENTS

Page

Page

Page

LIST OF TABLES

LIST OF FIGURES

Figure Page

ABBREVIATIONS

CI	cochlear implant
MP	monopolar
BP	bipolar
TP	tripolar
DR	dynamic range
QPVC	quadrupolar virtual channel
T-level	threshold level
M-level	most comfortable level
MCL	most comfortable level
HINT	hearing in noise test

ABSTRACT

Wu, Ching-Chih PhD, Purdue University, December 2014. Current Steering and Electrode Spanning with Partial Tripolar Stimulation Mode in Cochlear Implants. Major Professors: Xin Luo and Thomas M. Talavage.

Cochlear implants (CIs) partially restore hearing sensation to profoundly deaf people by electrically stimulating the surviving auditory neurons. However, CI users perform poorly in challenging listening tasks such as speech recognition in noise and music perception, possibly due to the small number of implanted electrodes and the large current spread of electric stimulation. Although current spread may be reduced using partial tripolar (pTP) stimulation mode, the number of electrodes may not be sufficient to preserve fine spectral details. Here, we propose to introduce current steering and electrode spanning to pTP mode to create additional spectral channels for CI users. Loudness and pitch perception with steered and spanned pTP modes were simulated using a computational model of CI stimulation and were tested in CI users. The excitation pattern of each stimulation mode was also measured at the physical (i.e., intra-cochlear electrical potential distribution), neural (i.e., spatial profile of evoked compound action potential), and perceptual levels (i.e., psychophysical forward masking pattern). Consistent with the model predictions, pitch-ranking results verified the feasibility and efficacy of the proposed stimulation modes in eliciting distinctive pitches for CI users. Pitch increased when the centroid of excitation pattern was shifted basally. When the centroid of excitation pattern did not move, higher pitches were perceived for narrower excitation patterns. These results suggest that in pTP-mode CI processing strategies, current steering and electrode spanning may provide additional spectral channels for better coding of spectral fine structures and for handling the cochlear dead region and defective electrode contact.

PUBLICATIONS

PUBLICATIONS

C. C. Wu and X. Luo, "Current steering with partial tripolar stimulation mode in cochlear implants," *Journal of the Association for Research in Otolaryngology*, vol. 14, no. 2, pp. 213–231, 2013.

C. C. Wu and X. Luo, "Electrode spanning with partial tripolar stimulation mode in cochlear implants," *Journal of the Association for Research in Otolaryngology*, 2014.

X. Luo, M. E. Masterson, and C. C. Wu, "Melodic interval perception by normal-hearing listeners and cochlear implant users," *The Journal of the Acoustical Society of America*, vol. 136, no. 4, pp. 1831–1844, 2014

X. Luo, M. E. Masterson, and C. C. Wu, "Contour identification with pitch and loudness cues using cochlear implants," *The Journal of the Acoustical Society of America*, vol. 135, no. 1, pp. EL8–EL14, 2014

1. INTRODUCTION

Cochlear implants can partially restore hearing sensation to profoundly deaf people by electrically stimulating the remaining auditory neurons. It has been used as a common treatment for profound hearing loss and benefited more than 324,000 people worldwide as of December 2012 [1]. CI users can understand speech well in quiet condition, but they have difficulties understanding speech in noise and appreciating music. The spectral information encoded for only 12–22 implanted electrodes is limited for high-level auditory processing. In addition, the most widely used monopolar (MP) stimulation mode can generate large current spread in the fluid-filled cochlea due to a long current pathway between an intra-cochlear electrode and an extra-cochlear ground. The large current spread can cause neural interaction between stimulation sites and further reduces the spectral resolution with CIs.

Recent studies have attempted to reduce channel interaction by current focusing techniques which aim to shorten the current pathway by returning current to one or more nearby electrodes. One example is partial tripolar (pTP) stimulation, which returns a major proportion of the current to both flanking electrodes and the rest to the extracochlear ground. Studies generally showed more restricted excitation pattern for pTP than MP stimulation across auditory processing levels, but the effect was not large especially in psychophysical studies with human subjects. Nevertheless, a speech processing strategy using pTP mode was shown to improve speech recognition in noise as compared to a matched MP strategy [2].

To fully explore the potential benefit of focused pTP stimulation, a few limitations of pTP stimulation need to be addressed. Although spectral resolution may be improved with pTP mode, the number of spectral channels is still limited by the number of physical electrodes. In addition, pTP stimulation is more susceptible to a poor electrode-neural interface such as dead regions (i.e., areas without functioning

hair cells or spiral ganglion neurons) [3, 4]. Stimulating such channels in pTP mode might have an adverse effect on speech recognition. Finally, when there are defective electrodes in the implanted array, we must find another way, such as using a modified pTP mode that avoids the defective electrode, to implement current focusing. Some field shaping technique studied in MP mode has been shown to create additional spectral channels (i.e., current steering) or bridge defective electrodes (i.e., electrode spanning). Introducing these techniques to pTP mode may be useful in providing additional spectral channels for better coding of spectral fine structures and for handling the cochlear dead region and defective electrode contacts.

1.1 Objectives

This study proposed to combine pTP stimulation with some field shaping techniques (i.e., current steering or electrode spanning) to increase the number of spectral channels or replace a spectral channel that involves a defective electrode while maintaining focused stimulation. The loudness and pitch of these experimental pTP modes were predicted using a computational model and tested in CI users. The excitation pattern of each stimulation mode was also measured at the physical (i.e., intra-cochlear electrical potential distribution), neural (i.e., spatial profile of evoked compound action potential), and perceptual levels (i.e., psychophysical forward masking pattern) to study the possible cause of any associated perceptual change.

1.2 Organization

Chapter 2 will provide background information on cochlear implants and the field shaping techniques used to improve spectral resolution (i.e., current focusing), increase the number of spectral channels (i.e., current steering), and tackle defective electrode contacts (i.e., electrode spanning). Chapter 3 investigated the pitch perception of pTP mode with current steering (i.e., steered pTP mode), which aimed to increase the number of spectral channels and provide a means to stimulate areas

around a dead region. Results showed steered pTP mode can generate additional spectral channels for most CI subjects. Chapter 4 investigated the mechanism by which steered pTP stimuli elicited distinctive pitch percepts by measuring and comparing the excitation patterns of different steered pTP stimuli. Chapter 5 investigated the pitch perception of pTP mode with electrode spanning (i.e., spanned pTP mode), which aimed to maintain focused stimulation when the original pTP channel had a defective return electrode. Results from Chapter 5 showed spanned pTP mode was not only useful for handling defective electrodes but also adding spectral channels. Chapter 6 investigated the mechanism by which spanned pTP mode elicited higher pitch than standard pTP mode by measuring and comparing the excitation patterns of spanned and standard pTP stimuli at physical, neural, and perceptual levels. Chapter 7 presented the conclusion of this research and future works.

The content in Chapter 3 and Chapter 5 has already been published in Journal of the Association for Research in Otolaryngology ([5] and [6], respectively).

2. BACKGROUND

2.1 Sound Perception with Normal Cochlea

In normal hearing, acoustic signal is converted to mechanical movements of basilar membrane within the cochlea. Since the basilar membrane varies in width and stiffness along the cochlea (i.e., narrower and stiffer near the base, and wider and less stiff near the apex), the vibration frequency which the BM is most sensitive to (i.e., characteristic frequency) also varies along the length of cochlea. The basal part of BM is more responsive to higher frequency, while the apical part is more responsive to low frequency. The motion of BM is converted to nerve signals by the sensory receptors, inner hair cells, for higher auditory processing. The inner hair cells located on BM are also tuned to high frequency near the base and low near the apex. This spatial arrangement of characteristic frequency, or tonotopic organization, can be observed throughout the auditory pathway, from cochlea, brain stem, to auditory cortex [7] [8].

2.2 Cochlear Implants

A cochlear implant (CI, Figure 2.1) is a neuroprothesis that can partially restore hearing sensation to profoundly deaf people with sensorineural hearing loss. These patients usually have damaged hair cells but still preserve some surviving auditory nerves which can be electrically stimulated to transmit signal to the brain. The CI consists of external (i.e., speech processor and transmitter coil) and internal (i.e., receiver/stimulator and electrode array) components. The incoming acoustic signal is processed and transmitted from an external transmitter coil to an internal receiver/stimulator with a radiofrequency link. The receiver/stimulator converts the received signal to electric pulses and delivers them to the implanted electrode array.

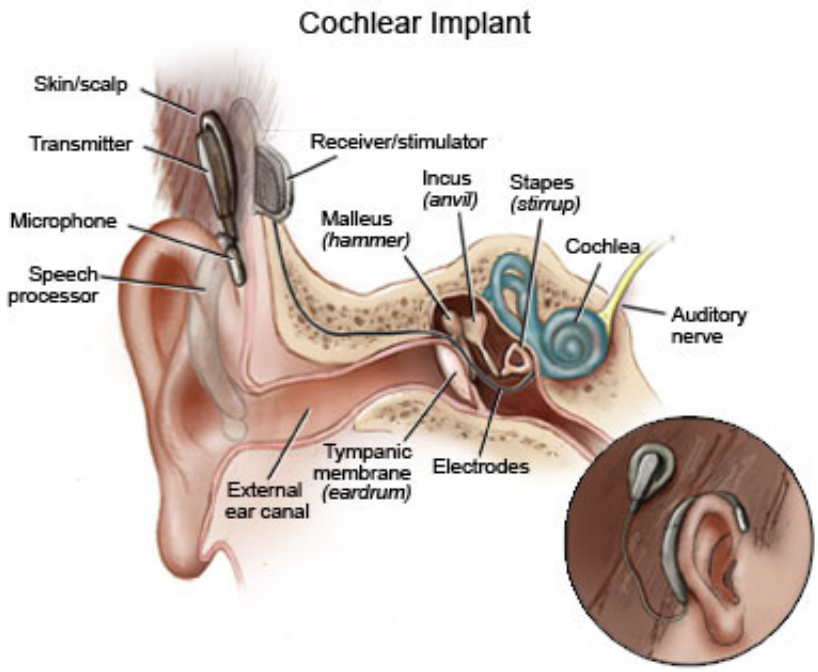

Fig. 2.1. Cochlear Implant [9]

Figure 2.2 shows a diagram of a four-channel CI using the widely used continuously interleaved sampling (CIS) [10] processing strategy. The sound received by the microphone is filtered into four different frequency bands. The envelope of each band is extracted by half-wave rectification and low-pass filtering, and then used to modulate biphasic pulses delivered to the corresponding electrodes, based on tonotopic organization of cochlea.

Modern CIs use 12–22 electrodes implanted in a patients cochlea to encode speech information. However, CI users have been shown to receive only 4–8 channels of spectral information [12], [13]. This is likely because the commonly used monopolar (MP) stimulation delivers current from an intracochlear electrode to an extracochlear ground (e.g., ball electrode in Figure 2.1). Such a long current pathway can generate a large spread of excitation and lead to strong neural interactions between channels. The limited spectral resolution with CIs may be enough for the recognition of simple sentences in quiet, but not for more complex materials or in noisy environments [14].

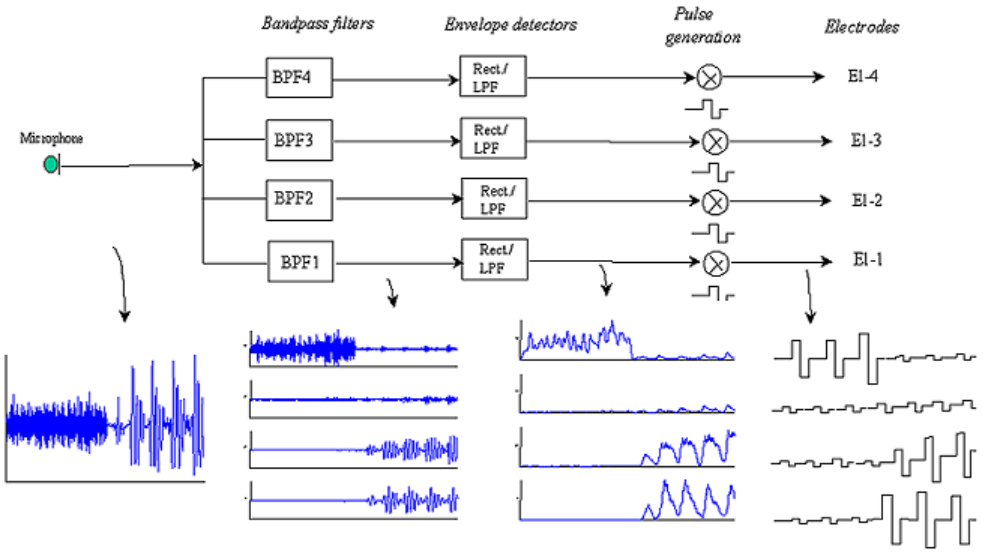

Fig. 2.2. Diagram of a four-channel CI using the CIS (i.e., continuously interleaved sampling) processing strategy. [11]

2.3 Current Focusing

Current focusing decreases the current spread of main electrode to increase the stimulation selectivity. Unlike MP mode (Fig. 2.3a) that returns the current to an extra-cochlear ground, full bipolar (BP) mode returns the current to an intra-cochlear electrode (e.g., the basal flanking electrode in Fig. 2.3b) to shorten the current return path. Further, full tripolar (TP) mode (Figure 2.3c) returns the current evenly to two intra-cochlear flanking electrodes to limit the current spread on both sides of the main electrode. The intra-cochlear electric field is narrower and channel interaction is reduced with full TP stimulation compared to full BP or MP stimulation in animal models [15], [16], [17], [18] and human CI listeners [19], [3]. With a smaller population of excited neurons, the focused full TP stimulation requires more current to reach the most comfortable level and sometimes cannot support full loudness growth (i.e., the perceived loudness cannot reach the most comfortable level) within the compliance limit of the implant, especially for patients with high electrode impedances.

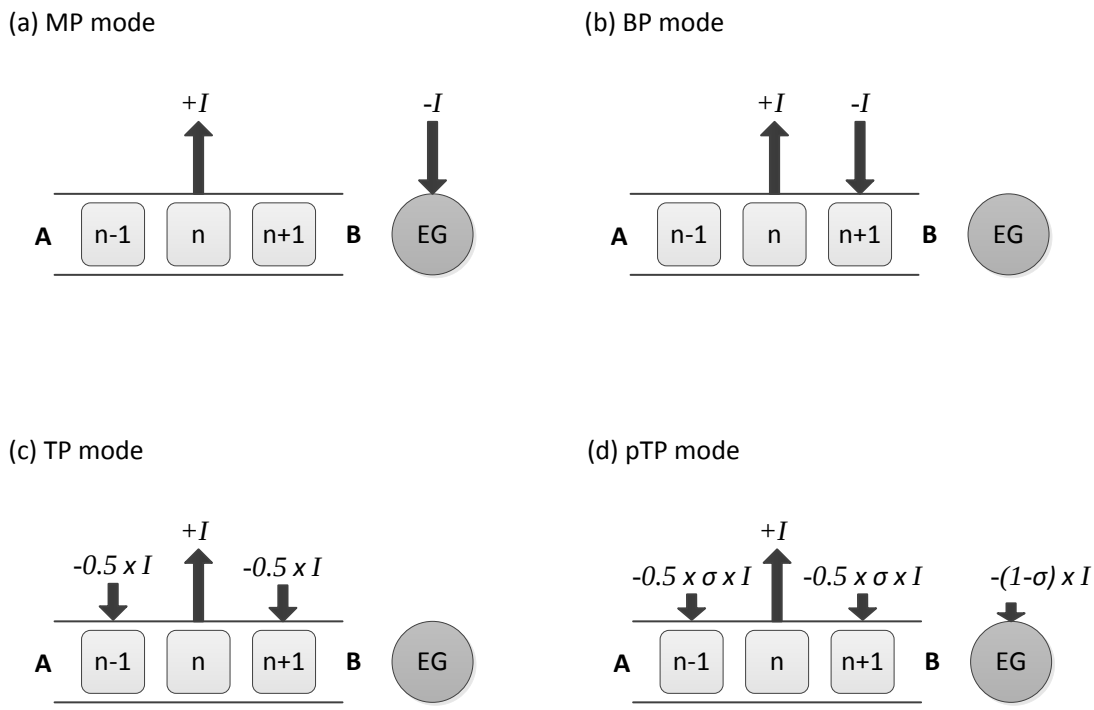

Fig. 2.3. Schematic illustration of stimulation modes with a fixed current level I on the main electrode n. The arrowhead direction indicates the phases of biphasic current pulses (upward: cathodic-leading; downward: anodic-leading), while the arrow length indicates the current level. A, B, and EG stand for apex, base, and extracochlear ground, respectively. (a) Monopolar (MP) mode: the current -I is fully returned to the EG. (b) Bipolar (BP) mode: the current -I is fully returned to the basal or apical (not shown) flanking electrode. (c) Tripolar (TP) mode: the current -I is split and returned evenly to both flanking electrodes. (d) Partial tripolar (pTP) mode: only a fraction of the current ($-\sigma\times$ I) is split and returned evenly to both flanking electrodes, while the rest [$-(1-\sigma)\times$ I] to the EG. Note that these plots differ in the current return pathways.

Partial tripolar (pTP) mode (Fig. 2.3d with α=0.5) was thus proposed to provide a trade-off between current focusing and loudness growth. It returns only a fraction (σ) of current to the intracochlear adjacent electrodes, and the rest ($1-\sigma$) to the extracochlear ground. The compensation coefficient σ can be varied from 0 (MP mode) to 1 (TP mode) to regulate the spread of excitation. At equal loudness, only

pTP mode with $\sigma > 0.5$ might have narrower spread of excitation than MP mode in some CI users [20]. A pTP strategy with σ fixed at 0.75 did significantly improve speech recognition in noise over a MP strategy that was matched in parameters such as the number of main electrodes and the rate of stimulation [2]. On average, there was no significant difference in performance with the pTP strategy and with subject's clinical strategies. Note that the clinical strategies may have had some advantages over the pTP strategy, because CI users experienced the pTP strategy only acutely. To reach the most comfortable level, the pTP strategy had to use a much longer pulse width than clinical strategies, leading to a much lower stimulation rate and possibly degraded temporal resolution. In addition, the most apical and basal electrodes could not be used as the main electrodes in pTP mode, because they do not have either an apical or a basal adjacent electrode for current return.

2.4 Current Steering

Current steering makes use of electrical interaction to stimulate neural population located between adjacent electrodes, so that the number of frequency channels could be increased beyond the number of physical electrodes. In the MP-mode current steering (Fig. 2.4a), a fixed amount of current was steered between two adjacent main electrodes. The fraction of current on the basal main electrode of the pair was controlled by a steering coefficient α. In general, higher pitch percepts were elicited with increasing α (i.e., more current injected to the basal main electrode). CI users perceived on average five intermediate pitch sensations per electrode pair [21], but their speech recognition with speech processing strategies using the MP-mode current steering only slightly improved [22] or remained similar [23]. The large current spread of MP stimulation may have limited the number of effective frequency channels with MP-mode current steering.

Current steering has also been implemented in partial bipolar (pBP) mode or with the phantom-electrode stimulation [24], which returns a fraction (σ) of current to the

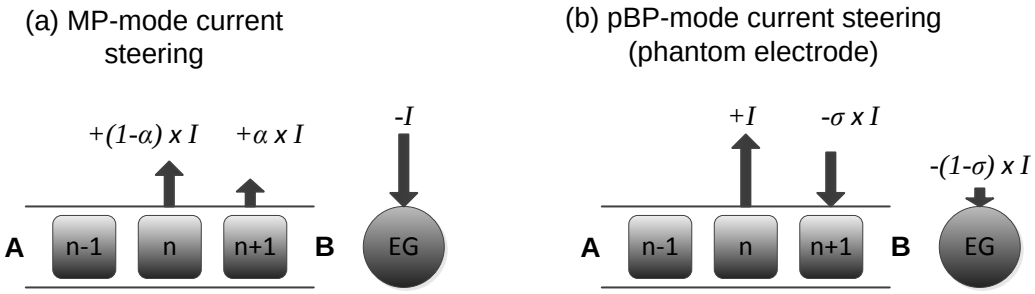

Fig. 2.4. Schematic illustration of current steering in MP and partial BP (pBP). Refer to Fig. 2.3 for annotations. (a) MP-mode current steering: two adjacent main electrodes are simultaneously stimulated in phase with varying ratios of current level (α and $1-\alpha$ on the basal and apical electrodes, respectively). (b) pBP-mode current steering or phantom electrode: a fraction of the current ($-\sigma\times$ I) is returned to the basal or apical (not shown) flanking electrode and the rest [$-(1-\sigma)\times$I] to the EG.

basal flanking electrode (Fig. 2.4b). pBP stimulation can elicit a pitch that is lower than the pitch elicited by its main electrode. The elicited pitch becomes lower when σ increases (i.e., more current returned to the basal flanking electrode). However, pitch reversal occurred for some subjects as σ neared one, possibly because the stimulation side-lobe around the basal flanking electrode became perceptually salient. The pBP-mode current steering can be applied to the most apical or basal electrode of a CI to extend its range of pitch perception (e.g., eliciting a lower pitch percept than that of the most apical electrode). The benefits of pBP-mode current steering in speech perception are yet to be investigated.

2.5 Electrode Spanning

The spectral channel that involves a defective electrode can prevent the use of current focusing and current steering. By delivering current to nonadjacent electrodes, electrode spanning can be used to bridge a defective electrode and restore the otherwise missing channel. Fig. 2.5a shows an example of MP-mode spanning with

stimulating electrodes n and n+2, which was shown to generate a pitch perception not significantly different from the elicited pitch of electrode n+1 [25]. MP-mode spanning can restore the intermediate spectral channel probably because their excitation patterns had comparable center of gravity [26] or peak position [27]. By introducing current steering to MP-mode spanning, Snel-Bongers [25] found that pitch increased monotonically as α increased. However, with increasing electrode separation, more current is required to maintain equal loudness, and pitch discrimination deteriorated. Frijns [28] showed a speech processing strategy with spanning (by deactivating six electrodes) could preserve sound quality and have similar speech perception score in quiet as subjects clinical program.

Electrode spanning can also be implemented in BP mode, without (Fig. 2.5c) or with current steering (Fig. 2.5d). In pBP-mode or phantom-electrode stimulation, Saoji [24] found that increasing the electrode separation reduced current required to maintain equal loudness, and produced progressively lower pitch percepts for some subjects.

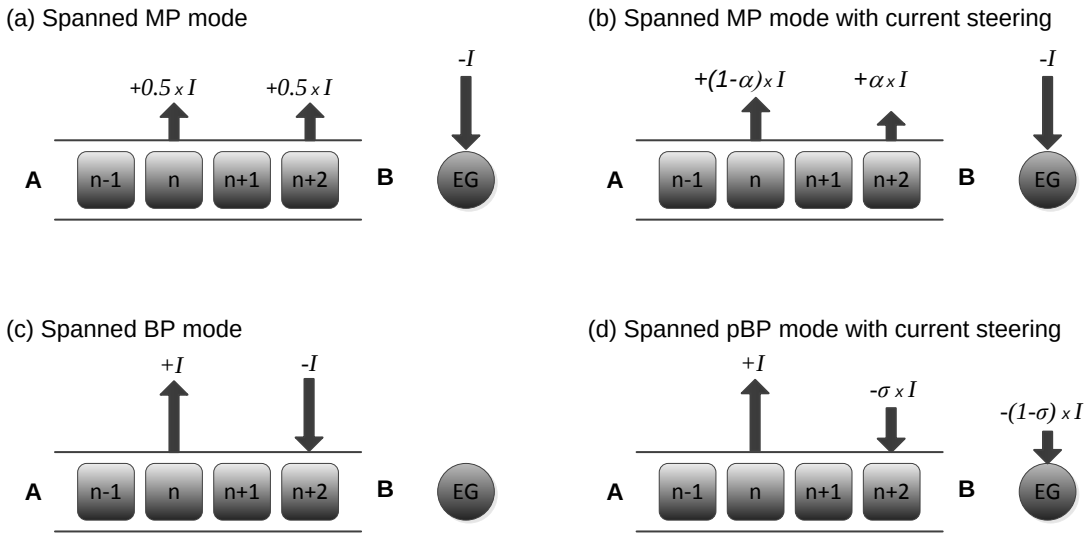

Fig. 2.5. Schematic illustration of electrode spanning in MP and pBP modes (top), and electrode spanning with current steering in MP and pBP modes (bottom).

3. CURRENT STEERING WITH PARTIAL TRIPOLAR STIMULATION MODE IN COCHLEAR IMPLANTS

3.1 Introduction

With focused pTP mode, CI users were more susceptible to poor electrode-neuron interface [3], which may adversely affect the perception of certain frequency information. Besides, the compensation coefficient σ may need optimization for different subjects and electrodes, so that the most focused pTP stimulation with full loudness growth could be utilized. Finally, while the stimulation on each main electrode was narrowed by pTP mode [20], the number of physical electrodes was still not enough to resolve fine spectral details such as the low-order harmonics of fundamental frequency, which have been shown by [29] to be important for speech recognition in noise and melody recognition.

In this study, current steering with focused pTP mode (Fig. 3.1) was proposed to increase the spectral or pitch cues for CI users. With a fixed compensation coefficient σ, steered pTP mode distributes the intra-cochlear return current to the basal and apical flanking electrodes with a proportion of α (the steering coefficient) and $1-\alpha$, respectively. With the basal and apical current spread limited to different degrees, the location of the peak or centroid of the excitation pattern can be changed to elicit different pitch percepts. The standard pTP mode (Fig. 2.3d) can be seen as a special case of steered pTP mode with $\alpha = 0.5$. When the intra-cochlear return current is distributed to either the basal ($\alpha = 1$; Fig. 2.4b) or apical flanking electrode alone ($\alpha = 0$), steered pTP mode is equivalent to pBP mode. Based on the results of phantom electrodes [24], steered pTP mode was expected to elicit lower pitch percepts with increasing α (i.e., more current returned to the basal flanking electrode). Because standard pTP stimulation may be more focused than pBP stimulation, we

also hypothesized that pitch discrimination would be better and the current required for equal loudness would be higher with $\alpha = 0.5$ than with $\alpha = 0$ or 1.

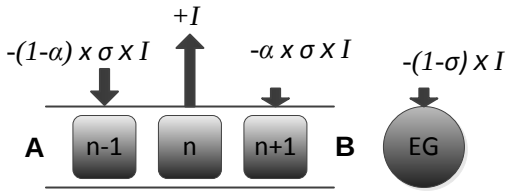

Fig. 3.1. Schematic illustration of pTP mode with current steering (i.e., steered pTP mode). A fraction of the current ($-\sigma \times I$) is split and returned to the basal and apical flanking electrodes with ratios of α and $1 - \alpha$ respectively, and the rest $[-(1 - \sigma) \times I]$ to the EG.

A computational model that simulates intra-cochlear potential fields and auditory neural response to CI stimulation [30] was used to investigate loudness and pitch perception with steered pTP mode. Similar models have been used to study loudness growth with standard pTP stimulation [31] and simulate current focusing and steering in various modes [32]. Modeling studies were less time consuming than testing human CI subjects and could provide valuable insights into human perceptual data, thanks to their capability of adjusting specific CI factors and examining conditions that were difficult to test in real CI users. However, a number of simplifying assumptions were necessary for a model to be computationally tractable. It was thus important to validate the model by other objective measures or psychophysical tests. As such, two psychophysical experiments with CI users were also conducted to investigate steered pTP mode. In Experiment 1, steered pTP stimuli with α from 0 to 1 on a main electrode were balanced in loudness and then ranked in pitch. Experiment 2 compared the pitches of loudness-balanced steered pTP stimuli on adjacent main electrodes to estimate the overlap between their pitch ranges.

3.2 Computational Model

Fig. 3.2 depicts the model of Goldwyn [30], which simulates the spatial pattern of neural activity along the cochlea in response to CI stimulation. The model is briefly described here and more details can be found in [30]. In this model, the scala tympani is simplified as a 33-mm subsection of an infinitely long cylinder with a fixed radius of 1 mm. The resistivity of the surrounding osseous spiral lamina is about a hundred times greater than that inside the fluid-filled scala tympani. The spiral ganglion cells are 0.3 mm away from the scala tympani. In case of full neural survival, 330 clusters of 100 spiral ganglion cells are evenly distributed along the cochlea (one cluster per 0.1 mm). A 16-electrode array with an inter-electrode spacing of 1.1 mm is placed in the center of the scala tympani to simulate the HiFocus1J electrode array from Advanced Bionics (Sylmar, CA). The most basal electrode (EL16) is 3 mm from the base of the cochlea. The electrode-neuron distance is 1.3 mm for all electrodes. These parameters were adapted from [30]. Real CI users would have variable neural survival [33] and electrode-neuron distances [34], but that information was not available and thus was not modeled for the subjects in this study. The inter-subject variability is likely evident in the psychophysical tests.

The first step of model computation is to derive the potential field of CI electric stimulation. For steered pTP mode, the overall potential field is thought to be the linear sum of those of the main and flanking electrodes with the proportional current levels shown in Fig. 3.1. In our model simulation, the compensation coefficient σ was 0.75 and the steering coefficient α varied from 0 to 1 in steps of 0.1, similar to those used for human subjects in Experiments 1 and 2. An activating function [35] is defined as the second spatial derivative of the potential field and was calculated at the midpoint of each neural cluster. The thresholds of neurons within each cluster were approximated by a normal distribution, with the mean and standard deviation determined from human psychophysical data [30] and animal studies [36], respectively. Together, the activating function value and threshold distribution were used

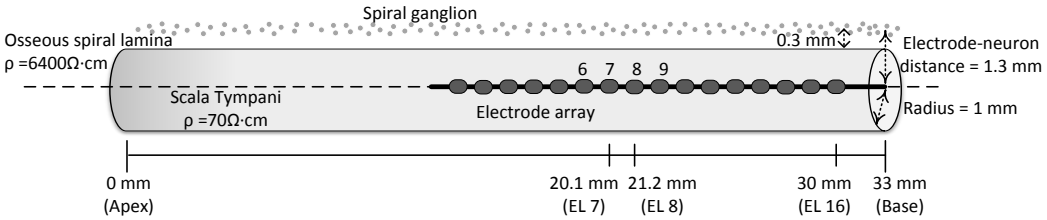

Fig. 3.2. Schematic illustration of the adapted model [30] and its parameters. The scala tympani is modeled by a 33-mm subsection of an infinitely long cylinder with a fixed radius of 1 mm. The resistivity inside the scala tympani (70 Ω·cm) is lower than that of the surrounding osseous spiral lamina (6400 Ω·cm). A 16-electrode array with an inter-electrode spacing of 1.1 mm is placed in the center of the scala tympani. The most basal electrode EL16 is 3 mm from the base of the cochlea. Spiral ganglion cells are evenly distributed along the entire length of the cochlea and located in the spiral lamina with a distance of 1.3 mm from the electrode array.

to calculate the number of activated neurons for each cluster. The final output of the computational model was the number of activated neurons as a function of cochlear position (i.e., an excitation pattern).

To simulate equal loudness with different α and to demonstrate the effect of α on the model excitation pattern, a simplifying assumption had to be made for the relation between loudness perception and activated neuron counts. Here, loudness-balanced pTP stimuli with different α were assumed to activate the same number of neurons, as in [30] and [31]. Although there was no evidence that a chosen neuron count corresponded to a particular value on a loudness perception scale, the current levels that activated 100 and 1000 neurons were assumed to be around the perceptual threshold and most comfortable level, respectively.

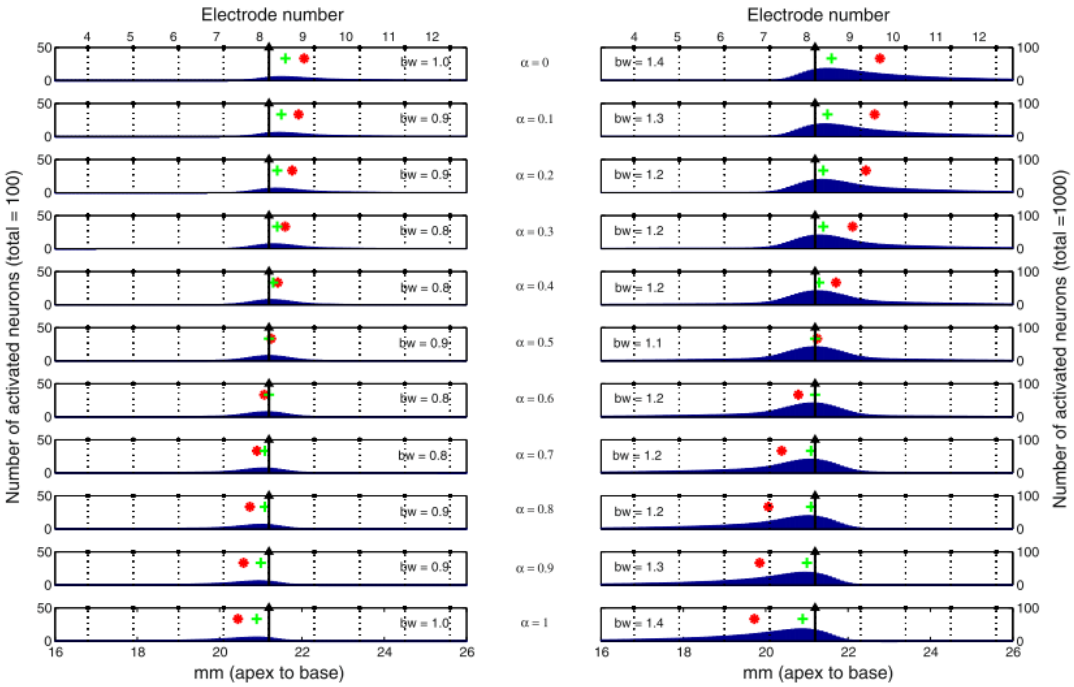

Fig. 3.3. The number of activated neurons (blue bars) calculated from the computational model is displayed as a function of cochlear position for different α (rows) and different activated neuron counts (left column: 100; right column: 1000). Except for the main electrode (EL8, black arrow), electrode positions are shown in dotted lines and their numbers are labeled on top of each column. Also shown for each excitation pattern are its bandwidth (bw: the width of excitation in mm at 75% peak value) and the location of peak (green cross) and centroid (red asterisk).

3.2.1 Simulated Excitation Patterns with Different α

Fig. 3.3 shows the simulated excitation patterns (blue areas) for steered pTP stimuli, which activated a total of 100 (left column) and 1000 neurons (right column), and were presented on the main electrode EL8 (black arrows) with α varying from 0 to 1 in steps of 0.1 (different rows). The peak (green "+") of excitation pattern was defined as the position of the neural cluster with the maximum number of activated neurons. The center of gravity (CoG; red "$*$") of excitation pattern was calculated as follows:

$$CoG = \frac{\sum_{i=1}^{330} N_i \times 0.1 \times i}{\sum_{i=1}^{330} N_i} \tag{3.1}$$

where i is the index of neural cluster, N_i is the number of activated neurons in the ith cluster, and $0.1 \times i$ is the distance from apex for the ith cluster (note that there was one cluster per 0.1 mm). The denominator was the total number of activated neurons across the whole cochlea (i.e., 100 or 1000 for the assumed threshold or most comfortable level). To quantify the spread of excitation, the bandwidth (bw) of excitation pattern was calculated at 75% of the peak value. The following sections will discuss the use of peak, CoG, and bandwidth of an excitation pattern to estimate its pitch and loudness perception.

3.2.2 Simulated Equal-loudness Contours across Different α

The current levels on the main electrode (in dB re 1 μA) needed to activate a total of 100 and 1000 neurons in the model are plotted as a function of the steering coefficient α in Fig. 3.4. Assuming that loudness-balanced stimuli would activate the same number of neurons, each contour in Fig. 3.4 represents an equal-loudness level with different α (triangles and circles for the assumed threshold and most comfortable level, respectively). Both equal-loudness contours peaked at $\alpha = 0.5$ and monotonically decreased for higher or lower α. These results may be explained by the spread of excitation with different α (Fig. 3.3). At both levels, standard pTP mode with $\alpha = 0.5$ reduced current spread on both the apical and basal sides to a similar degree and created a narrow excitation pattern centered on the main electrode. As α approached 0 or 1, the stimulation mode became more like pBP and current spread was more limited on one side of the main electrode than on the other side. The broader excitation patterns for α around 0 or 1 (as indicated by the greater bandwidths of excitation) thus required less current to achieve equal loudness. The two equal-loudness contours

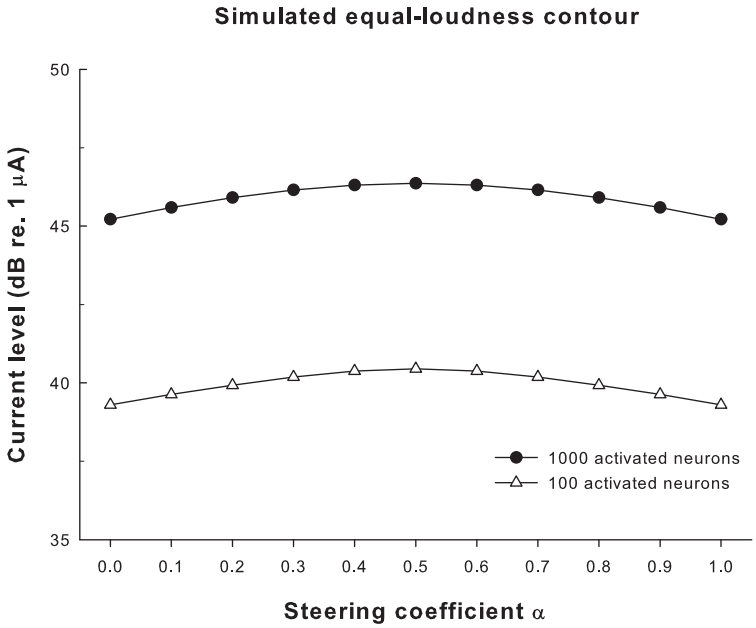

Fig. 3.4. Current levels (in dB re 1 μA) required to activate a total of 100 and 1000 neurons (open triangles and solid circles, respectively) in the model as a function of the steering coefficient α. The current levels that activated a total of 100 and 1000 neurons were assumed to be around the perceptual threshold and most comfortable level, respectively.

were parallel to each other, suggesting that the loudness growth and dynamic range were similar across α.

3.2.3 Simulated Pitch Changes with α on Adjacent Main Electrodes

Fig. 3.5 shows the simulated place-pitch changes with α in steered pTP mode. The peak (top row) and CoG (bottom row) of excitation pattern at the assumed threshold (triangles) and most comfortable level (circles) are shown against different α on EL8 (left column) and EL7 (right column). Note that in the simplified model, the peak and CoG curves for EL7 were identical to those for EL8 but shifted to the apex by 1.1 mm (i.e., the inter-electrode spacing). When α increased from 0 to 1, the peak of excitation only shifted 0.3 mm to the apex at both levels, while the CoG of

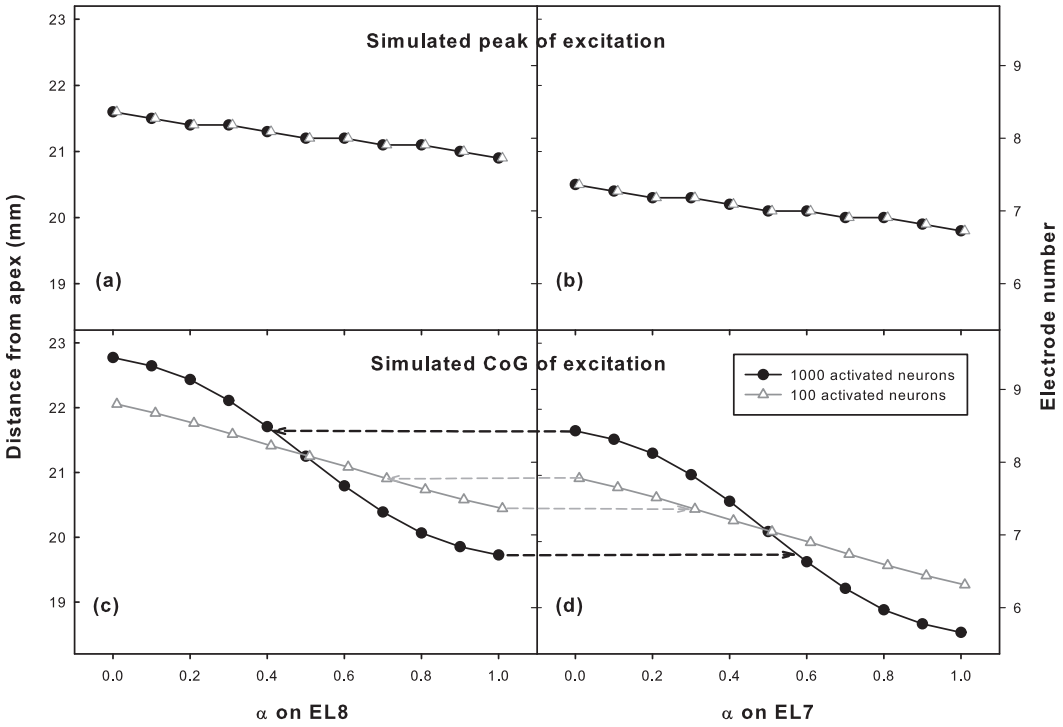

Fig. 3.5. Peak (top row) and center of gravity (CoG; bottom row) of simulated excitation pattern for various α on EL8 (left column) and EL7 (right column) with a total of 100 (triangles) and 1000 activated neurons (circles). Due to model simplification, the peak and CoG curves for EL7 were identical to those for EL8 but shifted to the apex by the inter-electrode spacing. For the two adjacent main electrodes, their excitation peaks did not overlap, while their CoGs of excitation overlapped with each other as indicated by the horizontal dashed lines in the bottom row.

excitation greatly shifted about 1.5 and 2.5 mm at the assumed threshold and most comfortable level, respectively. Close inspection of Fig. 3.3 reveals that returning more current to the basal flanking electrode (and less to the apical one) reduced the basal current spread but increased the apical current spread, leading to an apical shift of the overall excitation pattern. Therefore, if place pitch is mostly determined by the CoG of excitation, CI users would perceive lower pitches for higher α, and the pitch changes with steered pTP mode would be more salient at higher stimulation levels. Another effect that can be observed in Fig. 3.5 was that the CoG of excitation

at the assumed most comfortable level shifted more rapidly with the same α step of 0.1 when α was around 0.5, indicating better pitch discrimination for more focused pTP stimuli with α around 0.5 than for less focused pBP stimuli with α around 0 or 1. However, this effect was level dependent as the CoG of excitation at the assumed threshold shifted more linearly with α from 0 to 1.

The overlap of pitch ranges between adjacent main electrodes can be predicted by comparing the left and right columns of Fig. 3.5. Although the peaks of excitation for EL7 and EL8 were well separated, their CoGs of excitation greatly overlapped with each other. The pitch overlap estimated by the CoG of excitation was greater at the assumed most comfortable level than at the approximate threshold, as indicated by the horizontal dashed lines connecting Fig. 3.5c and 3.5d. At the assumed most comfortable level, the lowest pitch on EL8 with $\alpha = 1$ would be similar to the middle pitch on EL7 with $\alpha \approx 0.6$, and the highest pitch on EL7 with $\alpha = 0$ would be similar to the middle pitch on EL8 with $\alpha \approx 0.4$.

These model predictions of loudness and pitch perception were next tested with human CI subjects, using the same steered pTP stimuli but only at the most comfortable level. Although the modeling showed interesting results near threshold, related results in human listeners are difficult to obtain due to the time and strain associated with listening to stimuli that are barely audible.

3.3 Experiment 1: Pitch Ranking of Steered pTP stimuli on a main electrode

3.3.1 Methods

Subjects and Stimuli

Four post-lingually (S1, S2, S4, and S6) and two pre-lingually deafened (S3 and S5) adult CI users participated in Experiment 1. Table 3.1 shows their demographic details and sentence recognition scores obtained during the most recent clinical visit.

Percent correct scores for the Hearing in Noise Test (HINT) sentences in quiet at 60 dB SPL were available for all subjects except S5, who only had scores for the City University of New York (CUNY) sentences. Only users of the Advanced Bionics HiRes 90K implant were recruited because this device can stimulate multiple electrodes simultaneously and allows for the delivery of pTP stimulation. All subjects used the HiFocus1J electrode array with an electrode spacing of 1.1 mm, as simulated in the computational model. This study was reviewed and approved by the Purdue IRB committee. All subjects provided informed consent and were compensated for their participation.

All experimental stimuli were delivered to CI subjects using the Bionic Ear Data Collection System (BEDCS; Advanced Bionics, Sylmar, CA). As defined in Fig. 3.1, when current I was applied to the main electrode ELn, $-\alpha \times \sigma \times I$ was returned to the basal flanking electrode ELn+1, while $-(1-\alpha) \times \sigma \times I$ was returned to the apical flanking electrode ELn-1. The compensation coefficient σ was selected using the method described in the next section, while the steering coefficient α ranged from 0 to 1 in steps of 0.1. For brevity, $\text{pTP}_{ELn,\alpha=\alpha 1}$ denotes a steered pTP stimulus on the main electrode ELn with α equal to $\alpha 1$. Pulse trains were 300 ms long with 1000 pulses per second. The symmetric biphasic pulses (226 μs/phase) were cathodic-leading on the main electrode and anodic-leading on the flanking electrodes. The 226-μs phase duration was longer than those used in the clinic and was chosen to help achieve full loudness growth (up to the upper loudness limit) for pTP stimulation within the compliance limit of the implant (i.e., the voltage on each electrode should be lower than 8 V and the surface charge density should be lower than 100 $\mu\text{C}/cm^2$ [24]. To investigate performance variation across the electrode array, steered pTP stimuli on the apical (EL4), middle (EL8), and basal (EL12) main electrodes were tested. Stimuli on EL12 were not tested for S3 since EL11 to 16 were deactivated in her clinical speech processor. S5 was also not tested on EL12 after she failed in the attempts to balance loudness for several α values on EL12 within the compliance limit of the implant (see the procedure in the loudness balancing section).

Determining the Compensation Coefficient σ

For each tested main electrode ELn, the highest compensation coefficient σ that allowed for full loudness growth within the compliance limit was chosen. This σ value was expected to keep the overall excitation patterns of pTP stimuli as focused as possible and result in steered pTP mode with the greatest shift and the least channel interaction. During the search for the highest possible σ, the steering coefficient α was fixed at 0.5. Based on model predictions (Fig. 3.4), for a given σ, $\text{pTP}_{ELn,\alpha=0.5}$ would have the most focused excitation pattern and require the most current to reach the upper loudness limit among all $\text{pTP}_{ELn,\alpha=0,0.1,...,1}$. Therefore, if full loudness growth was achieved for $\alpha = 0.5$ within the compliance limit, it should also be possible for the other α values. Loudness growth for each tested σ was measured using a clinical 10-point scale from 1 ("just noticeable") to 10 ("too loud"). Starting from a sub-threshold level, the current level was increased in 8-μA steps until loudness level 9 on the scale ("upper loudness limit") was perceived or the implant compliance limit was reached.

The binary search algorithm [37] was used to speed up the search for the highest possible σ. The initial search range for σ was [0, 1] and $\sigma = 1$ (i.e., the most focused full TP mode) was tested first. If the upper loudness limit could be reached within the compliance limit for $\sigma = 1$, the search stopped with an output of $\sigma = 1$. Otherwise, the midpoint of the initial search range (i.e., $\sigma = 0.5$) was tested. If the upper loudness limit could be reached within the compliance limit for $\sigma = 0.5$, the search range for σ was limited to the higher half [0.5, 1]. Otherwise, the search range for σ was limited to the lower half [0, 0.5]. The midpoint of the reduced search range was then tested. This search continued in a similar fashion until the size of the search range was reduced to 0.05 (i.e., the search result had a precision of 0.05). The output of σ was then applied to steered pTP stimuli with different α on the same main electrode. With the found σ, full loudness growth was indeed achieved for each α within the compliance limit, except for several α values on EL12 of S5. The dynamic

range (DR) from loudness level 1 (defined as T-level) to 9 (defined as C-level) was measured using the method described above.

Loudness Balancing across Different α

On each main electrode ELn, pTP stimuli with different α from 0 to 1 in steps of 0.1 were loudness balanced to avoid loudness effects on the next pitch-ranking tests. The reference stimulus was $\mathrm{pTP}_{ELn,\alpha=0.5}$ at the most comfortable level (M-level: loudness level 6 during the DR measurement), while the target stimulus was $\mathrm{pTP}_{ELn,\alpha}$ with $\alpha \neq 0.5$. Different α values were tested separately in a random order. As mentioned above, $\alpha = 0.5$ was predicted to require the most current for M-level among all current steering coefficients for steered pTP stimuli. Therefore, using $\mathrm{pTP}_{ELn,\alpha=0.5}$ as the reference would leave a greater range of current adjustment for the target, so as to improve the reliability of loudness balancing. A two-alternative, forced-choice (2AFC), double-staircase procedure [38] was used to balance the loudness of the target and reference. A 2-down/1-up and a 2-up/1-down adaptive sequence were randomly interleaved. In each trial, the reference and target stimuli were presented in a random order. Subjects were asked to choose the louder stimulus regardless of possible pitch and timbre differences. The target current level on the main electrode was adjusted based on subject response using the corresponding adaptive rule and was always limited within the compliance limit. The current level step size was 20 μA for the first four reversals and 12 μA thereafter. Each sequence was terminated after 12 reversals or 60 trials, and the average current level over the last eight reversals and across the two sequences was the loudness-balanced level for the target stimulus. If the number of reversals in a sequence was less than eight after 60 trials, the attempt to balance loudness for the target stimulus failed.

Pitch Ranking of Steered pTP Stimuli

On each main electrode ELn, a 2AFC task was used to compare the pitches of 10 consecutive pairs of loudness-balanced steered pTP stimuli with a 0.1 interval in α, ranging from 0 to 1. In each trial, a stimulus pair (e.g., $\text{pTP}_{ELn,\alpha=0.2}$ vs. $\text{pTP}_{ELn,\alpha=0.3}$) was randomly chosen and the stimuli in this pair were presented also in a random order. Amplitude roving of ± 0.5 dB was applied to all stimuli to further reduce possible loudness effects. The task of the subject was to indicate which stimulus had higher pitch. Subjects were allowed to repeat the stimuli as many times as desired before responding. No feedback was provided as to the correctness of each response, because pitch reversals could occur when the side-lobes around the flanking electrodes became perceptually salient [24]. Twenty trials of each stimulus pair were tested in a run and data from two runs were averaged. For $\alpha = 0.1, 0.2, \ldots, 1$, the percentages that $\text{pTP}_{ELn,\alpha}$ was judged as higher in pitch than $\text{pTP}_{ELn,\alpha-0.1}$ were recorded and converted to d' values [39] to indicate the perceptual distance or sensitivity index between steered pTP stimuli with an α interval of 0.1. The overall cumulative d' calculated by successively summing the d' values from $\alpha = 0.1$ to $\alpha = 1$, could be used to estimate the overall pitch changes on a main electrode in steered pTP mode.

3.3.2 Results

Subject- and Electrode-specific Compensation Coefficient σ

Fig. 3.6 shows the highest possible compensation coefficient σ that allowed for full loudness growth within the compliance limit for each subject on the three main electrodes. A one-way repeated-measures (RM) analysis of variance (ANOVA) revealed no significant effect of electrode on the highest possible σ ($F_{2,8} = 0.17, p = 0.85$). The variation of σ across the three electrodes of each subject was usually 0.05 (i.e., equal to the minimum step for σ search), except for S2 who had a variation of 0.1. In contrast, the highest possible σ varied greatly from 0.6 to 0.9 for different subjects.

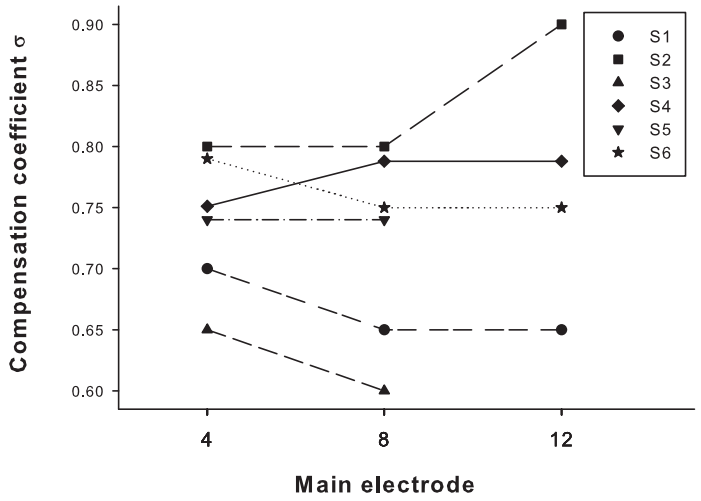

Fig. 3.6. Compensation coefficient σ for individual subjects (different symbols and line types) across the apical (EL4), middle (EL8), and basal (EL12) main electrodes.

Dynamic Range between T/C Levels

Fig. 3.7 shows the DRs (dynamic ranges, denoted by shaded area) between T- (thresholds, denoted by upward triangles) and C-levels (upper loudness limits, denoted by downward triangles) on each main electrode as a function of the steering coefficient α. All current levels are in dB re 1 μA. The applied compensation coefficient σ is also included in each plot. Two-way RM ANOVAs were performed to analyze the effects of electrode and α on T/C levels and DRs, respectively. Both T-levels and DRs were not significantly affected by either electrode ($F_{2,8} = 3.71, p = 0.07$ for T-levels; $F_{2,8} = 2.89, p = 0.11$ for DRs) or α ($F_{10,50} = 0.87, p = 0.57$ for T-levels; $F_{10,50} = 0.11, p = 1.00$ for DRs). However, C-levels were significantly affected by both electrode ($F_{2,8} = 9.19, p = 0.01$) and α ($F_{10,50} = 2.11, p = 0.04$). There was no significant interaction between electrode and α for T-levels ($F_{20,80} = 0.09, p = 1.00$), C-levels ($F_{20,80} = 0.33, p = 1.00$), and DRs ($F_{20,80} = 0.14, p = 1.00$). Post-hoc t-tests with Bonferroni correction showed that C-levels were only significantly higher on EL8

than on EL4 ($p = 0.01$), but not significantly different between any α pair. Future examination of neural survival and imaging of electrode placement may help explain the increased C-levels on EL8. Also note that, T/C levels of steered pTP stimuli were only measured on three main electrodes, which did not explore the possible threshold variation across the electrode array as shown in [19].

Equal-loudness Contour at M-level

Fig. 3.7 also shows the equal-loudness contours at the most comfortable level (M-level, denoted by circles) for individual subjects and electrodes. As can be seen, M-levels were well above T-levels but close to C-levels. In a few cases (e.g., $\text{pTP}_{EL8,\alpha=0.7}$ for S2 and $\text{pTP}_{EL12,\alpha=0.9}$ for S6), the M-level obtained from loudness balancing across α even exceeded the C-level obtained from loudness growth within α, most likely due to their different methods of measurement (i.e., method of adjustment for M-level and method of limits for T/C levels). The patterns of equal-loudness contours at M-level varied across subjects and electrodes. For EL12 of S2 and all electrodes of S4 and S5, the M-level contours peaked at α around 0.5 and decreased toward both ends at α equal to 0 or 1. For EL8 of S2 and EL4 and EL12 of S6, the M-level contours peaked at α around 0 or 1 and decreased toward the other end. For the other electrodes including those of S1 and S3, the contours of M-level were relatively flat. A two-way RM ANOVA revealed significant effects of both electrode ($F_{2,8} = 18.22, p = 0.001$) and α ($F_{10,50} = 3.43, p = 0.002$) on M-levels. Electrode and α did not significantly interact with each other ($F_{20,80} = 0.70, p = 0.82$). Post-hoc Bonferroni t-tests showed that M-levels were significantly higher on EL8 than on EL4 ($p = 0.004$) and EL12 ($p = 0.002$), a pattern similar to that of C-levels. As α varied, M-levels were only significantly higher for standard pTP mode with $\alpha = 0.5$ than for pBP mode with $\alpha = 0 (p = 0.03) or 1 (p = 0.05)$. Unlike T/C levels, M-levels were carefully loudness balanced across α using the adaptive procedures and thus may better reflect the different current requirements for different α.

Table 3.1.
Subject demographic details

Subject	Age (years)	Years of Profound Deafness	Etiology	Processing Strategy	CI use (years)	HINT scores* (%)
S1	82	3	Sudden hearing loss	HiRes-P 120	3	96
S2	62	25	Gestational hypertension	HiRes-P	6	88
S3	37	34	Spinal meningitis	HiRes-S 120	2	14
S4	42	N/A	Sudden hearing loss	HiRes-P 120	7	94
S5	60	55	Unknown	Emulated CIS	2	N/A
S6	64	19	Hereditary deafness	HiRes-P	6	94

*The Hearing In Noise Test (HINT) sentences were tested in quiet at 60 dB SPL during the most recent clinical visit. S5 was only tested with the CUNY sentences and scored 14 % correct.

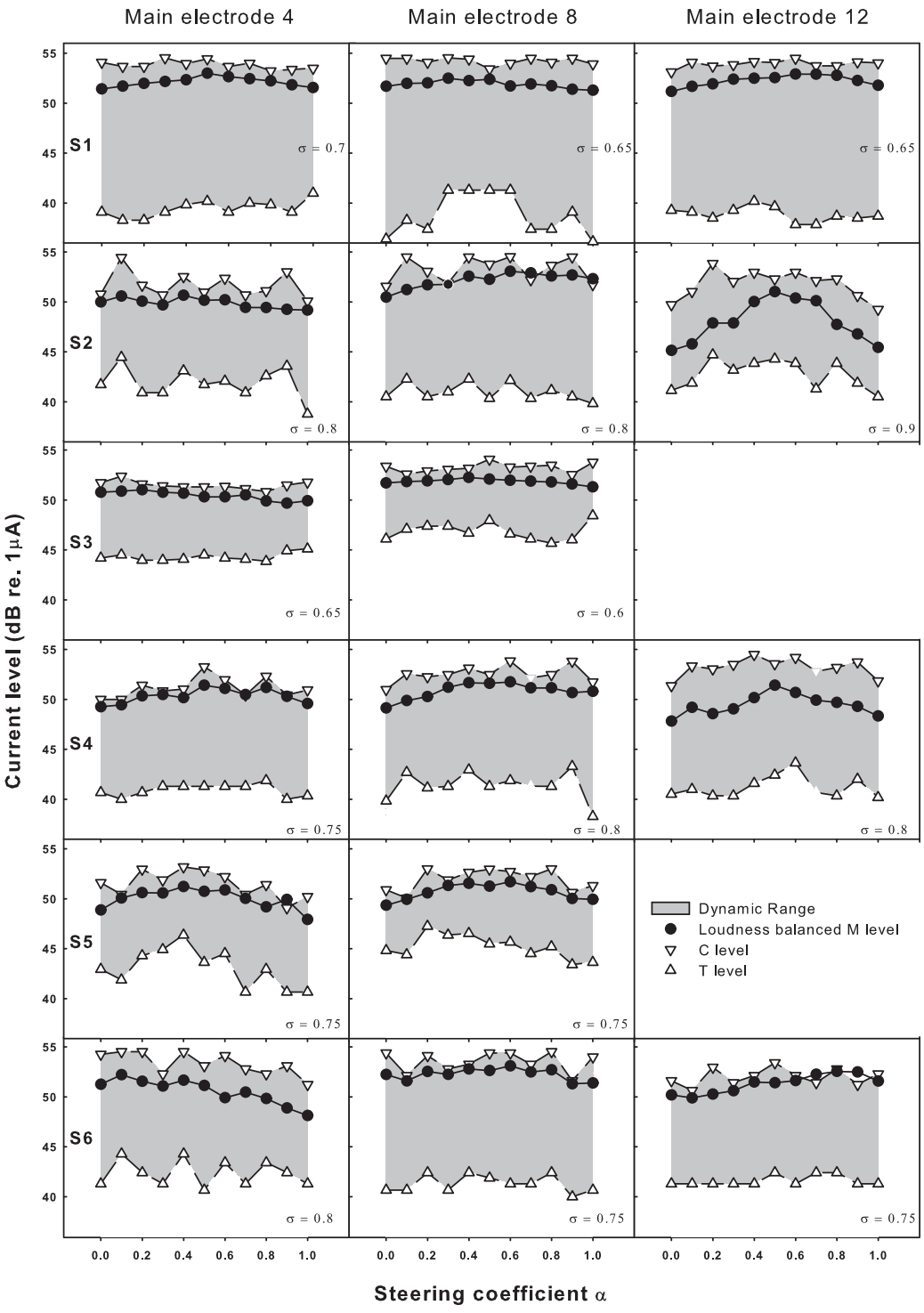

Fig. 3.7. Thresholds (T-levels: upward open triangles), upper loudness limits (C-levels: downward open triangles), and loudness-balanced most comfortable levels (M-levels: solid circles) as a function of the steering coefficient σ for individual subjects (different rows) and main electrodes (different columns). The dynamic ranges between T/C levels are shown as the shaded areas. All current levels are in dB re 1 μA. The applied compensation coefficient σ is included in each plot.

Pitch Ranking of Steered pTP Stimuli

Pitch-ranking results (i.e., the percentages that $\text{pTP}_{ELn,\alpha}$ was judged as higher in pitch than $\text{pTP}_{ELn,\alpha-0.1}$, where $\alpha = 0.1, 0.2, \ldots, 1$) were converted to d' values, which are shown in Fig. 3.8 as a function of α (gray circles), with the ordinate for d' labeled on the right. Also shown in Fig. 3.8 are the cumulative d' functions (black circles with the ordinate labeled on the left) across subjects and electrodes. The cumulative d' started from 0 at $\alpha = 0$ and was the summation or running total of successive d' values with increasing α. The cumulative d' at $\alpha = 1$ was called the overall cumulative d' and would be used to derive the number of discriminable pitch steps on a main electrode later.

Positive d' values indicate higher pitches for higher α (with percentages $> 50\%$), while negative d' values indicate lower pitches for higher α (with percentages $< 50\%$). The d' values shown in Fig. 3.8 had a mean of -0.56 and a standard deviation of 0.73, which suggests that for the tested electrodes and α, the perceived pitch of $\text{pTP}_{ELn,\alpha}$ was usually lower, but occasionally similar or higher, than that of $\text{pTP}_{ELn,\alpha-0.1}$. This somewhat agrees with the model prediction that higher α pushes the excitation pattern to the apex and results in lower pitch percepts. A two-way RM ANOVA performed on the d' values showed a nearly significant effect of α ($F_{9,45} = 2.03, p = 0.06$), but not of electrode ($F_{2,8} = 0.62, p = 0.56$), or their interaction ($F_{18,72} = 0.68, p = 0.81$).

Since the d' values were mostly negative or close to zero, the cumulative d' was in general a monotonic decreasing function of α for most subjects except S2 and S3. Fig. 3.8 also shows that for some of the tested electrodes (e.g., EL4 and EL8 of S1, EL4 and EL12 of S4), the cumulative d' function decreased faster in the middle than at the two ends of α. However, as revealed by the above analysis of the d' values, the change in cumulative d' with a 0.1 interval in α was not significantly different across α. The overall cumulative d' (i.e., the cumulative d' at $\alpha = 1$) ranged from -0.74 to -14.42 for different subjects and electrodes with a mean of -7.44. The overall cumulative

d' can be converted to the number of discriminable pitch steps when divided by a d' threshold corresponding to the just-noticeable-difference in pitch [40]. Using the same d' threshold (1.16 or 79.4% correct in a 2AFC task) as in previous studies such as [21], it was found that steered pTP mode created on average six pitch steps on a main electrode in this study. A one-way RM ANOVA revealed no significant effect of electrode ($F_{2,8} = 0.17, p = 0.85$) on the overall cumulative d', indicating similar pitch changes with steered pTP stimuli on different main electrodes. The compensation coefficient σ (shown in each plot of Fig. 3.8) was not correlated with the overall cumulative d' ($r^2 = 0.11, p = 0.22$), thus the variable pitch changes across subjects cannot be explained by different degrees of current focusing. Instead, the inter-subject variability in pitch changes may be partially due to different onsets of hearing loss, which can result in different degrees of neural survival. The two pre-lingually deafened subjects (S3 and S5) did have poorer pitch discrimination and less overall cumulative d'.

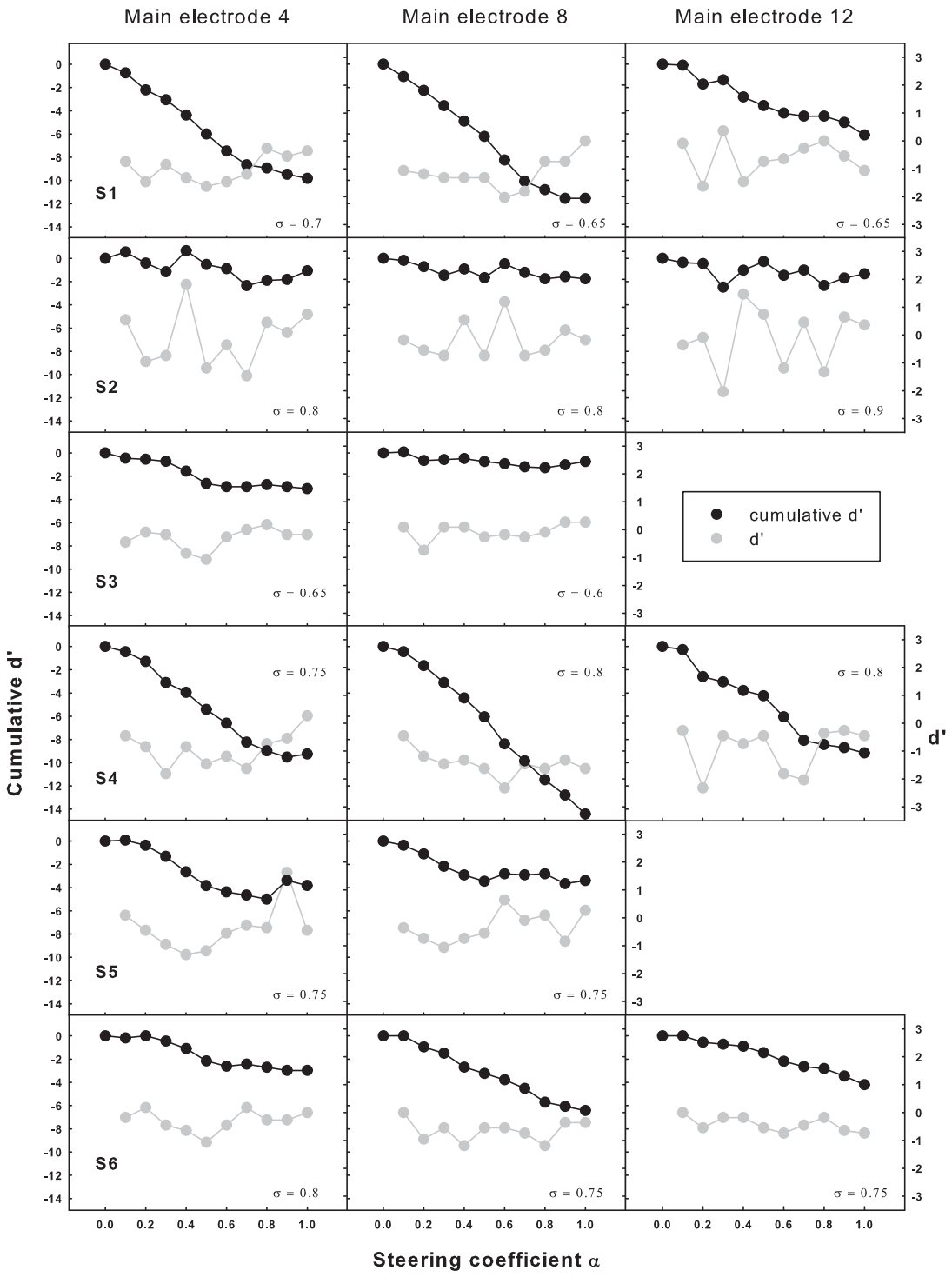

Fig. 3.8. Cumulative d' from $\alpha = 0$ (black circles; left ordinate) and d' values between adjacent α (gray circles; right ordinate) for pitch ranking as a function of the steering coefficient α for individual subjects (different rows) and main electrodes (different columns). The applied compensation coefficient σ is shown in each plot.

3.3.3 Discussion

Experiment 1 tested loudness and pitch perception with steered pTP mode on three main electrodes. Although variable across subjects and electrodes, the loudness-balancing data confirmed the hypothesis that steered pTP stimuli with $\alpha = 0.5$ required more current to achieve equal loudness than stimuli with $\alpha = 0$ or 1. As expected, lower pitches were generally perceived with increasing α in the pitch-ranking tests. However, there was no clear evidence that pitch discrimination with steered pTP mode was better for α around 0.5 than for α around 0 or 1, except for some subjects and electrodes.

Subject- and Electrode-specific Compensation Coefficient σ

The highest possible σ values found for individual subjects were in a range (> 0.6) that has been shown to generate narrower excitation patterns than $\sigma = 0$ (MP stimulation) with equal loudness [32], and thus should be able to support more effective current steering. Previous studies of pTP mode [41] [31] [23] did not attempt to find the highest possible σ and only tried σ values of 0.25, 0.5, or 0.75, which may have underestimated the benefits of current focusing to CI users. Assuming that higher σ values would improve speech perception with more focused stimulation, our results suggest that finer adjustments of σ may be necessary for individual CI users, but not for individual electrodes within each patient. Although it may still be time consuming, our method for searching the highest possible σ can be useful for such fitting optimization of pTP-mode processing strategies.

Inconsistent Patterns of Various Loudness Contours

Measurements of T/C levels for individual subjects and electrodes (Fig 3.7) did not show consistent patterns across α as in model predictions (3.4), possibly due to the susceptibility of focused pTP stimulation to variable local electrode-neuron interface,

which was not simulated in the basic model. Also note that the model levels across α were simply assumed to generate equal loudness with the same total number of activated neurons, which may or may not be a valid hypothesis. On the other hand, the measured T/C levels were also not strictly loudness balanced across α using the adaptive procedure because loudness perception at these two levels was either too weak or too strong to be tested. Bierer [19] found significantly higher thresholds for full TP stimulation ($\sigma = 1$, $\alpha = 0.5$) compared to full BP stimulation ($\sigma = 1$, $\alpha = 0$) across the whole electrode array. However, similar T-levels were found for standard pTP ($\sigma < 1$, $\alpha = 0.5$) and pBP modes ($\sigma < 1$, $\alpha = 0$ or 1) in this study. The smaller σ or less proportion of intra-cochlear return current may have reduced the T-level differences between standard pTP and pBP modes. Our results also did not show evidence that standard pTP mode would generate larger DRs than pBP mode, at least for the tested σ. The similar DRs across α had implications for a quick yet efficient fitting of steered pTP mode. For example, the DR measured for $\alpha = 0.5$ can be used to estimate the C levels for the other α from the corresponding T levels.

Somewhat similar to model predictions (3.4), the equal-loudness contours at M-level (3.7) for S2, S4, and S5 exhibited higher current requirement for α around 0.5 than for α around 0 and 1, supporting the hypothesis that more focused stimulation of standard pTP mode requires more current to achieve equal loudness than pBP stimulation. For S6, the peaks of M-level contours shifted to $\alpha = 0$ or 1. It is possible that her neural survival was poorer and/or her electrode-neuron distance was longer around one of the flanking electrodes. Thus more current was required for pBP mode with $\alpha = 0$ or 1, which had a side-lobe of excitation near the apical or basal flanking electrode, respectively. The relatively flat M-level contours of S1 and S3 may have been visually compressed because the y-axis of 3.7 was scaled to show the complete DRs. It also happened that the compensation coefficients σ of S1 and S3 were smaller than those of the other subjects. The variation of M-level contour, quantified by the difference between the maximum and minimum M-levels of each contour, was indeed positively correlated with σ across all subjects and electrodes (Pearsons correlation:

$r^2 = 0.66, p < 0.001$). The moderate correlation suggests that at least for some tested electrodes, higher σ of steered pTP mode required more variable current levels to keep equal loudness perception with different α.

Variable Pitch-ranking Results across Electrodes and α

Fig. 3.8 shows that in general, subjects perceived lower pitches when α increased from 0 to 1, and their pitch discrimination was not better with any specific α value. The lack of significant difference in d' values between $\alpha = 0.5$ (standard pTP mode) and $\alpha = 0$ or 1 (pBP mode) was not consistent with the simplified model predictions. Again, the different local electrode-neuron interfaces of individual electrodes may be a major factor underlying the irregular d' functions. Besides, the α step of 0.1 may have been too small for some subjects to reliably rank the pitches of consecutive pairs of steered pTP stimuli and this floor effect may have contributed to the variable d' values. A larger α step (e.g., 0.2) may help ease the task of pitch ranking and better estimate the d' values, especially in cases where performance was near chance (i.e., d' close to 0).

The variable pitch-ranking results also exhibited pitch reversals (i.e., higher rather than lower pitches with increasing α), which occurred most often for S2. Pitch reversals with steered pTP mode did not necessarily occur around $\alpha = 0$ or 1, and thus were not caused by the perceptually salient side-lobe around the return electrode as in pBP mode or phantom electrode [24]. It is also unlikely that such pitch reversals were due to the $\pm$0.5-dB amplitude roving used in the pitch-ranking tests, because the added random loudness changes across trials should not have consistently reversed pitch ranking. To examine S2's susceptibility to amplitude roving, she was retested on EL8 without amplitude roving. The results (right panel in Fig. 3.9) did show improved pitch discrimination (or greater negative d' values) between consecutive pairs of steered pTP stimuli than those with amplitude roving (left panel). However, even without amplitude roving, pitch reversals still occurred for different α than with

amplitude roving, showing inconsistent pitch judgments. Future measurements of the actual excitation patterns may be necessary to explain the cause of pitch reversals in steered pTP mode.

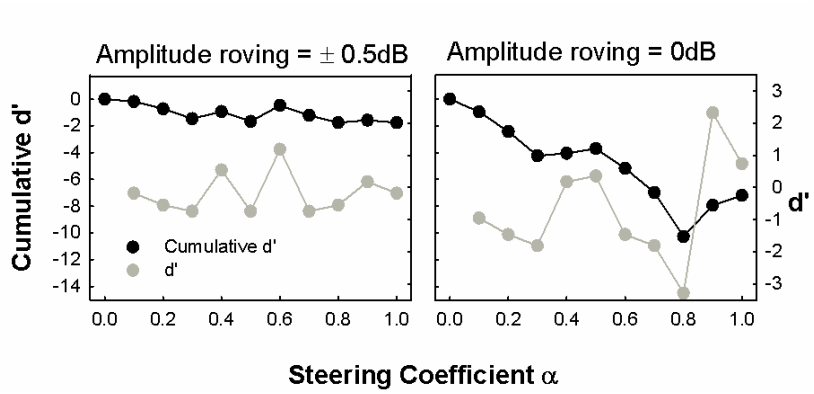

Fig. 3.9. Pitch-ranking results of subject S2 on EL8 with or without amplitude roving.

Comparison with Phantom Electrodes

Due to the different working principles (i.e., varying the proportion of current on return or main electrodes), the proposed pTP-mode current steering may not be directly comparable with monopolar- or quadrupolar-mode current steering (e.g., [21] [42]). However, it is worth comparing the present results with those of phantom electrodes proposed by [24]. Phantom-electrode stimuli were indeed pBP stimuli with a basal return electrode or pTPELn, α=1 in this study. Instead of varying the steering coefficient α, Saoji [24] varied the compensation coefficient σ to control the proportion of current returned to the basal electrode. Similar to our results, their subjects also perceived lower pitches for higher σ (or with more current returned to the basal flanking electrode). However, when σ was 0.6 or higher, many of their subjects were affected by the perceptually salient side-lobe and perceived higher instead of lower pitches for higher σ (i.e., pitch reversals). In contrast, as mentioned above, the side-lobe effect cannot explain the pitch reversals observed with steered pTP mode

in this study. The overall pitch changes created by phantom electrodes were actually similar to those of steered pTP mode. [24] only tested phantom electrodes with the basal return electrode and the overall cumulative d' (from $\sigma = 0$ to the highest σ without pitch reversals) ranged from -2 to -5 for their subjects. If phantom electrodes with the apical return electrode were similarly perceived, the overall cumulative d' would presumably double and match well with those of steered pTP mode in this study.

3.4 Experiment 2: Pitch ranking on steered pTP stimuli on adjacent main electrodes

Experiment 1 tested the relative pitch changes with steered pTP stimuli on a main electrode and found that, in general, pitch monotonically decreased as the steering coefficient α increased from 0 to 1. To implement steered pTP mode along the electrode array, it is important to know if the pitch ranges of adjacent main electrodes both in steered pTP mode would overlap. To answer this question, pitch was compared between steered pTP stimuli on two adjacent main electrodes EL7 and EL8 in Experiment 2.

3.4.1 Methods

Subjects and Stimuli

Subjects S1, S4, and S6 from Experiment 1 participated in Experiment 2. These subjects had relatively better pitch discrimination and hardly any pitch reversals with steered pTP mode on EL8 in Experiment 1. Their well-perceived pitch ranges from $\alpha = 0$ to $\alpha = 1$ on EL8 and EL7 could thus be reliably compared using the following procedure. Stimuli were the same as those defined in Experiment 1.

Loudness Balancing and Pitch Ranking between EL7 and EL8

Loudness balancing and pitch ranking of steered pTP stimuli on EL7 were first tested using the same procedure as in Experiment 1, except that the stimuli on EL7 (i.e., $\mathrm{pTP}_{EL7,\alpha=0}$, $\mathrm{pTP}_{EL7,\alpha=0.1}$, ..., $\mathrm{pTP}_{EL7,\alpha=1}$) were loudness balanced to $\mathrm{pTP}_{EL8,\alpha=1}$ at M-level. These tests aimed to confirm that pitch changed in a similar fashion (i.e., lower pitches for higher α) with steered pTP stimuli on both EL7 and EL8.

Based on the tonotopic organization of cochlea, the pitch range on EL8 (from $\alpha = 0$ to $\alpha = 1$) was expected to be higher than that on EL7. To determine if there was overlap between the two pitch ranges, the lowest pitch on EL8 elicited by $\mathrm{pTP}_{EL8,\alpha=1}$ was compared with the various pitches on EL7, while the highest pitch on EL7 elicited by $\mathrm{pTP}_{EL7,\alpha=0}$ was compared with the various pitches on EL8. If the lowest-pitch stimulus on EL8 ($\mathrm{pTP}_{EL8,\alpha=1}$) was perceived as higher in pitch even than the highest-pitch stimulus on EL7 ($\mathrm{pTP}_{EL7,\alpha=0}$), then the two pitch ranges did not overlap. Otherwise, it was possible to find a stimulus on EL7 ($\mathrm{pTP}_{EL7,\alpha=\alpha1}$) that was pitch-matched to $\mathrm{pTP}_{EL8,\alpha=1}$ and a stimulus on EL8 ($\mathrm{pTP}_{EL8,\alpha=\alpha2}$) that was pitch-matched to $\mathrm{pTP}_{EL7,\alpha=0}$. In other words, the pitch range between $\mathrm{pTP}_{EL8,\alpha=\alpha2}$ and $\mathrm{pTP}_{EL8,\alpha=1}$ overlapped with that between $\mathrm{pTP}_{EL7,\alpha=0}$ and $\mathrm{pTP}_{EL7,\alpha=\alpha1}$. Also, with matched pitch percepts, $\mathrm{pTP}_{EL7,\alpha=\alpha1}$ indicated the apically shifted excitation of $\mathrm{pTP}_{EL8,\alpha=1}$, while $\mathrm{pTP}_{EL8,\alpha=\alpha2}$ indicated the basally shifted excitation of $\mathrm{pTP}_{EL7,\alpha=0}$.

Pitch ranking was tested using the same 2AFC task as in Experiment 1. In one test, the reference was $\mathrm{pTP}_{EL8,\alpha=1}$ and the signal was randomly selected from $\mathrm{pTP}_{EL7,\alpha=0}$, $\mathrm{pTP}_{EL7,\alpha=0.1}$, ..., and $\mathrm{pTP}_{EL7,\alpha=1}$. In the other test, the reference was $\mathrm{pTP}_{EL7,\alpha=0}$ and the signal was randomly selected from $\mathrm{pTP}_{EL8,\alpha=0}$, $\mathrm{pTP}_{EL8,\alpha=0.1}$, ..., and $\mathrm{pTP}_{EL8,\alpha=1}$. In each trial, the reference and signal were presented in a random order and the subject had to judge which stimulus was higher in pitch. Amplitude roving of ± 0.5 dB was applied to all stimuli to reduce possible loudness effects. All stimulus pairs were repeated 20 times in a run and data from two runs were averaged to obtain the percentages that the signals were perceived as higher in pitch than the

reference. These scores were fitted with a sigmoid function to estimate the signal that was pitch-matched to the reference.

3.4.2 Results

The cumulative d' for pitch ranking on EL7 is plotted as a function of α in the right column of Fig. 3.10. Similar to that on EL8 (obtained from Experiment 1 and re-plotted in the left column), the cumulative d' on EL7 generally decreased as more current was returned to the basal flanking electrode, or when α increased. The overall cumulative d' (i.e., the cumulative d' at $\alpha = 1$) on EL7 was also similar to that on EL8 for each subject. Also note that the highest possible compensation coefficient σ that allowed for full loudness growth within the compliance limit of the implant was identical on the two adjacent main electrodes, as shown in the upper right corner of each plot. This may indicate that for these selected subjects, the adjacent main electrodes EL7 and EL8 had similar neural survival, electrode-neuron distances, and impedances.

Fig. 3.11 shows the pitch-ranking data between steered pTP stimuli on EL7 and EL8. The left column shows the percentages that signals on EL7 were judged as higher in pitch than the reference $\text{pTP}_{EL8,\alpha=1}$, while the right column shows the percentages that signals on EL8 were judged as higher in pitch than the reference $\text{pTP}_{EL7,\alpha=0}$. As shown in the left column, the lowest pitch on EL8 elicited by $\text{pTP}_{EL8,\alpha=1}$ fell in the middle of the pitch range on EL7 (i.e., higher than the pitch of $\text{pTP}_{EL7,\alpha=1}$ but lower than that of $\text{pTP}_{EL7,\alpha=0}$). Similarly, in the right column, the highest pitch on EL7 elicited by $\text{pTP}_{EL7,\alpha=0}$ also fell in the middle of the pitch range on EL8 (i.e., higher than the pitch of $\text{pTP}_{EL8,\alpha=1}$ but lower than that of $\text{pTP}_{EL8,\alpha=0}$). The only exception was that S6 did not reliably perceive $\text{pTP}_{EL7,\alpha=0}$ as lower in pitch than $\text{pTP}_{EL8,\alpha=0}$. Nevertheless, the results suggest that the pitch ranges of adjacent main electrodes did overlap with each other. Each S-shaped psychometric function in Fig. 3.11 was fitted with a 3-parameter sigmoid function:

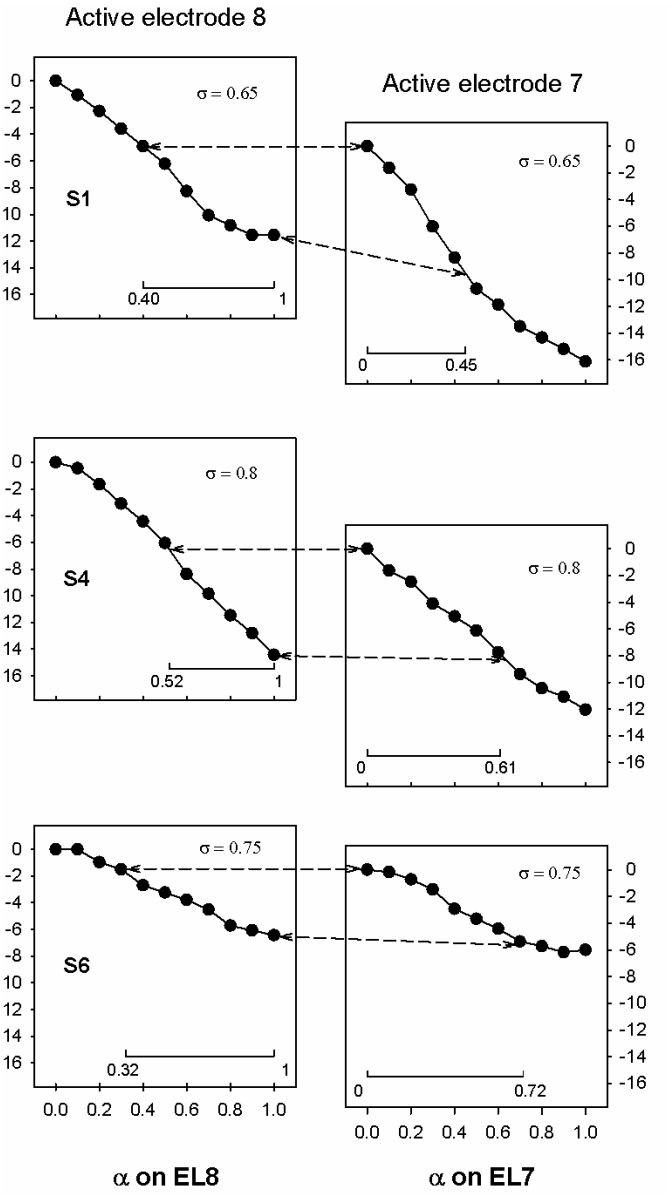

Fig. 3.10. Cumulative d' from $\alpha = 0$ for pitch ranking on EL8 (left column; data from Experiment 1) and EL7 (right column) as a function of the steering coefficient α for subjects S1, S4, and S6. The applied compensation coefficient σ is included in each plot. The pitch-ranking results between the two adjacent main electrodes (shown in Fig. 3.11) were used to determine their overlapped pitch ranges, which are aligned with each other along the ordinate and connected by the dashed lines. The interval of α for the overlapped pitch range is also indicated by the horizontal line at the bottom of each plot.

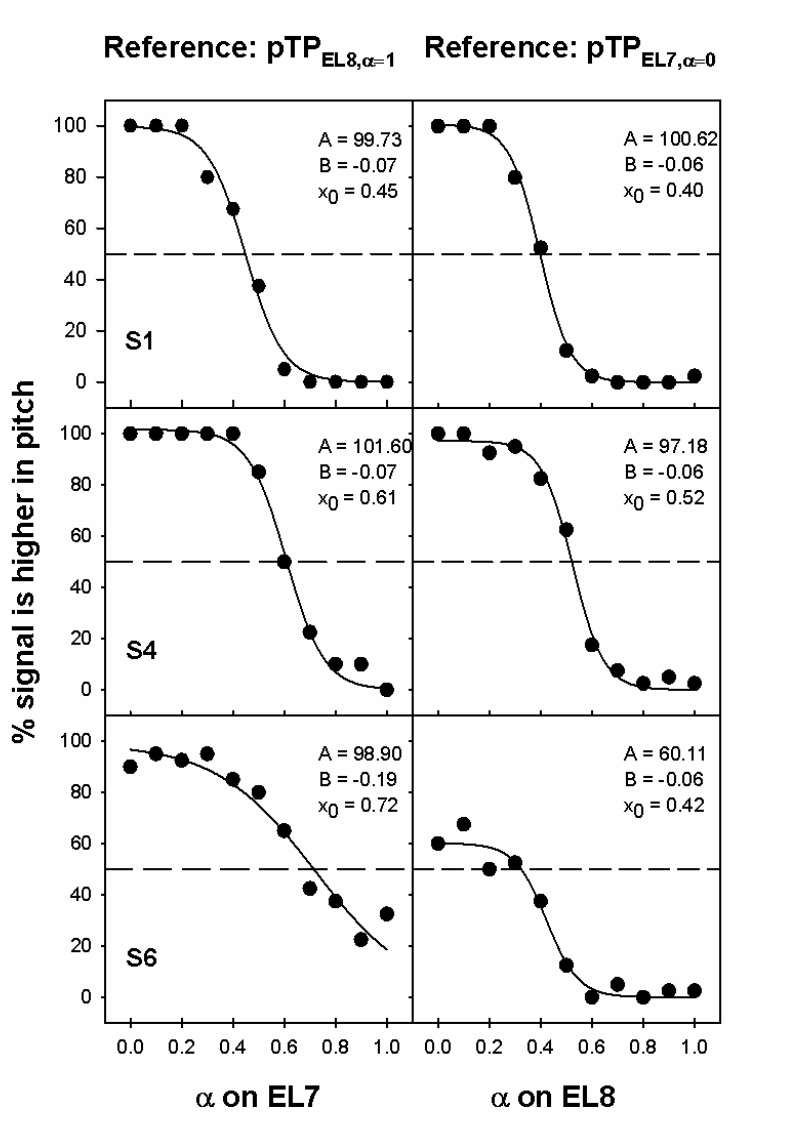

Fig. 3.11. Pitch-ranking results between EL7 and EL8 for subjects S1, S4, and S6. The left column shows the percentages that signals on EL7 ($\mathrm{pTP}_{EL7,\alpha=0,0.1,\ldots,1}$) were judged as higher in pitch than the lowest-pitch reference on EL8 (i.e., $\mathrm{pTP}_{EL8,\alpha=1}$). The right column shows the percentages that signals on EL8 ($\mathrm{pTP}_{EL8,\alpha=0,0.1,\ldots,1}$) were judged as higher in pitch than the highest-pitch reference on EL7 (i.e., $\mathrm{pTP}_{EL7,\alpha=0}$). The solid curves show the best-fit sigmoid functions for the data (solid circles), with the function parameters indicated in each plot. The dashed lines correspond to 50% responses on the function where the signal and reference were matched in pitch.

$$y = \frac{A}{1 + \exp(\frac{x - x_0}{B})} \tag{3.2}$$

where y is the percentage that the signal was judged as higher in pitch than the reference and x is the α of signal. The best-fit sigmoid functions (all with $r^2 > 0.94$ and $p < 0.005$) are shown by solid curves and the corresponding parameters are included in each plot. The parameter B was in inverse proportion to the slope of the function. The parameter A represented the highest percentage of the function and was near 100 except for S6 with the reference $\text{pTP}_{EL7,\alpha=0}$. When A was 100, the parameter x_0 represented α of the signal that was pitch-matched to the reference (i.e., with 50% responses in pitch ranking). For S6 with the reference $\text{pTP}_{EL7,\alpha=0}$, α of the pitch-matched signal on EL8 was calculated by solving for x with y equal to 50% responses in the best-fit sigmoid function.

Take S4 for example. Her x_0 parameters showed that $\text{pTP}_{EL7,\alpha=0}$ was pitch-matched to $\text{pTP}_{EL8,\alpha=0.52}$, while $\text{pTP}_{EL8,\alpha=1}$ was pitch-matched to $\text{pTP}_{EL7,\alpha=0.61}$. In other words, the pitch range between $\text{pTP}_{EL8,\alpha=0.52}$ and $\text{pTP}_{EL8,\alpha=1}$ overlapped with that between $\text{pTP}_{EL7,\alpha=0}$ and $\text{pTP}_{EL7,\alpha=0.61}$. The overlapped pitch range was indicated in the second row of Fig. 3.10 by aligning $\text{pTP}_{EL7,\alpha=0}$ with $\text{pTP}_{EL8,\alpha=0.52}$ and $\text{pTP}_{EL8,\alpha=1}$ with $\text{pTP}_{EL7,\alpha=0.61}$ along the ordinate. The interval of α for the overlapped pitch range was also indicated by the horizontal line at the bottom of each plot. The cumulative d' was calculated within the overlapped pitch range and was similar on EL7 (-7.97) and EL8 (-7.69). Similar results were found for S6. However, for S1, the cumulative d' of the overlapped pitch range was less on EL8 (-6.77) than on EL7 (-9.20). This suggests that the estimated cumulative d' of the same pitch range may differ due to different intermediate stimuli used for d' measurements [40]. S1's poorer pitch discrimination on EL8 for α from 0.7 to 1 in steps of 0.1 may have underestimated the cumulative d' of the overlapped pitch range.

3.4.3 Discussion

Pitch Overlap between Adjacent Main Electrodes

For a subset of better-performing subjects, the lower half of the pitch range on EL8 overlapped with the higher half of the pitch range on EL7. The overlapped pitch ranges between adjacent main electrodes at the loudness-balanced M-level in these CI subjects were better matched with the model predictions based on the CoG rather than the peak of excitation (Fig. 3.5). Therefore, place-pitch perception elicited by steered pTP stimuli was more likely determined by the CoG than by the peak of excitation.

Fig. 3.10 shows that, on average, $\text{pTP}_{EL8,\alpha=1}$ had a similar pitch to $\text{pTP}_{EL7,\alpha=0.6}$. Their simulated CoGs of excitation were also close together in Fig. 3.5. The excitation pattern of $\text{pTP}_{ELn,\alpha=0.5}$ was centered on ELn because of its symmetric current return to the two flanking electrodes. When α varied from 0.5 to 1 for steered pTP stimuli on EL8, the CoG of excitation was steered apically from EL8 to EL7 (i.e., a shift of about one physical electrode). Similarly, the average pitch match between $\text{pTP}_{EL7,\alpha=0}$ and $\text{pTP}_{EL8,\alpha=0.4}$ suggests that when α varied from 0.5 to 0 for steered pTP stimuli on EL7, the CoG of excitation shifted about one physical electrode basally from EL7 to EL8. Such amounts of CoG shifts were similar to those with phantom electrodes [24]. Although pitch ranking was only tested between steered pTP stimuli on EL7 and EL8, similar results were expected for the other electrodes, because pitch perception with steered pTP stimuli was not significantly different on different electrodes in Experiment 1.

Selection of α Range for Each Main Electrode

To implement steered pTP mode along the electrode array in a CI speech processor, the range of steering coefficient α on each electrode should be chosen so that pitch changes continuously from one electrode to the next without overlap. Based

on Fig. 3.5 and 3.10, it is reasonable to assume that on average, the pitch range between $\text{pTP}_{EL8,\alpha=0.4}$ and $\text{pTP}_{EL8,\alpha=0.6}$ may overlap with that between $\text{pTP}_{EL7,\alpha=0}$ and $\text{pTP}_{EL7,\alpha=0.3}$. Similarly, the pitch range between $\text{pTP}_{EL7,\alpha=0.4}$ and $\text{pTP}_{EL7,\alpha=0.6}$ is expected to overlap with that between $\text{pTP}_{EL6,\alpha=0}$ and $\text{pTP}_{EL6,\alpha=0.3}$. To elicit continuous non-overlapped pitch changes, one can use α values from 0.4 to 0.6 on each electrode. In this way, pitch decreases as the stimuli change from $\text{pTP}_{EL8,\alpha=0.4}$ to $\text{pTP}_{EL8,\alpha=0.6}$, continues to decrease as the stimuli change from $\text{pTP}_{EL7,\alpha=0.4}$ to $\text{pTP}_{EL7,\alpha=0.6}$, and so on. On the other hand, instead of using the same α range from 0.4 to 0.6 on each electrode, one can use a wider α range on the electrode with better pitch discrimination and more discriminable pitch steps than its adjacent electrode. This alternative selection of α range may provide more spectral resolution but requires sophisticated pitch tests during fitting.

3.5 General Discussion and Summary

Loudness and pitch perception with steered pTP mode was predicted using model simulations and tested in psychophysical experiments. Although CI subjects had similar T/C levels and dynamic ranges across α on a main electrode, their loudness-balanced M-levels were significantly higher with $\alpha = 0.5$ than with $\alpha = 0$ or 1. This is consistent with the model prediction that more current is required for more focused standard pTP mode ($\alpha = 0.5$) than for less focused pBP mode ($\alpha = 0$ and 1) to achieve equal loudness. CI subjects generally perceived lower pitches (with an average overall cumulative d' of -7) as α increased from 0 to 1. However, their pitch discrimination was not better with α around 0.5 (i.e., more focused standard pTP mode) than with α around 0 or 1 (i.e., less focused pBP mode), except for some subjects and electrodes. For three better-performing CI subjects, pitch comparisons between steered pTP stimuli on adjacent main electrodes showed that about half of the pitch ranges of EL7 and EL8 overlapped with each other (e.g., the lower half of EL8 matched with the higher half of EL7). Compared with the model predictions,

these results suggest that pitch changes elicited by steered pTP stimuli were largely driven by the shifted CoG rather than by the peak of excitation.

The small heterogeneous subject group (i.e., N = 6 with two being pre-lingually deafened) may not be ideal for this proof-of-concept study. The inter-subject variability in loudness and pitch perception was high, which unfortunately weakened the overall findings of this study and made the results somewhat anecdotal. The underlying reasons for inter-subject variability were unclear, but individual subjects' different electrode-neuron interfaces and various onsets of hearing loss (i.e., pre- or post-lingually deafened) most likely contributed to their different performances. In future studies, variations in electrode-neuron distance and neural survival will be introduced to the computational model to predict their effects on loudness and pitch perception with steered pTP mode. A more straightforward way to explain the variable perceptual data is to directly estimate the excitation patterns of steered pTP stimuli with different α in each subject. This can be achieved by measuring the forward masking patterns of steered pTP stimuli using psychophysical methods (e.g., [43] [44] [45] [20]) or using electrically evoked compound action potentials (e.g., [46] [47]).

In summary, both the model and psychophysical data verified the feasibility and efficacy of pTP-mode current steering, which can be readily incorporated into the pTP-mode processing strategies [23] to improve CI performance. For example, Bierer [3] argued that with the more focused standard pTP mode, CI users were more susceptible to cochlear "dead regions" which required more current to reach T/C levels and had less spatial selectivity of electric stimulation. In such a case, an α value different from 0.5 may be used to steer pTP stimuli away from the dead region to more efficiently transmit the corresponding spectral information. In addition, as discussed in Experiment 2, α values from 0.4 to 0.6 can be applied to steered pTP stimuli on each main electrode to create additional frequency channels and encode fine spectral details. The long pulse phase duration (226 μs) in this study helped achieve full loudness growth with steered pTP mode, but may limit the stimulation rate available in CI processors. As suggested by Landsberger [42], this issue may

be partially addressed by using an n-of-m strategy that only stimulates a subset of largest-amplitude channels in each cycle. The proposed idea of combining current steering with focusing (see also [42]) may provide CI users with more distinctive pitches and frequency channels than MP-mode current steering in the HiRes-120 strategy. Future studies will implement pTP-mode current steering in multi-channel CI speech processors and test the potential benefits to CI users using appropriate psychophysical, speech, and music tests.

4. EXCITATION PATTERNS OF STANDARD AND STEERED PARTIAL TRIPOLAR COCHLEAR IMPLANT STIMULATION

4.1 Introduction

To investigate the mechanism by which steered pTP stimulation can generate progressively lower pitch with increasing α, the stimulation or excitation patterns of steered pTP stimulation with various α were measured at physical, physiological, and perceptual levels. At physical level, potential distribution can be recorded via the implant back-telemetry system and provides information about the volume conduction or what the current spread looks like in the cochlea. This method, also called "Electrical field imaging" (EFI) in Advanced Bionics devices, has been used to record the potential distribution of multiple electrodes stimulating in phase [27, 48] or out of phase [49] and showed that spatial interaction at the physical level can be adequately modeled by linear summation of the potential distribution of each current source. At physiological level, evoked compound action potential (ECAP) can be recorded again using the implant telemetry system to assess the spread of neural excitation [26, 27, 46, 50, 51]. At behavioral level, the spread of excitation can be characterized by psychophysical forward masking pattern (PFM; [43, 52–55]). The goal of this study was to investigate how steered pTP stimulations elicit different pitch perception by comparing their spatial profiles at physical, physiological, and behavioral levels. Previous studies have shown the perceived place pitch usually agree with the centroid [5, 52, 56] or peak location [27] of excitation. The peak and centroid location of each spatial profile would be identified to see if they can be used to predict the perceived pitch. The width of excitation would also be calculated to quantify the spatial selectivity. The spatial representation of steered pTP stimulation measured at dif-

ferent processing levels may also reveal how steered pTP stimulation were processed and coded spectrally along the auditory pathway.

4.2 Methods

4.2.1 Subjects

Four postlingually deafened CI users of the Advanced Bionics HiRes 90K implant with the HiFocus1J electrode array participated in this study. Subject demographic details can be found in Table 4.1. Subject S3 received bilateral CIs and her left and right implants (S3L and S3R, respectively) were both tested. This study was reviewed and approved by the Purdue IRB committee. Subjects provided informed consent and were compensated for their time.

Table 4.1.
Subject demographic details

Subject	**Age (yrs)**	**Etiology**	**CI use (yrs)**	**Cumulative d' from α=0.5 to α=0**	**Cumulative d' from α=0.5 to α=1**	**σ used in pitch ranking**	**σ used in ECAP recording**
S1	85	Sudden hearing loss	5	6.22	-5.33	0.60	0.55
S2	45	Meningitis	9	6.06	-8.37	0.80	0.50
S3L	67	Hereditary deafness	3	-0.90	-2.04	0.75	0.40
S3R	67	Hereditary deafness	8	3.23	-3.19	0.65	0.55
S4	64	Unknown	5	2.45	-0.97	0.60	0.60

4.2.2 Pitch Ranking of Steered pTP stimuli

Steered pTP stimuli on the main electrode EL8 were balanced in loudness at the most comfortable level (MCL) and then ranked in pitch by each subject using the method in Chapter 3. During the psychophysical pitch-ranking test, the highest possible compensation coefficient σ that allowed for full loudness growth within the compliance limit of the CI was used for all subjects except S4. S4 experienced pitch reversals between adjacent main electrodes in standard pTP mode with the highest possible σ (0.8). Thus, a smaller σ (0.6) was used for S4 to rank the pitches of steered pTP stimuli on EL8 in this study. The results were consistent with those of Chapter 3, showing that pitch generally decreased with higher steering coefficient α. The cumulative d' of pitch ranking from $\text{pTP}_{EL8,\alpha=0.5}$ to $\text{pTP}_{EL8,\alpha=0}$ or from $\text{pTP}_{EL8,\alpha=0.5}$ to $\text{pTP}_{EL8,\alpha=1}$ was listed in Table 1 together with the compensation coefficient σ used for each subject. There was a large inter-subject variability in the pitch sensitivity to current steering in pTP mode. The electrical fields and excitation patterns of $\text{pTP}_{EL8,\alpha=0}$, $\text{pTP}_{EL8,\alpha=0.5}$, and $\text{pTP}_{EL8,\alpha=1}$ were thus measured in each subject to reveal the mechanism of pTP-mode current steering and to explain variable pitch-ranking results across subjects.

4.2.3 EFI: Stimuli and Procedure

Intracochlear potential distributions of $\text{pTP}_{EL8,\alpha=0}$, $\text{pTP}_{EL8,\alpha=0.5}$, and $\text{pTP}_{EL8,\alpha=1}$ were measured using the Electrical Field Imaging and Modeling software (EFIM v1.4, Advanced Bionics, Antwerp, Belgium). The stimulus used for EFI measurement was a 2.5-ms, 3000-Hz sinusoid at a sub-threshold level of 32 μA [27, 49]. The σ of the stimulus for each subject was the same as in the pitch-ranking test (Table 4.1). For each steered pTP stimulus, electrical potentials were recorded on all the non-stimulated electrodes along the electrode array (e.g., the open diamonds in Fig. 4.1 for $\text{pTP}_{EL8,\alpha=0.5}$ in S4). The recordings on the stimulated electrodes EL7, EL8, and EL9 could not be used because they were dominated by the reactive impedance between the

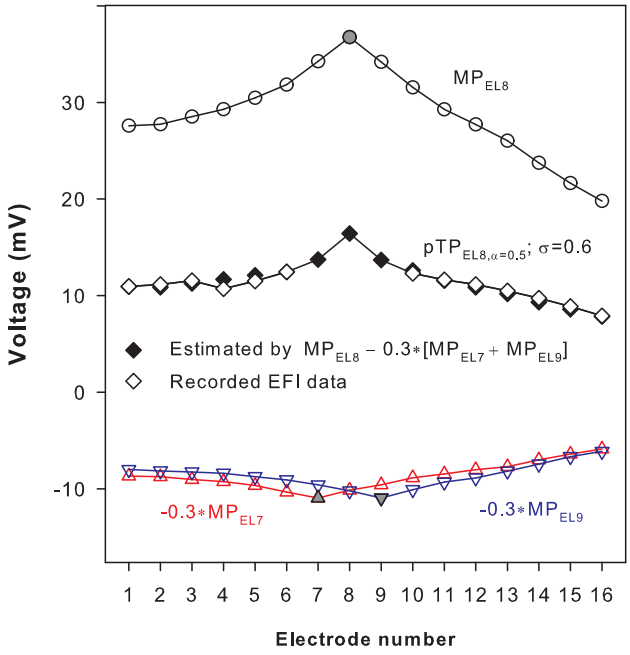

Fig. 4.1. The intracochlear potential distribution of $\text{pTP}_{EL8,\alpha=0.5}$ with $\sigma = 0.6$ recorded on the non-stimulated electrodes (open diamonds) and estimated (black diamonds) by summing the potential distribution of MP_{EL8} (circles), 0.3^*MP_{EL7} (upward triangles), and 0.3^*MP_{EL9} (downward triangles).

stimulated electrodes and the surrounding tissue rather than the resistive impedance between the stimulated electrodes and the remote ground [49]. To obtain the full intracochlear potential distribution of a steered pTP stimulus (e.g., $\text{pTP}_{EL8,\alpha=0.5}$ in S4), the electrical fields of MP stimuli on EL7, EL8, and EL9 were separately measured, each scaled by its corresponding current level and polarity in the steered pTP stimulus (e.g., the upward triangles, circles, and downward triangles in Fig. 4.1, respectively), and then linearly summed (e.g., the black diamonds in Fig. 4.1). Note that for each MP stimulus, the electrical potential on the stimulated electrode (e.g., the gray circle in Fig. 4.1 for MP_{EL8}) was estimated by fitting the EFI recordings (e.g., the open circles) on the apical (e.g., EL1–EL7) and basal non-stimulated electrodes (e.g., EL9–EL16) with separate exponential curves and averaging the extrapolated

values of both curves on the stimulated electrode [49]. Fig. 4.1 shows that the linear summation of the electrical fields of individual stimulated electrodes (e.g., the black diamonds) adequately approximated the electrical field of a steered pTP stimulus (e.g., the open diamonds) on the non-stimulated electrodes (with an average percent error of 7.14% across subjects and stimuli). This was consistent with the findings of [48, 49]. The final EFI pattern or the potential distribution of a steered pTP stimulus comprised the recorded values on the non-stimulated electrodes and the estimated values on the stimulated electrodes.

4.2.4 ECAP: Stimuli and Procedure

ECAP for steered pTP stimuli was recorded using the Bionic Ear Data Collection System (BEDCS v1.17, Advanced Bionics, Sylmar, CA). A forward masking subtraction method [57–60] was used to remove electrical stimulation artifacts while preserving neural responses. To determine the spread of neural excitation for steered pTP stimuli, the ECAP spatial profile (e.g., [46]) was measured by keeping the steered pTP-mode probe on EL8 (i.e., $\text{pTP}_{EL8,\alpha=0}$, $\text{pTP}_{EL8,\alpha=0.5}$, and $\text{pTP}_{EL8,\alpha=1}$) while moving the MP-mode masker along the electrode array from EL1 to EL16. Both probe and masker used a biphasic cathodic-leading, charge-balanced pulse. The phase duration (32 μs) was much shorter than that used in the pitch-ranking test (226 μs) to avoid prolonged stimulus artifacts. The interval between the probe and masker pulses was 500 μs so that the neurons recruited by the masker stayed in the refractory state and did not respond to the probe [61, 62]. For each pair of masker and probe, ECAP responses were averaged across 128 repeats with a repetition rate of 20 Hz. Ideally, ECAP recording should occur at MCL as in the pitch-ranking test. However, MCL could not be reached within the compliance limit of the CI for the steered pTP-mode probe, due to the much shorter phase duration (32 μs) and slower stimulation rate (20 Hz) than those in the pitch-ranking test (226 μs and 1000 Hz, respectively). To achieve sufficient loudness for ECAP recording, the compensation coefficient σ for the

steered pTP-mode probe (originally the same as in the pitch-ranking test) was reduced (Table 4.1) until the soft but comfortable level could be reached. In light of the poor loudness perception of the steered pTP-mode probe, the masker was presented in MP rather than pTP mode and at MCL rather than the soft but comfortable level. The growth of ECAP amplitude between the negative N1 and positive P2 peaks with increasing current levels for the probe $\mathrm{pTP}_{EL8,\alpha=0.5}$ was measured using the MP-mode masker on EL8. The ECAP growth function confirmed that the probe $\mathrm{pTP}_{EL8,\alpha=0.5}$ at the soft but comfortable level could generate reliable ECAP responses.

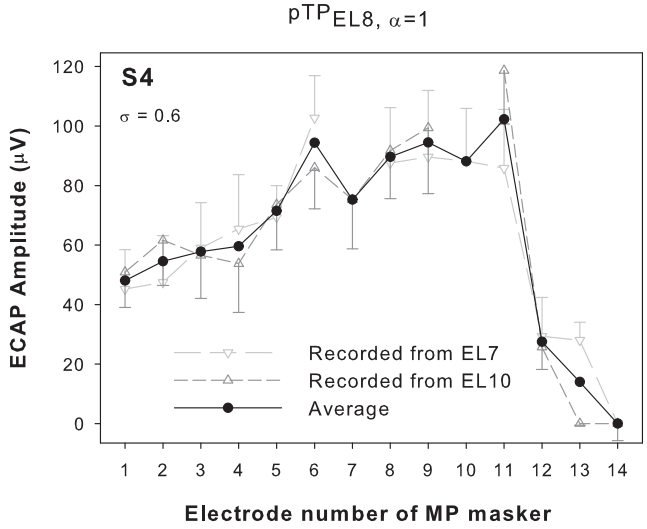

Fig. 4.2. The evoked compound action potential (ECAP) as a function of masker electrode for $\mathrm{pTP}_{EL8,\alpha=1}$ in S4. The ECAP spatial profile of probe $\mathrm{pTP}_{EL8,\alpha=1}$ is recorded from EL7 (downward triangles) and EL10 (upward triangles) and averaged (circles).

Fig. 4.2 shows the example ECAP spatial profiles (i.e., the N1-P2 amplitude of ECAP response as a function of masker electrode) for $\mathrm{pTP}_{EL8,\alpha=1}$ in S4. An apical and a basal recording electrode (e.g., EL7 and EL10 for $\mathrm{pTP}_{EL8,\alpha=1}$) adjacent to the stimulated electrodes of the steered pTP-mode probe (e.g., EL8 and EL9 for $\mathrm{pTP}_{EL8,\alpha=1}$) were both used for ECAP recording. Note that ECAP responses could not be recorded when the masker was on the recording electrode, due to amplifier saturation. As such, the ECAP spatial profile recorded from each recording elec-

trode had a missing data point on the recording electrode (e.g., the downward and upward triangles in Fig. 4.2 show the spatial profiles recorded from EL7 and EL10, respectively). Averaging the ECAP spatial profiles recorded from the two recording electrodes yielded a final ECAP spatial profile without missing data (e.g., the black circles in Fig. 4.2). The sampling rate of ECAP responses was 56 kHz and the gain was 300. The ECAP responses were processed with a band-pass smoothing filter from 400 to 6000 Hz and the ECAP amplitudes were set to zero if the estimated signal-to-noise ratio (SNR) was below 1.7 dB [63]. The error bars in Fig. 4.2 represent the 95% confidence intervals of the ECAP amplitudes.

The ECAP spatial profile of a MP-mode probe on EL8 (i.e., MP_{EL8}) at MCL was also measured using the same method as mentioned above. The ECAP spatial profiles of MP_{EL8} and $\mathrm{pTP}_{EL8,\alpha=0.5}$ were compared to see if the compensation coefficient σ used for ECAP recording narrowed the spread of excitation at the neural level.

4.2.5 PFM: Stimuli and Procedure

The excitation patterns of steered pTP stimuli at the psychophysical level were measured using a forward-masking technique [43] [64] [44]. In this technique, thresholds of probes along the electrode array are measured with or without a forward masker. The difference between the masked and unmasked probe thresholds (i.e., the masked threshold shift) indicates the channel interaction between the masker and probe. The probe threshold shift as a function of probe electrode may reflect the neural excitation pattern of the masker. The three maskers used in this study (i.e., $\mathrm{pTP}_{EL8,\alpha=0}$, $\mathrm{pTP}_{EL8,\alpha=0.5}$, and $\mathrm{pTP}_{EL8,\alpha=1}$ with the highest possible σ presented at MCL) were exactly the same stimuli as in the pitch-ranking test (section 4.2.2). The excitation pattern of a MP masker on EL8 was also of interest but not tested due to the time limitation. The probes were standard pTP stimuli on the main electrodes from EL3 to EL13 with σ fixed at 0.75 for all subjects except S1. The oldest subject S1 could only detect probes with a lower σ (0.65) in the presence of the maskers, pos-

sibly because she experienced slower psychophysical recovery and stronger masking from the maskers than younger subjects [65]. Both maskers and probes were 1000-Hz, biphasic (226 μs/phase), charge-balanced, cathodic-leading pulse trains. The probes were 20 ms while the maskers were 300 ms. The interval between masker and probe was 10 ms. All stimuli were presented using the BEDCS.

The unmasked probe threshold was measured using a three-interval, forced-choice (3IFC), 2-down/1-up adaptive procedure. In each trial, two intervals of silence and one interval containing the probe were presented in random order. The onsets of consecutive intervals were separated by 500 ms. The color of the corresponding button on a computer screen changed to indicate the presentation of each interval, especially those of silence or with sub-threshold levels. Subjects were allowed to repeat the stimuli before responding by clicking on the button corresponding to the interval with the probe. Visual feedback was provided. The probe level was adjusted based on subject response using a 20-μA step size in the first three intervals and a 5-μA step size thereafter. Each run stopped after 9 reversals, and the probe threshold was the average level across the last six reversals.

The masked probe threshold was also measured using the same 3IFC, 2-down/1-up adaptive procedure, except that in each trial, two intervals of the masker only and one interval of the masker followed by the probe were presented in random order.

4.2.6 Data Analysis

The measured spatial profile of each stimulus at each level (EFI, ECAP, and PFM) for each subject was normalized to its peak amplitude to better compare the relative shape of excitation pattern across α values and measurement levels. Fig. 4.3 shows an example of the normalized ECAP pattern of $\mathrm{pTP}_{EL8,\alpha=0.5}$ for S3R. The long and short dashed lines represent the normalized values of 0.95 and 0.75, respectively. The peak location of each normalized pattern was defined as the median location of the electrodes with normalized values greater than 0.95. For the example in Fig. 4.3, the

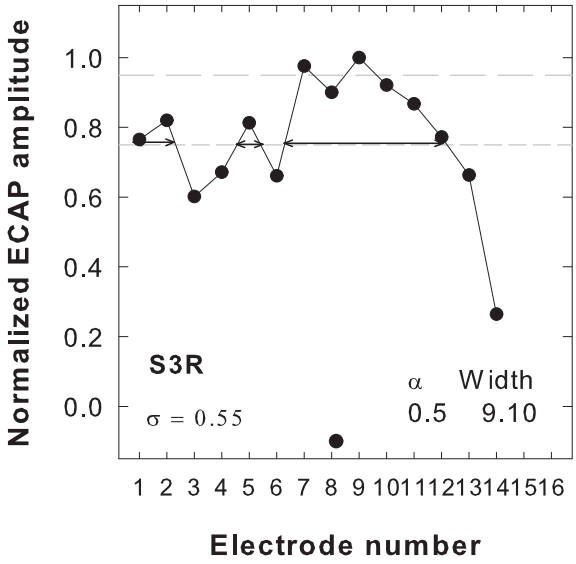

Fig. 4.3. An example of the normalized ECAP pattern for $\text{pTP}_{EL8,\alpha=0.5}$ for S3R (connected circles). The centroid of the ECAP pattern (unconnected circle) is plotted near the x-axis. The width at 75% peak amplitude (i.e., the total width of the horizontal double-arrow lines) is also listed (9.10 in units of electrode spacings).

normalized values of EL7 and EL9 both exceed 0.95, and their median location (i.e., EL8) was taken as the peak location of the ECAP pattern. As in Chapter 3, the center of gravity or the centroid of each normalized pattern was calculated as follows:

$$Centroid = \frac{\sum_k k \times |SP(k)|}{\sum_k |SP(k)|} \tag{4.1}$$

where k indicates the electrode number and $SP(k)$ is the normalized value at electrode k. In Fig. 4.3, the centroid of the ECAP pattern was 8.16 in the unit of electrode number, as indicated by the circle near the x-axis. The width at 75% of the peak amplitude was also calculated to characterize the degree of focusing for each normalized pattern. For the example in Fig. 4.3, the width of the ECAP pattern was the total width of the horizontal double-arrow lines and was 9.10 in the unit of electrode spacing.

4.3 Results

4.3.1 EFI Patterns

MP vs. standard pTP stimulation

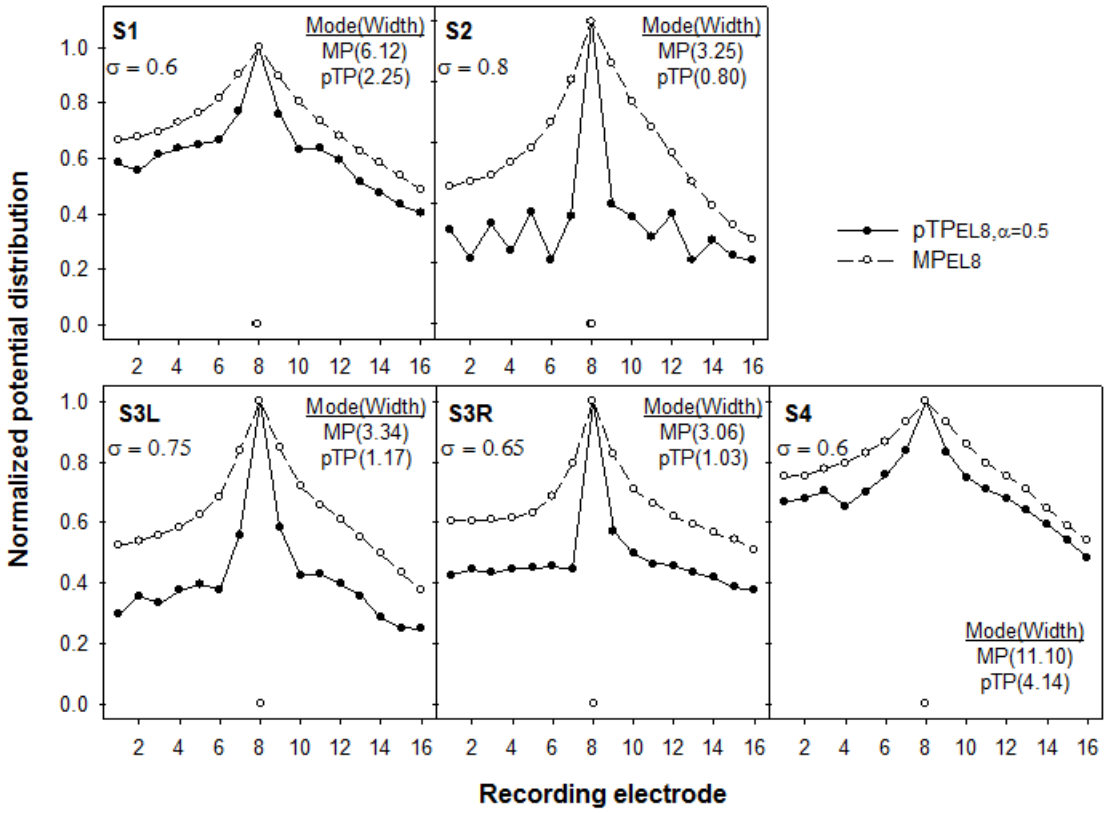

Fig. 4.4. The normalized EFI patterns as a function of recording electrode for the MP (open circles) and standard pTP stimuli (filled circles) on EL8

Fig. 4.4 shows the normalized EFI patterns as a function of recording electrode for the MP (open circles) and standard pTP stimuli (filled circles) on EL8 for each subject. The original un-normalized electrical potentials generated by the MP stimulation (ranging from 20 to 100 mV) were much higher than those generated by the standard pTP stimulation (ranging from 8 to 45 mV). The electrical fields of both the MP and standard pTP stimuli had a single sharp peak on EL8. The centroid of

the EFI pattern (as indicated by the circles near the x-axis) was also around EL8 for both stimuli. The potentials fell off more quickly on both sides of the peak, suggesting less current spread beyond the activated electrodes, for the standard pTP stimulation than for the MP stimulation. The width at 75% of the peak amplitude of the EFI pattern (as shown in parenthesis in the unit of electrode spacing) was significantly narrower for the standard pTP stimulation than for the MP stimulation (paired t-test: $t4 = 3.78, p = 0.02$). Although several modeling studies [30, 32] suggested that larger σ for pTP stimulation may lead to more focused or narrower excitation patterns, no correlation ($r = -0.73, p = 0.16$) was found between the width of the EFI pattern and σ across subjects, possibly because the statistical power (0.26) was limited by the small number of subjects.

Steered pTP stimuli

Fig. 4.5 shows the normalized EFI patterns as a function of recording electrode for $\text{pTP}_{EL8,\alpha=0}$, $\text{pTP}_{EL8,\alpha=0.5}$, and $\text{pTP}_{EL8,\alpha=1}$ for each subject. The original un-normalized electrical potentials on EL8 (i.e., the peak amplitudes of the un-normalized EFI patterns) were similar for the three steered pTP stimuli within each subject, but varied from 15 to 38 mV across subjects. It is possible that different subjects may have different cochlear conditions (e.g., fibrous tissues and bone growth), which may affect current conduction during electrical CI stimulation. The standard $\text{pTP}_{EL8,\alpha=0.5}$ stimulation returned the same amount of current to both flanking electrodes and thus generated roughly symmetric EFI patterns with a similar suppression of current spread on both sides of EL8 (circles). The $\text{pTP}_{EL8,\alpha=0}$ stimulation applied the intracochlear return current completely to the apical flanking electrode EL7 and thus the electrical potentials were strongly reduced on the apical side (i.e., EL1–EL7) but not on the basal side (i.e., EL9–EL16) (upward triangles). For S2, S3L, and S3R, the large amount of current returned to EL7 (due to the high σ values) even caused a strong dip of the EFI pattern on EL7. In contrast, the $\text{pTP}_{EL8,\alpha=1}$ stimulation

generated reversed EFI patterns, which were strongly attenuated on the basal side (i.e., EL9–EL16) but not on the apical side (i.e., EL1–EL7) (downward triangles).

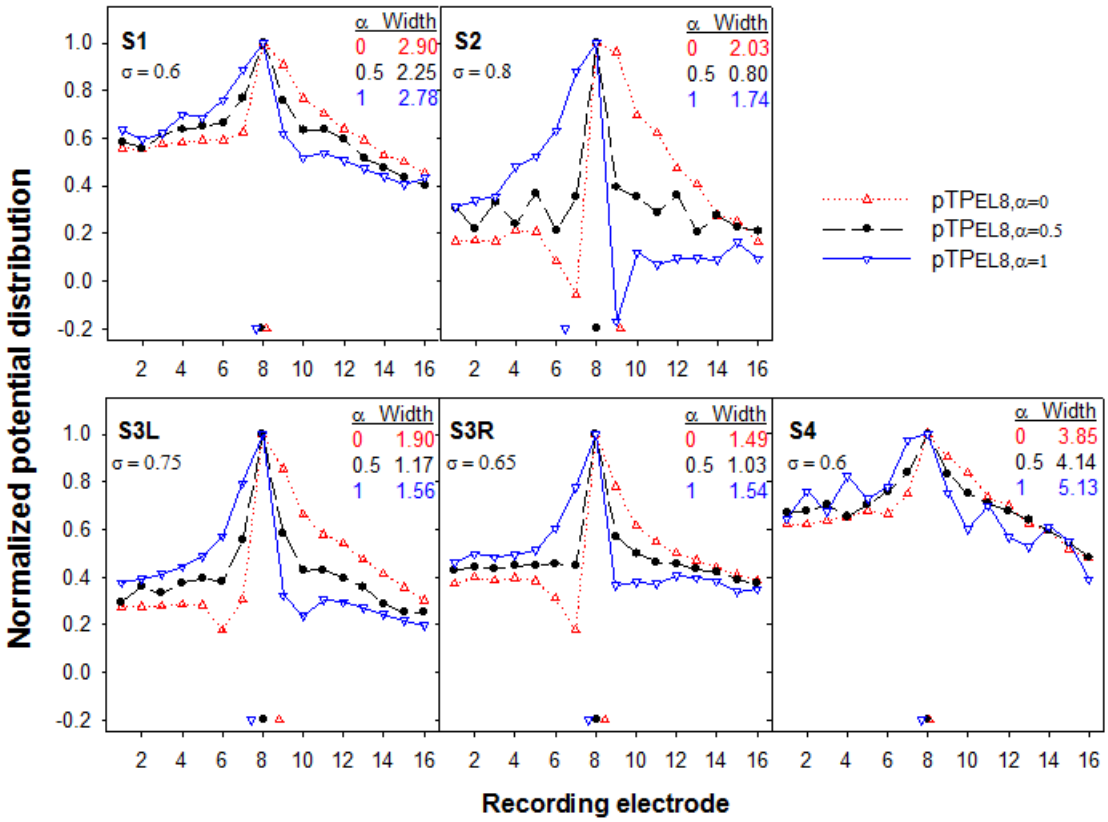

Fig. 4.5. The normalized EFI patterns as a function of recording electrode for $\mathrm{pTP}_{EL8,\alpha=0}$ (upward triangles), $\mathrm{pTP}_{EL8,\alpha=0.5}$ (circles), and $\mathrm{pTP}_{EL8,\alpha=1}$ (downward triangles).

On average, the centroid of the EFI pattern shifted apically as α increased ($\mathrm{pTP}_{EL8,\alpha=0}$: 8.55, $\mathrm{pTP}_{EL8,\alpha=0.5}$: 8.00, and $\mathrm{pTP}_{EL8,\alpha=1}$: 7.37, as shown by the corresponding symbols near the x-axis). A one-way repeated-measures (RM) analysis of variance (ANOVA) showed a significant effect of α value on the location of the EFI centroid ($F_{2,8} = 7.59, p = 0.01$). Post-hoc pair-wise comparisons using the Holm-Sidak method showed that the centroid locations were significantly different between $\mathrm{pTP}_{EL8,\alpha=0}$ and $\mathrm{pTP}_{EL8,\alpha=1}$ (p = 0.01), but not between $\mathrm{pTP}_{EL8,\alpha=0}$ and $\mathrm{pTP}_{EL8,\alpha=0.5}$ ($p = 0.11$) or between $\mathrm{pTP}_{EL8,\alpha=0.5}$ and $\mathrm{pTP}_{EL8,\alpha=1}$ ($p = 0.14$). The width at 75% of the peak

amplitude of the EFI pattern was narrower for $\text{pTP}_{EL8,\alpha=0.5}$ than for $\text{pTP}_{EL8,\alpha=0}$ and $\text{pTP}_{EL8,\alpha=1}$ (on average, 1.88, 2.44, and 2.56 in the unit of electrode spacing, respectively). A one-way RM ANOVA showed that the effect of α value on the width of the EFI pattern was of borderline significance ($F_{2,8} = 4.74, p = 0.04$). Post-hoc pair-wise comparisons showed that there was no significant difference in the width between any pair of the steered pTP stimuli, although the width difference between $\text{pTP}_{EL8,\alpha=0.5}$ and $\text{pTP}_{EL8,\alpha=1}$ just missed significance ($p = 0.06$).

4.3.2 ECAP Patterns

MP vs. standard pTP stimulation

Fig. 4.6 shows the normalized ECAP patterns as a function of masker electrode for the MP (open circles) and standard pTP probes (filled circles) on EL8 for each subject. The original un-normalized ECAP amplitudes were consistently larger for the MP probe (e.g., 150-180 μV with the masker on EL8) than for the standard pTP probe (e.g., 70-130 μV with the masker on EL8). This may be because the pTP probe had a lower loudness level (soft but comfortable) than the MP probe (most comfortable). The smaller neural population recruited by the more focused pTP probe may also result in less probabilistic response characteristics [66] and thus weaker neural responses. S2 had much larger un-normalized ECAP amplitudes than the other subjects, possibly because more neurons were survived for S2 with a younger age and a shorter duration of profound deafness following meningitis. For the bilateral CI user S3, the ECAP responses of her first implant (S3R) were stronger with higher SNRs than those of her second implant (S3L), which may also be attributed to the better neural survival with a shorter duration of deafness [67] in her first implanted ear.

The normalized ECAP patterns of the MP and pTP probes were similar to each other, both showing a broad peak around EL8 and decreasing more rapidly on the basal side than on the apical side of the peak. The calculated peak location of the

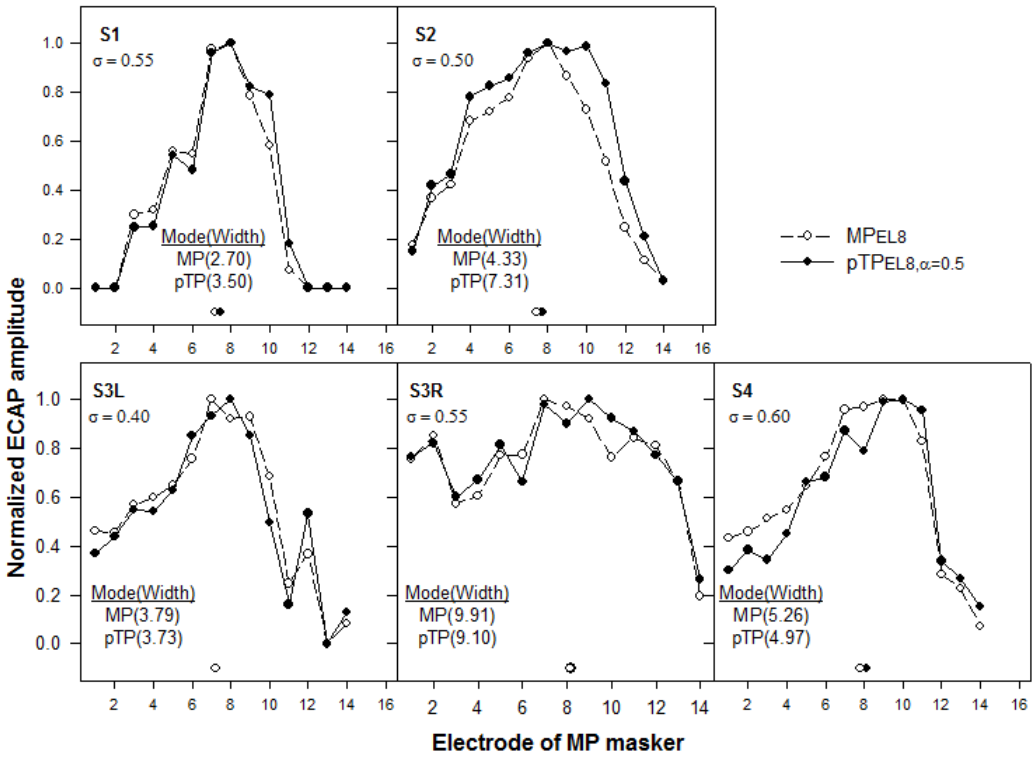

Fig. 4.6. The normalized ECAP patterns as a function of recording electrode for the MP (open circles) and standard pTP stimuli (filled circles) on EL8.

ECAP pattern was on average 7.7 for the MP probe and 8.4 for the pTP probe. This difference in the peak location, although approaching statistical significance (paired t-test: $t4 = -2.75, p = 0.05$), was difficult to interpret due to the lack of a prominent peak in both the MP and pTP ECAP patterns. Plotted near the x-axis, the centroid of the ECAP pattern was on average 7.42 for the MP probe and 7.72 for the pTP probe. Because the normality assumption was not met, the ECAP centroids of the MP and pTP probes were compared using a Wilcoxon signed ranked test, which showed that the centroid locations were not significantly different ($Z = 1.75, p = 0.13$). The width at 75% of the peak amplitude of the ECAP pattern was also not significantly different between the pTP and MP probes (on average, 5.72 and 5.20 in the unit of electrode spacing, respectively) (paired t-test: $t4 = -0.79, p = 0.47$).

Steered pTP stimuli

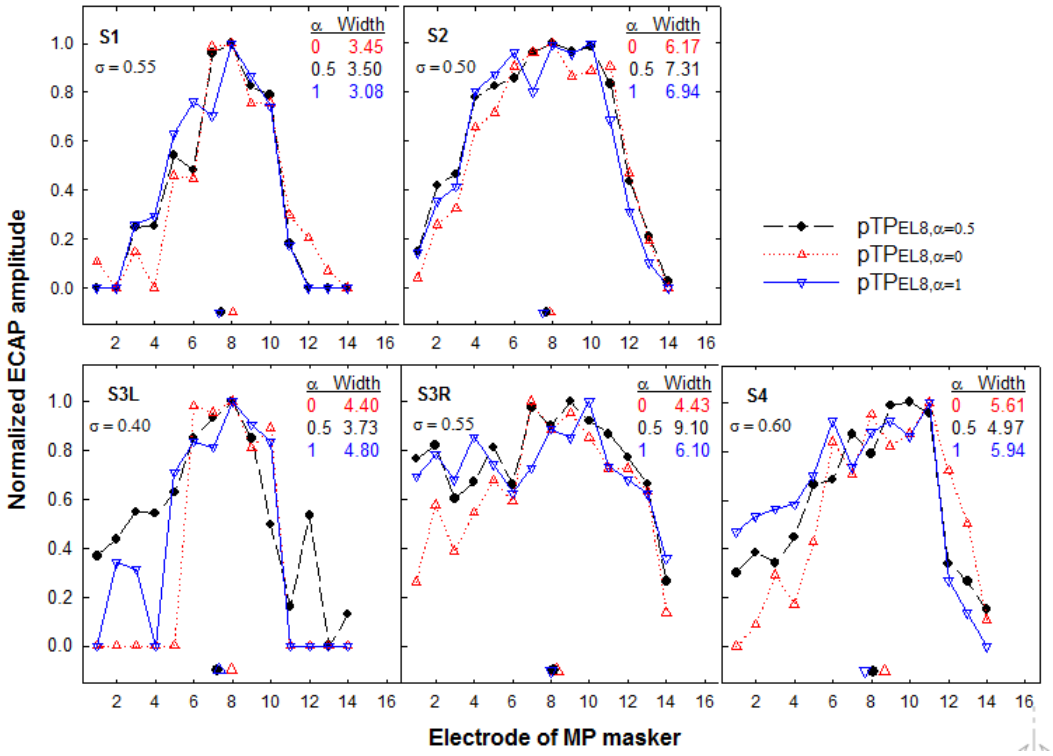

Fig. 4.7. The normalized ECAP patterns as a function of recording electrode for $\text{pTP}_{EL8,\alpha=0}$ (upward triangles), $\text{pTP}_{EL8,\alpha=0.5}$ (circles), and $\text{pTP}_{EL8,\alpha=1}$ (downward triangles).

Fig. 4.7 shows the normalized ECAP patterns for the probes $\text{pTP}_{EL8,\alpha=0}$ (upward triangles), $\text{pTP}_{EL8,\alpha=0.5}$ (circles), and $\text{pTP}_{EL8,\alpha=1}$ (downward triangles) as a function of masker electrode for each subject. The weak neural responses of focused pTP stimuli were prone to the influence of electrical stimulation artifacts during ECAP recording. The low SNRs in ECAP recording might lead to irregular changes (e.g., those on the apical electrodes of S3R) or zero values of the ECAP amplitudes (e.g., those on the apical/basal electrodes of S3L). For subjects with higher σ values (e.g., S4, S1, and S3R), there was a trend that, as α increased, the normalized ECAP amplitudes slightly increased on the apical side of EL8 but decreased on the basal side of EL8. Contrary to our prediction, on average, the estimated peak location

of the ECAP pattern shifted from apex to base as α increased ($\text{pTP}_{EL8,\alpha=0}$: 7.9, $\text{pTP}_{EL8,\alpha=0.5}$: 8.4, and $\text{pTP}_{EL8,\alpha=1}$: 9.1). A one-way RM ANOVA showed a significant effect of α value on the ECAP peak location ($F_{2,8} = 8.55, p = 0.01$). Post-hoc pair-wise comparisons using the Holm-Sidak method showed that the estimated peak for $\text{pTP}_{EL8,\alpha=1}$ was significantly more basal to that for $\text{pTP}_{EL8,\alpha=0}$ ($p = 0.01$). Again, the lack of a prominent peak in the ECAP patterns made it difficult to interpret these results. The centroid of the ECAP pattern was also estimated for each steered pTP probe (as shown by the corresponding symbol near the x-axis). On average, the centroid of the ECAP pattern shifted from base to apex as α increased ($\text{pTP}_{EL8,\alpha=0}$: 8.07, $\text{pTP}_{EL8,\alpha=0.5}$: 7.72, and $\text{pTP}_{EL8,\alpha=1}$: 7.51). The centroid and peak of the ECAP pattern shifted in the opposite directions with α. Due to the violation of the normality assumption, a Friedman RM ANOVA on ranks was used to analyze the ECAP centroids and showed a significant effect of α value ($\chi^2 = 8.40, p = 0.01$). Post-hoc pair-wise comparisons using the Tukey method showed that the location of the ECAP centroid was significantly more basal for $\text{pTP}_{EL8,\alpha=0}$ than for $\text{pTP}_{EL8,\alpha=1}$ ($p < 0.05$), but was not significantly different between any other pair of the steered pTP stimuli. The width at 75% of the peak amplitude of the ECAP pattern did not significantly change with α (on average, $\text{pTP}_{EL8,\alpha=0.5}$: 5.72, $\text{pTP}_{EL8,\alpha=0}$: 4.81, and $\text{pTP}_{EL8,\alpha=1}$: 5.37 in the unit of electrode spacing) (one-way RM ANOVA: $F_{2,8} = 0.77, p = 0.49$).

4.3.3 PFM Patterns

Fig. 4.8 shows the normalized threshold shift of pTP probe (calculated as the dB difference between the masked and unmasked probe thresholds) with the forward masker $\text{pTP}_{EL8,\alpha=0}$ (upward triangles), $\text{pTP}_{EL8,\alpha=0.5}$ (circles), and $\text{pTP}_{EL8,\alpha=1}$ (downward triangles) as a function of probe electrode for each subject. The normalized PFM patterns mostly had a single peak and decreased monotonically towards the apex and base when the probe moved away from the masker. For all subjects, the PFM patterns

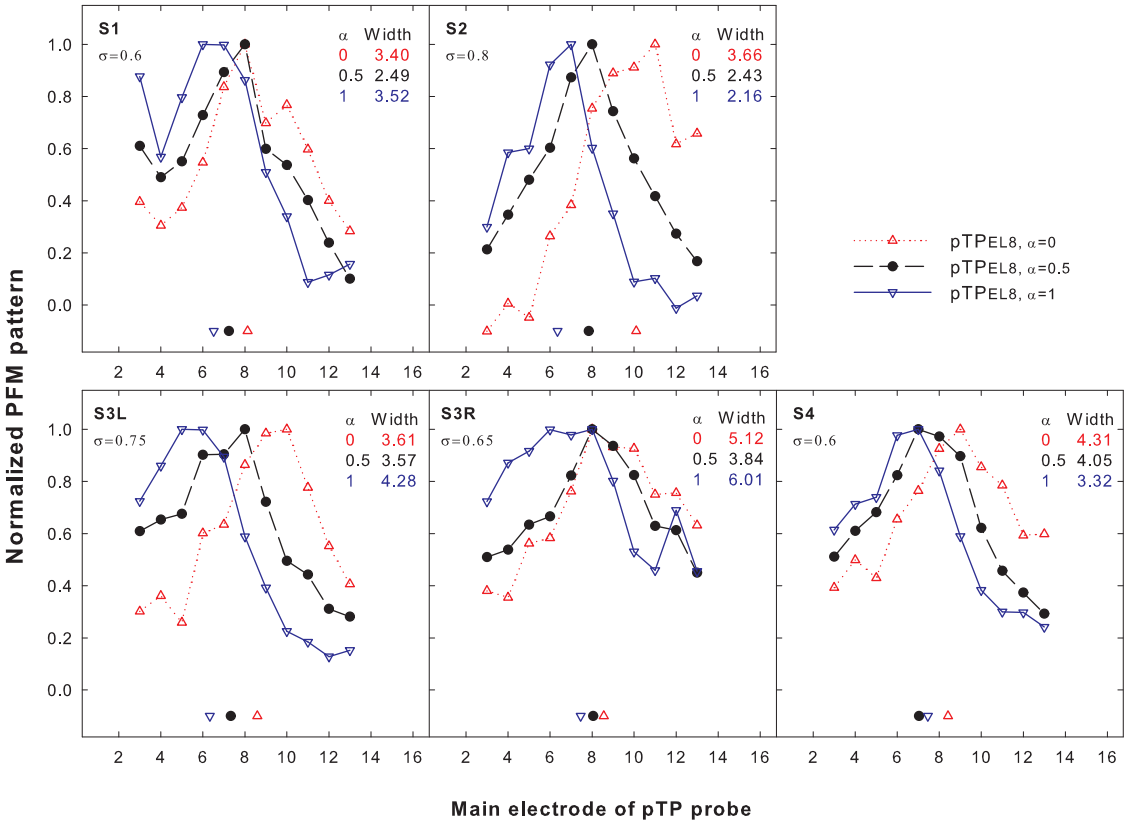

Fig. 4.8. The normalized PFM patterns as a function of recording electrode for $\text{pTP}_{EL8,\alpha=0}$ (upward triangles), $\text{pTP}_{EL8,\alpha=0.5}$ (circles), and $\text{pTP}_{EL8,\alpha=1}$ (downward triangles).

gradually shifted from base to apex as α increased. Although the steered pTP maskers had the same main electrode EL8, current steering between flanking electrodes shifted the peak of the PFM pattern for all subjects except S3R. The estimated peak location of the PFM pattern was on average 9.1, 7.9, and 6.5 for $\text{pTP}_{EL8,\alpha=0}$, $\text{pTP}_{EL8,\alpha=0.5}$, and $\text{pTP}_{EL8,\alpha=1}$, respectively. A one-way RM ANOVA showed a significant effect of α value on the PFM peak location ($F_{2,8} = 12.94, p = 0.003$). Post-hoc pair-wise comparisons using the Holm-Sidak method showed that the PFM peak locations were significantly different between any pair of the steered pTP maskers ($p < 0.05$). The centroid of each PFM pattern was shown by the corresponding symbol near the x-axis. On

average, the PFM centroid also shifted from base to apex as α increased ($\text{pTP}_{EL8,\alpha=0}$: 8.76, $\text{pTP}_{EL8,\alpha=0.5}$: 7.60, and $\text{pTP}_{EL8,\alpha=1}$: 6.74). A one-way RM ANOVA showed a significant effect of α value on the PFM centroid location ($F_{2,8} = 17.92, p = 0.001$). Post-hoc pair-wise comparisons using the Holm-Sidak method showed significantly different PFM centroid locations between $\text{pTP}_{EL8,\alpha=0}$ and $\text{pTP}_{EL8,\alpha=0.5}$ ($p = 0.02$) and between $\text{pTP}_{EL8,\alpha=0.5}$ and $\text{pTP}_{EL8,\alpha=1}$ (p = 0.03). The width at 75% of the peak amplitude of the PFM pattern was on average 3.28, 3.86, and 4.02 in the unit of electrode spacing for $\text{pTP}_{EL8,\alpha=0.5}$, $\text{pTP}_{EL8,\alpha=1}$, and $\text{pTP}_{EL8,\alpha=0}$, respectively. No significant effect of α value was found on the PFM width (one-way RM ANOVA: $F_{2,8} = 1.70, p = 0.24$).

4.3.4 Comparisons across Measurement Levels

Fig. 4.9 shows the peak, centroid, and width of the EFI, ECAP, and PFM patterns as a function of α for the steered pTP stimuli. To investigate how the excitation patterns of the steered pTP stimuli varied at the physical, neural, and perceptual levels, the pattern features (peak, centroid, and width) were analyzed by separate two-way RM ANOVAs with α value and measurement level as the two factors, followed by the Holm-Sidak post-hoc t-tests.

For the excitation peak, there were no significant effects of α value ($F_{2,16} = 2.83, p = 0.12$) and measurement level ($F_{2,16} = 1.21, p = 0.35$), but the interaction between the two factors was significant ($F_{4,16} = 16.39, p < 0.001$). The significant interaction reflected the fact that the EFI peak did not move, while the ECAP and PFM peaks moved in the opposite directions with increasing α (as described in previous sections). Post-hoc t-tests showed that the peak locations of $\text{pTP}_{EL8,\alpha=0}$ and $\text{pTP}_{EL8,\alpha=0.5}$ did not vary across different measurement levels, while that of $\text{pTP}_{EL8,\alpha=1}$ was significantly different between any two measurement levels ($p < 0.05$).

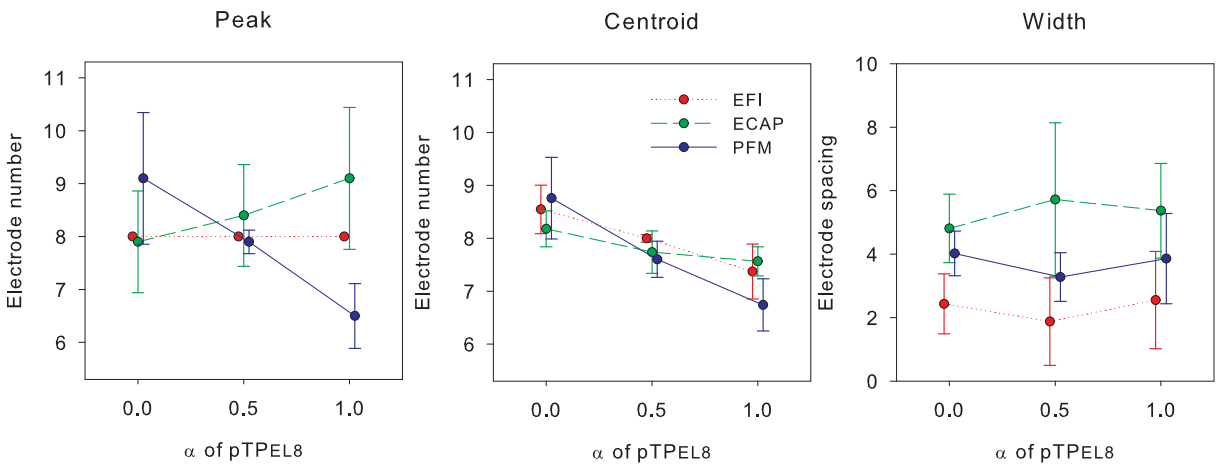

Fig. 4.9. The peak, centroid, and width of the EFI, ECAP, and PFM patterns as a function of α for the steered pTP stimuli.

For the excitation centroid, there was no significant effect of measurement level ($F_{2,16} = 1.51, p = 0.28$). However, the effect of α value ($F_{2,16} = 20.96, p < 0.001$) and the interaction between α value and measurement level ($F_{4,16} = 5.04, p = 0.008$) were both significant. The significant interaction was driven by greater shifts of the PFM centroid than the EFI and ECAP centroids with increasing α as described in previous sections. Post-hoc t-tests showed that the centroid locations of $\text{pTP}_{EL8,\alpha=0}$ and $\text{pTP}_{EL8,\alpha=0.5}$ did not vary across different measurement levels, while the excitation centroid of $\text{pTP}_{EL8,\alpha=1}$ was significantly more apical at the perceptual level (measured by PFM) than at the physical or neural level (measured by EFI or ECAP) ($p < 0.03$).

The width of the excitation pattern was similar with different α values but varied across measurement levels (i.e., in the descending order: ECAP, PFM, and EFI widths). There was a significant effect of measurement level ($F_{2,16} = 7.14, p = 0.02$), but not of α value ($F_{2,16} = 0.96, p = 0.42$) or their interaction ($F_{4,16} = 1.33, p = 0.30$). Post-hoc t-tests showed that the width was significantly different between the ECAP

and EFI patterns (p = 0.02), but was similar between the ECAP and PFM patterns or between the PFM and EFI patterns ($p > 0.11$).

4.3.5 Correlation between Pitch Sensitivity and Excitation Pattern Shift

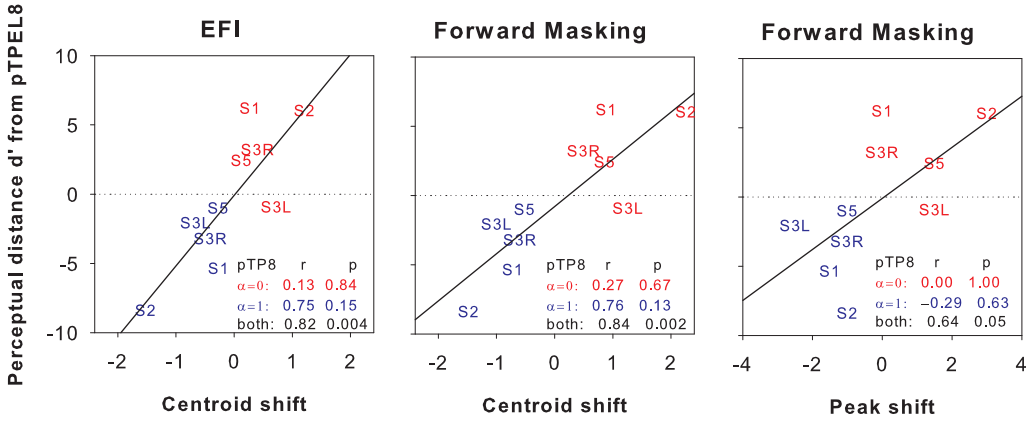

Fig. 4.10. The cumulative d' from $\text{pTP}_{EL8,\alpha=0.5}$ to $\text{pTP}_{EL8,\alpha=0}$ (in red) and from $\text{pTP}_{EL8,\alpha=0.5}$ to $\text{pTP}_{EL8,\alpha=1}$ (in blue) as a function of their corresponding centroid shifts at the physical (left panel) and perceptual levels (middle panel), and peak shifts at the perceptual level (right panel)

The cumulative d' of pitch ranking from $\text{pTP}_{EL8,\alpha=0.5}$ to $\text{pTP}_{EL8,\alpha=0}$ or from $\text{pTP}_{EL8,\alpha=0.5}$ to $\text{pTP}_{EL8,\alpha=1}$ was listed in Table 1. The cumulative d' values were usually positive from $\text{pTP}_{EL8,\alpha=0.5}$ to $\text{pTP}_{EL8,\alpha=0}$ and negative from $\text{pTP}_{EL8,\alpha=0.5}$ to $\text{pTP}_{EL8,\alpha=1}$. That means $\text{pTP}_{EL8,\alpha=0}$ was generally higher in pitch than $\text{pTP}_{EL8,\alpha=0.5}$, while $\text{pTP}_{EL8,\alpha=1}$ was lower in pitch than $\text{pTP}_{EL8,\alpha=0.5}$. This pitch lowering from $\alpha = 0$ to $\alpha = 0.5$ and then to $\alpha = 1$ was consistent with the significant apical shifts of the EFI and PFM centroids, as well as the PFM peak (as summarized in previous sections). Fig. 4.10 shows the cumulative d' from $\text{pTP}_{EL8,\alpha=0.5}$ to $\text{pTP}_{EL8,\alpha=0}$ (in red) and from $\text{pTP}_{EL8,\alpha=0.5}$ to $\text{pTP}_{EL8,\alpha=1}$ (in blue) as a function of their corresponding centroid shifts at the physical (left panel) and perceptual levels (middle panel), and peak shifts at the perceptual level (right panel). Apical shifts were represented

as negative values, while basal shifts as positive values. Across subjects, the pitch-ranking sensitivity from $\text{pTP}_{EL8,\alpha=0.5}$ to either $\text{pTP}_{EL8,\alpha=0}$ or $\text{pTP}_{EL8,\alpha=1}$ was not correlated with the amount of displacement of the excitation pattern, as quantified by the shift of the EFI centroid, PFM centroid, or PFM peak. This suggests that the inter-subject variability in pitch-ranking sensitivity with either increasing or decreasing α cannot be predicted by the measures of excitation pattern shift. When the data for both $\text{pTP}_{EL8,\alpha=0}$ and $\text{pTP}_{EL8,\alpha=1}$ were included in the correlation analysis, the pitch-ranking sensitivity was significantly correlated with the shifts of the EFI and PFM centroids, and marginally correlated with the shift of the PFM peak. These correlations, however, were driven by the distribution of the data for $\text{pTP}_{EL8,\alpha=0}$ and $\text{pTP}_{EL8,\alpha=1}$ in the upper-right and lower-left quadrants, respectively.

4.4 Discussion

This study investigated the excitation pattern changes with steered pTP stimuli at the physical (measured with EFI), neural (measured with ECAP), and perceptual levels (measured with PFM). Steered pTP stimuli shifted the excitation centroid from base to apex with increasing α at all measurement levels, consistent with the lowering of pitch observed in the pitch-ranking test. Similar peak shifts were only observed for the PFM patterns at the perceptual level. However, the shift of excitation centroid or peak was not correlated with the pitch-ranking sensitivity across subjects. The excitation patterns were similarly wide with different α values, but were wider at the neural level than at the physical and perceptual levels, most likely due to the smaller σ values used for ECAP recording than for EFI and PFM measurements. These results provided insights into the efficacy of electrical field shaping techniques on the excitation patterns along the auditory pathway.

4.4.1 Current focusing with standard pTP stimulation

In this study, the electrical field generated by $\text{pTP}_{EL8,\alpha=0.5}$ was significantly more restricted than that of MP_{EL8}, consistent with previous results in animal or human studies (e.g., [15,49]). For example, Berenstein [49] also found a significantly reduced EFI width as long as the σ of pTP stimulation was greater than 0.5. However, the effect of current focusing was not observed at the neural level in this study, where $\text{pTP}_{EL8,\alpha=0.5}$ generated a similarly wide ECAP pattern as MP_{EL8}. Note that the ECAP recording used a smaller σ (i.e., 0.4–0.6 for different subjects) than the EFI recording (i.e., 0.6–0.8 for different subjects) to obtain reliable neural responses. The σ used for ECAP recording may not be high enough to effectively narrow the spread of neural excitation. Zhu [51] found that the ECAP pattern of full TP stimulation with $\sigma = 1$ was significantly narrower than that of MP stimulation, although the measured MP and full TP patterns were both irregular with multiple peaks. In our pilot study, the 226-μs phase duration and the highest possible σ of 1 used by Zhu [51] produced weak ECAP responses masked by prolonged electrical stimulation artifacts and thus the difficulty of identifying the N1 and P2 peaks in the ECAP responses greatly increased. This partially explained the irregular ECAP patterns in Zhu [51] and motivated us to use a smaller σ and shorter phase duration for ECAP recording. The inferior colliculus responses recorded from guinea pigs [32] and the PFM patterns measured in human subjects [20] both suggest that σ needs to be greater than 0.75 to generate significantly narrower pTP excitation patterns than MP excitation patterns. In this study, the PFM pattern of MP stimulation was not measured due to the time limitation and thus the effect of current focusing for the experimental pTP stimuli could not be confirmed at the perceptual level.

4.4.2 Current steering with steered pTP stimuli

The effect of pTP-mode current steering on the excitation pattern was different at different measurement levels. At the physical level, the peak of the EFI pattern

did not move while the EFI centroid shifted apically with increasing α. The effects resulted from the linear summation of the electrical fields of involved electrodes (i.e., EL7, EL8, and EL9) in the steered pTP stimuli. As α increased, the negative electrical field of the basal return electrode EL9 (downward triangles in Fig. 4.5) increased while that of the apical return electrode EL7 (upward triangles in Fig. 4.5) decreased. Thus, the electrical field of the main electrode EL8 (circles in Fig. 4.5) had more reduction on the basal side than on the apical side, resulting in apically shifted EFI centroids. However, the peak electrical potential remained on EL8 after the linear summation of the electrical fields. Different subjects had different shifts of the EFI centroid from $\alpha = 0.5$ to $\alpha = 0$ or 1, which can be attributed to the subject-specific σ values (or the total amounts of current steered between the two flanking electrodes), as shown by the significant Pearson correlations between σ and EFI centroid shift ($r = 0.97$, $p = 0.006$ for $\alpha = 0$; $r = 0.91$, $p = 0.03$ for $\alpha = 1$). At the neural level, the peak of the ECAP pattern slightly shifted to the base while the ECAP centroid significantly shifted to the apex with increasing α. When α was 0 or 1, relatively high ECAP amplitudes were observed around the single return electrode (i.e., EL7 for $\alpha = 0$ and EL9 for $\alpha = 1$), although it was unlikely to have side-lobe effects (e.g., [31]) with the small σ values used for ECAP recording. For the electrodes that were further away from the main and return electrodes, the ECAP amplitudes were instead lower on the side of the single return electrode than on the other side. This caused the ECAP centroid to shift in the opposite direction as the ECAP peak with increasing α. Compared to the EFI and PFM centroids, the ECAP centroid shifted in the same direction but to a lesser degree as α increased. This may be because the smaller σ values used for ECAP recording limited the amount of current steered between the flanking electrodes and reduced the effect of pTP-mode current steering at the neural level. Across subjects, the small σ value was not correlated with the generally small amount of ECAP centroid shift from $\alpha = 0.5$ to $\alpha = 0$ or 1 ($r = 0.20$, $p = 0.75$ and $r = 0.73$, $p = 0.16$, respectively). At the perceptual level, both the PFM peak and centroid significantly shifted from base to apex as α increased. Several studies

have recently measured the psychophysical spatial tuning curves and PFM patterns for (partial or full) BP and TP stimuli (e.g., [20, 51, 54]). For these relatively focused stimuli, shifted and split tips of spatial tuning and peaks of forward masking have been reported and attributed to possible dead region or poor neural survival around the tested electrode (see [51] for a schematic illustration). However, in this study, the PFM pattern of the standard $\text{pTP}_{EL8,\alpha=0.5}$ showed a single peak on the main electrode EL8, suggesting that a dead region was unlikely to exist around EL8 for our subjects. The significant peak shifts of $\text{pTP}_{EL8,\alpha=0}$ and $\text{pTP}_{EL8,\alpha=1}$ relative to $\text{pTP}_{EL8,\alpha=0.5}$ only occurred at the perceptual level (measured by PFM) but not at the physical or neural level (measured by EFI or ECAP), and thus may have resulted from central processing beyond the electrode-neuron interface. A psychophysical mechanism that may account for the PFM peak shifts is the off-electrode listening in electric hearing ([68]), analogous to the off-frequency listening in acoustic hearing [69]. For $\text{pTP}_{EL8,\alpha=0}$ and $\text{pTP}_{EL8,\alpha=1}$, the largest amount of masking was not found on EL8 where the peak electrical potential was located (Fig. 4.8), suggesting that subjects may have attended to the responses of neurons far from EL8 for the detection of the probe. The largest amount of masking and the minimum contribution of off-electrode listening may be found around the geometric center rather than the peak of the EFI pattern. On the other hand, the apical shift of the excitation centroid with increasing α was consistently preserved from the physical level to the perceptual level along the auditory pathway of CI processing and was the greatest at the perceptual level. Again, central processing such as the off-electrode listening may have exaggerated the effect of pTP-mode current steering on the PFM centroid. Similar to the EFI centroid shift, the PFM centroid shift also had borderline or significant Pearson correlations with the σ value across subjects ($r = 0.84$, $p = 0.08$ for $\alpha = 0$; $r = 0.92$, $p = 0.03$ for $\alpha = 1$).

5. ELECTRODE SPANNING WITH PARTIAL TRIPOLAR STIMULATION MODE IN COCHLEAR IMPLANTS

5.1 Introduction

To increase the number of spectral channels with focused excitation patterns, Chapter 3 proposed to incorporate current steering into pTP mode (Fig. 5.1a) by varying the proportions of current returned to the basal and apical adjacent electrodes (α and 1-α, respectively). Subjects generally perceived a lowering of pitch as the steering coefficient α increased from 0 to 1, which was consistent with the apical shifts of centroid of neural excitation pattern in a computational model [30]. However, the pitch-ranking results of pTP-mode current steering varied across subjects, with one out of six subjects exhibiting pitch reversals. Similar pitch reversals were also seen in phantom electrode or partial BP (pBP) stimuli with an increasing amount of current returned to the basal adjacent electrode alone [24]. For those who are less sensitive to the pitch changes caused by the different distributions of return current, alternative ways to create additional spectral channels in pTP mode may be necessary.

This study tested if moving the apical or basal return electrode away from the main electrode in pTP mode (i.e., apical or basal electrode spanning; Fig. 5.1b and 5.1c, respectively, with $\alpha = 0.5$) may also elicit distinctive pitch percepts and create additional spectral channels. The asymmetrically spanned pTP stimuli can be viewed as quadrupolar virtual channel (QPVC) stimuli [42] with only a single activated main electrode. QPVCs generally stimulate four adjacent electrodes at the same time, using two middle electrodes as the main electrodes for current steering and two outer electrodes as the return electrodes for current focusing. QPVCs have been shown to reduce current spread and improve pitch discrimination in either a single- or multi-channel context more than MP virtual channels [42] [45] [70]. The increased

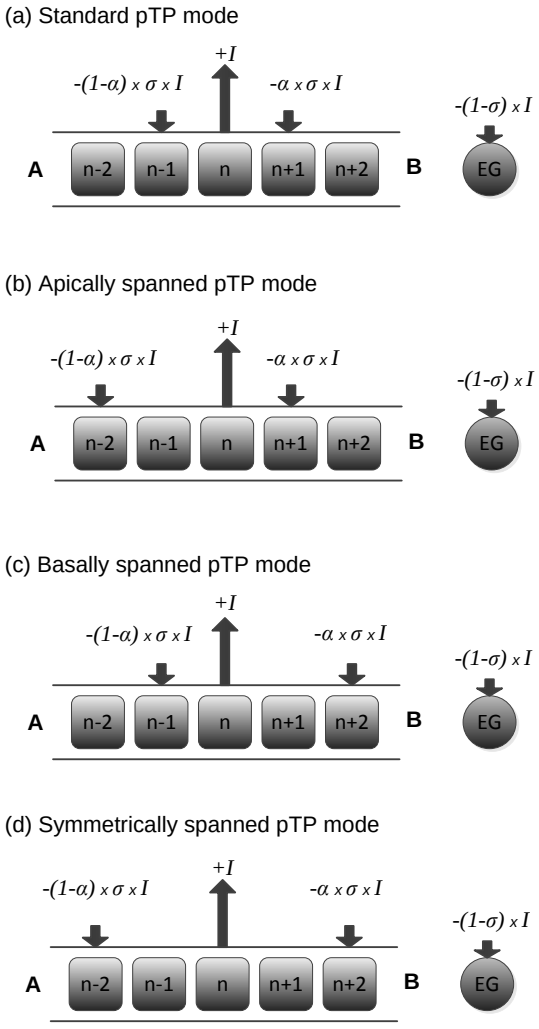

Fig. 5.1. Schematic illustration of various partial tripolar (pTP) stimulation modes with a fixed current level I on the main electrode ELn. A fraction of the current ($\sigma \times I$) is split and returned to two intracochlear electrodes with varying ratios (α and 1-α for the basal and apical return electrodes, respectively), while the rest $[(1-\sigma)\times I]$ to the extra-cochlear ground (EG). The arrowhead direction indicates the phases of biphasic current pulses (upward: cathodic-leading; downward: anodic-leading), while the arrow length indicates the current level. A and B stand for apex and base, respectively. Note that α is fixed at 0.5 for the named pTP modes in Fig. 5.1. When current steering is used, α can vary between 0 and 1.

number of discriminable pitches with QPVCs may be partially due to a larger steering range caused by the asymmetric current distribution when either main electrode is activated alone. This possibility was tested in this study by comparing the pitches of standard and asymmetrically spanned pTP stimuli on the same main electrode. Basal electrode spanning has been used in the technique of phantom electrode, which stimulates the most apical electrode in pBP mode. When a fraction of current was returned to the adjacent basal electrode, the neural excitation pattern was pushed apically ([54]), resulting in a pitch lower than that of MP stimulation ([24]). In addition, pitch generally decreased as the spatial separation between the main and basal return electrodes increased up to 2–3 mm or there were 1–2 intermediate electrodes. Compared to the adjacent basal return electrode, the nonadjacent (or spanned) basal return electrode may have further reduced the spread of excitation towards the basal end and pushed the neural excitation pattern more apically. Based on these results, basal electrode spanning in pTP mode was expected to elicit lower pitch percepts, while apical electrode spanning may elicit higher pitch percepts. Experiment 1 tested these hypotheses using both the computational model of [30] and human CI users.

From another perspective, electrode spanning may be inevitable when realizing a pTP strategy in CI users with a defective electrode. According to Hughes [71], 10–15% of CI users have at least one defective electrode. Note that when one electrode (e.g., EL9) is defective, three (rather than one) pTP channels are not available, including one using the defective electrode as the main electrode [e.g., $\mathrm{pTP}_{(8,9,10)}$] and two using the defective electrode as the apical or basal return electrode [e.g., $\mathrm{pTP}_{(7,8,9)}$ and $\mathrm{pTP}_{(9,10,11)}$]. The pTP channel with a defective main electrode may be replaced using quadrupolar-mode current steering [42] between two non-adjacent main electrodes on both sides of the defective electrode. It is possible to generate the same pitch percept as the intermediate defective electrode when current is evenly distributed in phase to the two non-adjacent main electrodes. Similar electrode spanning has been successfully used in MP-mode current steering to recover missing MP channels [25] and restore speech performance with the HiRes-120 processing strategy [28].

This study focused on alternate ways to replace the pTP channel with a defective return electrode. As hypothesized earlier, simply spanning the defective return electrode may vary the perceived pitch. The current steering technique in Chapter 3 may be applied to the apically or basally spanned pTP channel (Fig. 5.1b and 5.1c with various α) to approximate the pitch of the missing standard pTP channel, or to create a more discriminable channel from the neighboring available standard pTP channels. Another way to replace the pTP channel with a defective return electrode is to move both return electrodes away from the main electrode. The symmetric electrode spanning (Fig. 5.1d with $\alpha = 0.5$) may change the width but not the centroid of the neural excitation pattern. The compensation coefficient σ may thus need to be adjusted for the symmetrically spanned pTP channel to approximate the pitch of the missing standard pTP channel. Experiments 2 and 3 tested these two methods separately, using both the model of [30] and human CI users.

5.2 Experiment 1: Asymmetric Electrode Spanning

For brevity, $\mathrm{pTP}_{(ELa,ELn,ELb),\alpha=\alpha 1}$ denotes a general form of pTP stimulation on the main electrode ELn with the apical return electrode ELa, the basal return electrode ELb, and the steering coefficient $\alpha = \alpha 1$. For example, a standard pTP stimulus on the main electrode EL8 would be denoted by $\mathrm{pTP}_{(7,8,9),\alpha=0.5}$. The compensation coefficient σ, not shown in this form, was customized for each subject to be the highest value that allowed for full loudness growth within the compliance limits of CIs (see below for details).

Saoji [54] have shown that for phantom electrode stimuli, the centroid of forward-masking pattern shifted in directions consistent with the pitch changes. Similarly, a computational model [30] has been successfully used in Chapter 3 to predict the relative pitch changes of pTP-mode current steering based on the shifts of centroid (rather than peak) of simulated neural excitation pattern (i.e., the number of activated neurons as a function of cochlear position). In this study, the model with the same

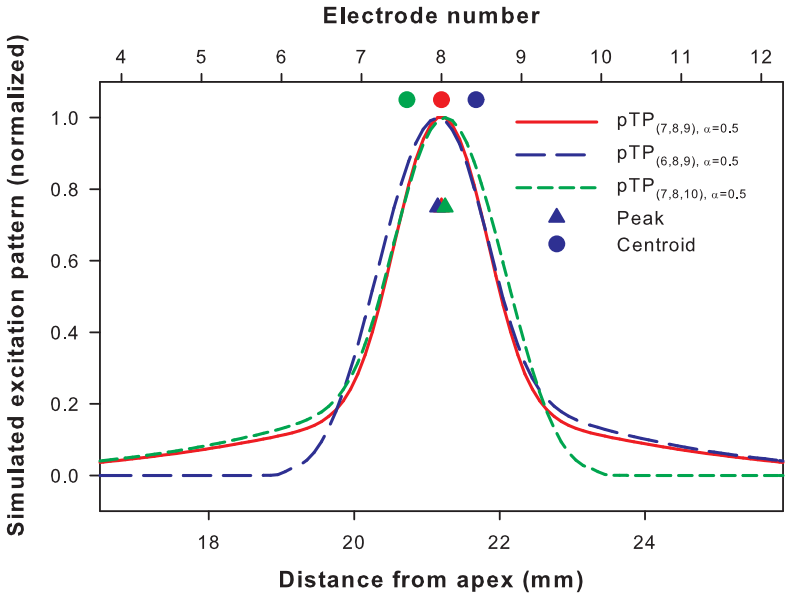

Fig. 5.2. Simulated neural excitation patterns for $\text{pTP}_{(7,8,9),\alpha=0.5}$ (red curve), $\text{pTP}_{(6,8,9),\alpha=0.5}$ (blue curve), and $\text{pTP}_{(7,8,10),\alpha=0.5}$ (green curve). The number of activated neurons is normalized and shown as a function of the distance from the apex of cochlea (bottom abscissa) or electrode number (top abscissa). For each pTP mode, the centroid (circle) and peak (triangle) of excitation are shown in the corresponding color. The compensation coefficient σ is fixed at 0.75 for all the simulations.

parameters (e.g., full neural survival and a fixed electrode-neuron distance of 1.3 mm) and assumptions (e.g., a total of 1000 activated neurons corresponds to equal loudness at MCL) was used to simulate the neural excitation patterns. Fig. 5.2 shows the normalized neural excitation patterns for the standard, apically spanned, and basally spanned pTP stimuli [i.e., $\text{pTP}_{(7,8,9),\alpha=0.5}$, $\text{pTP}_{(6,8,9),\alpha=0.5}$, and $\text{pTP}_{(7,8,10),\alpha=0.5}$, respectively]. Although their excitation peaks (triangles) all remained near the main electrode EL8, the excitation centroids (circles) of asymmetrically spanned pTP stimuli shifted away from EL8. As shown in Fig. 5.2, $\text{pTP}_{(6,8,9),\alpha=0.5}$ (blue curve) had similar spread of excitation as $\text{pTP}_{(7,8,9),\alpha=0.5}$ (red curve) on the basal side of EL8, but less excitation around the non-adjacent return electrode EL6. As such, the excitation centroid of $\text{pTP}_{(6,8,9),\alpha=0.5}$ (blue circle) shifted towards the base by 0.41 mm and was

located between EL8 and EL9. The pitch of $pTP_{(6,8,9),\alpha=0.5}$ was thus predicted to be between those of standard pTP stimuli on main electrodes EL8 and EL9. The model also predicted that the excitation centroid of $pTP_{(7,8,10),\alpha=0.5}$ (green circle) would shift towards the apex by the same amount and elicit a pitch between those of standard pTP stimuli on main electrodes EL7 and EL8. However, the model had inherently simplified assumptions and uncertainties in results. For example, it did not consider the different sensitivity of auditory neurons to cathodic- and anodic-leading pulses on the main and return electrodes, respectively (e.g., [72]). Also, the uniform electrode-neuron distance, neural survival, and impedance along the cochlea, as well as the fixed compensation coefficient σ (0.75) may have had great quantifiable effects on the side lobes and centroid shifts of simulated excitation patterns.

To study the effects of asymmetric electrode spanning on pitch perception in CI users, apically or basally spanned pTP stimuli on the main electrode EL8 were compared in pitch to standard pTP stimuli on main electrodes from EL6 to EL10. As a prerequisite, pitch ranking of standard pTP stimuli on main electrodes from EL6 to EL10 was first tested to make sure that distinctive pitches in tonotopic order were elicited by standard pTP stimuli on these main electrodes. Results of electrode ranking in standard pTP mode may also indicate the place-pitch sensitivity of individual CI subjects.

5.2.1 Methods

Subjects

Five post-lingually deafened female adult CI users participated in this study. One subject (S3) had bilateral implants and was tested in each ear separately. Table 5.1 shows CI subject demographics. All subjects used the Advanced Bionics HiRes 90K implant, which can stimulate multiple electrodes simultaneously to deliver various types of pTP stimuli. The HiFocus1J electrode array with an electrode spacing of 1.1 mm was used by all subjects. This study was reviewed and approved by the Purdue

IRB committee. All subjects provided informed consent and were compensated for their time.

Table 5.1.
Subject demographic details

Subject	Age (yrs)	Etiology	Processing Strategy	CI use (yrs)	HINT scores* (%)
S1	84	Sudden hearing loss	HiRes-P 120	4	96
S2	42	Meningitis	HiRes-P 120	8	94
S3L	64	Hereditary deafness	HiRes-P	2	N/A
S3R	64	Hereditary deafness	HiRes-P	7	94
S4	70	NF2 tumor	HiRes-P 120	4	7
S5	63	Unknown	HiRes-P 120	4	91

*The Hearing In Noise Test (HINT) sentences were tested in quiet at 60 dB SPL.

Pitch Ranking of Standard pTP Stimuli

Each main electrode from EL6 to EL10 was stimulated with 300-ms, 1000-Hz pulse trains in standard pTP mode. The symmetric biphasic pulses were cathodic-leading on the main electrode and anodic-leading on the return electrodes. A phase duration (226 μs) longer than those in clinical strategies was used so that the experimental pTP stimuli can reach the upper loudness limit within the compliance limits of CIs (i.e., the voltage on each electrode should be lower than 8 V and the surface charge density should be lower than 100 μC/cm2; [24]). The Bionic Ear Data Collection System (BEDCS; Advanced Bionics, Sylmar, CA) was used to bypass the clinical processors and directly present the experimental stimuli.

For the standard pTP stimulus on each main electrode, the highest compensation coefficient σ_{max} that allowed for full loudness growth within the compliance limits was first found using a binary search algorithm (see Chapter 3). For each subject,

the smallest σ_{max} among different main electrodes was selected and used for all the standard pTP stimuli in this experiment. This σ value kept a similar degree of current focusing while allowing for full loudness growth on all the main electrodes from EL6 to EL10.

The most comfortable level (MCL) for the standard pTP stimulus on the main electrode EL8 [i.e., $\text{pTP}_{(7,8,9),\alpha=0.5}$] was determined during the search of σ_{max} and was then used as the reference for loudness balance. The target standard pTP stimulus on the main electrode EL6, EL7, EL9, or EL10 was matched in loudness to the reference using a two-alternative, forced-choice (2AFC), double-staircase adaptive procedure [38]. Details of the loudness balance procedure can also be found in Chapter 3.

After loudness balancing, the pitches of standard pTP stimuli on two adjacent main electrodes [e.g., $\text{pTP}_{(5,6,7),\alpha=0.5}$ vs. $\text{pTP}_{(6,7,8),\alpha=0.5}$] were compared in a 2AFC task. In each trial, a pair of adjacent main electrodes was randomly chosen and the standard pTP stimuli on the two main electrodes were presented also in random order. Subjects were allowed to repeat the stimulus pair before indicating which stimulus had a higher pitch. There were four pairs of adjacent main electrodes and each pair was presented ten times, resulting in a total of 40 trials in each run. The percentages that the stimulus on the higher numbered main electrode was judged as higher in pitch were recorded. If the results of two runs differed by more than 30% for any stimulus pair, an additional run was tested. The final pitch-ranking results were averaged across all runs.

Pitch Ranking between Asymmetrically Spanned and Standard pTP Stimuli

With the same stimulation parameters (e.g., the pulse rate, phase duration, and compensation coefficient σ, etc.), the apically spanned $\text{pTP}_{(6,8,9),\alpha=0.5}$ and basally spanned $\text{pTP}_{(7,8,10),\alpha=0.5}$ were loudness balanced to the standard $\text{pTP}_{(7,8,9),\alpha=0.5}$ at MCL. The apically or basally spanned pTP stimulus was then separately compared

to the five equally loud standard pTP stimuli on main electrodes from EL6 to EL10 in a 2AFC pitch-ranking task. In each trial, the apically or basally spanned pTP stimulus and a randomly selected standard pTP stimulus were presented in random order. Each standard pTP stimulus was tested ten times, resulting in a total of 50 trials in a run. The percentages that the standard pTP stimuli were judged as higher in pitch than the spanned pTP stimulus were recorded. If the results of two runs differed by more than 30% for any stimulus pair, an additional run was tested. The final pitch-ranking results were averaged across all runs.

5.2.2 Results

Pitch Ranking of Standard pTP Stimuli

Fig. 5.3 shows the percentages that standard pTP stimuli on the main electrode ELn were judged as higher in pitch than those on ELn-1, where n = 7, 8, 9, and 10. The σ_{max} value used for each subject is indicated in the figure legend. The initially found σ_{max} for S5 was actually 0.8. However, with such a large σ value, pitch reversals occurred for S5 between pairs of adjacent main electrodes (EL6 vs. EL7 and EL9 vs. EL10), possibly due to perceptually salient side lobes ([24]). Less focused stimuli with a smaller σ value 0.6 were thus tested for S5 to avoid pitch reversals.

All the data points in Fig. 5.3 were well above the 50% chance level (gray solid line). In fact, most of the data points (except some from S4 and all from S5) were above the 76% perceptual threshold (defined by d' = 1; gray dashed line). This suggests that with the customized σ_{max} values, standard pTP stimuli on main electrodes from EL6 to EL10 elicited distinctive pitches as in the expected tonotopic order. A one-way repeated-measures (RM) analysis of variance (ANOVA) did not reveal any significant difference in the pitch-ranking results across electrode pairs ($F_{3,15} = 2.00, p = 0.16$). In other words, different pairs of adjacent main electrodes were similarly discriminable. However, pitch ranking of adjacent main electrodes in standard pTP mode was variable across subjects, with the best performance in S1

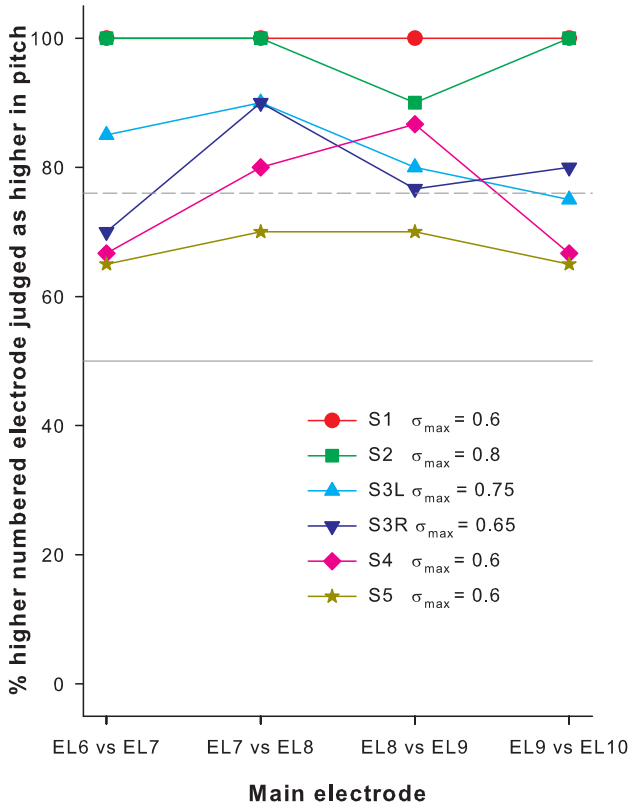

Fig. 5.3. Pitch-ranking results for main electrodes from EL6 to EL10 in standard pTP mode. The percentages that the higher-numbered main electrode was judged as higher in pitch are shown as a function of the adjacent stimulus pair. The gray solid line indicates the 50% chance level; dashed line indicates the 76% threshold level (with d' = 1). The applied compensation coefficient σ_{max} is included for each subject.

and S2, and the worst performance in S5. For all subjects except S1, the average pitch-ranking performance across electrode pairs was significantly correlated with the used σ_{max} value ($r = 0.92, p = 0.029$). In contrast, S1 used the smallest σ_{max} value but had the best pitch-ranking performance among subjects.

Pitch Ranking between Asymmetrically Spanned and Standard pTP Stimuli

The current levels required to reach equal loudness did not significantly differ for the standard [i.e., $\text{pTP}_{(7,8,9),\alpha=0.5}$], apically spanned [i.e., $\text{pTP}_{(6,8,9),\alpha=0.5}$], or basally spanned [i.e., $\text{pTP}_{(7,8,10),\alpha=0.5}$] pTP stimuli (one-way RM ANOVA: $F_{2,10} = 3.18, p = 0.09$), although the statistical power (0.34) was low due to the limited number of subjects. $\text{pTP}_{(7,8,9),\alpha=0.5}$ and $\text{pTP}_{(7,8,10),\alpha=0.5}$ tended to need more current than $\text{pTP}_{(6,8,9),\alpha=0.5}$ for equal loudness.

Fig. 5.4 shows the percentages that standard pTP stimuli on main electrodes from EL6 to EL10 were judged as higher in pitch than the apically spanned $\text{pTP}_{(6,8,9),\alpha=0.5}$ (top panel) or the basally spanned $\text{pTP}_{(7,8,10),\alpha=0.5}$ (bottom panel). Most of the psychometric functions monotonically increased with the main electrode number of standard pTP stimuli, in line with the tonotopic order in pitch. Each psychometric function was fitted with a three-parameter sigmoid function:

$$y = \frac{A}{1 + \exp(\frac{x - x_0}{B})} \tag{5.1}$$

to find the standard pTP stimulus with a virtual main electrode that may be pitch matched to the apically or basally spanned pTP stimulus (or with 50% responses). If the sigmoid function did not provide a good fit, data points of adjacent main electrodes were linearly interpolated to find the virtual main electrode with 50% responses. Fig. 5.4 also shows the interpolated virtual main electrode that may elicit a similar pitch as the apically or basally spanned pTP stimulus for each subject.

The virtual main electrodes with 50% responses suggest that the perceived pitch of $\text{pTP}_{(6,8,9),\alpha=0.5}$ fell between those of $\text{pTP}_{(7,8,9),\alpha=0.5}$ and $\text{pTP}_{(}8, 9, 10), \alpha = 0.5$ for most cases, but was slightly higher than that of $\text{pTP}_{(}8, 9, 10), \alpha = 0.5$ for S3R and S5. On the other hand, the perceived pitch of $\text{pTP}_{(7,8,10),\alpha=0.5}$ fell between those of $\text{pTP}_{(6,7,8),\alpha=0.5}$ and $\text{pTP}_{(7,8,9),\alpha=0.5}$ for all subjects except S4 who perceived $\text{pTP}_{(7,8,10),\alpha=0.5}$ as slightly higher in pitch than $\text{pTP}_{(7,8,9),\alpha=0.5}$. The dashed lines in

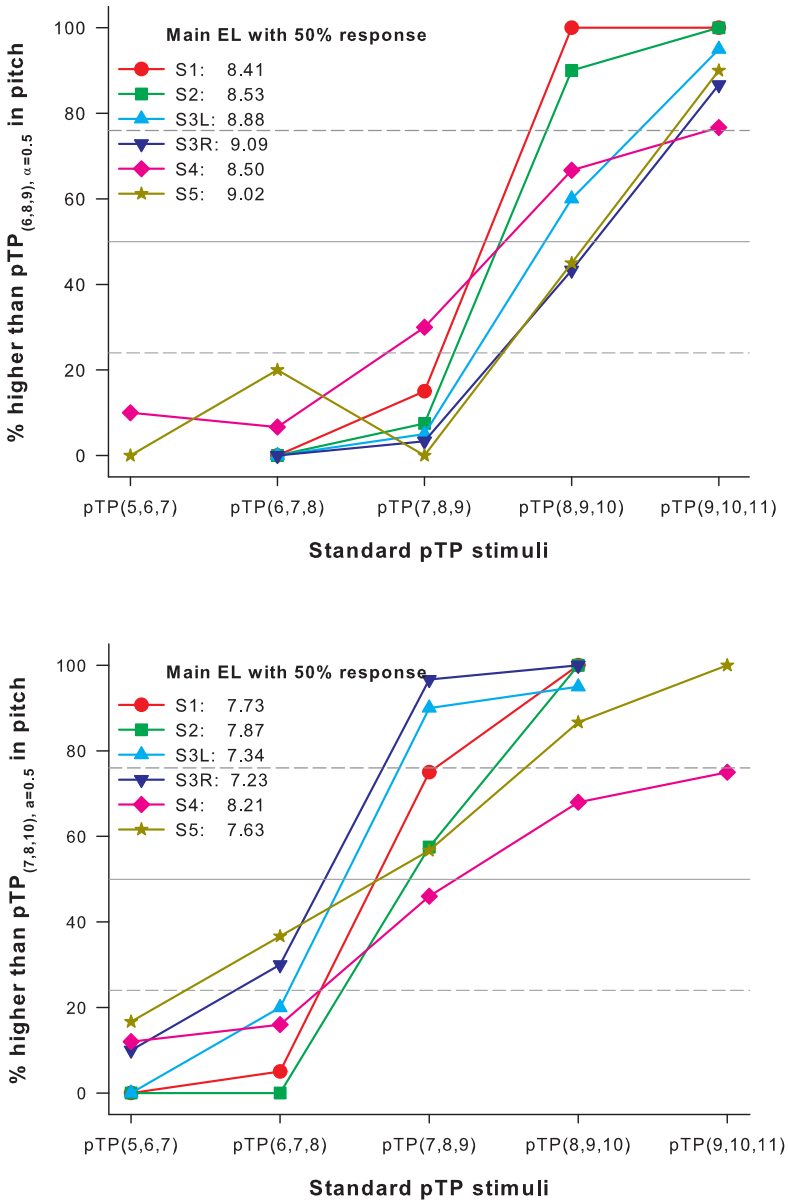

Fig. 5.4. Percentages that standard pTP stimuli on main electrodes from EL6 to EL10 were judged as higher in pitch than $\mathrm{pTP}_{(6,8,9),\alpha=0.5}$ (top panel) or $\mathrm{pTP}_{(7,8,10),\alpha=0.5}$ (bottom panel). The gray solid lines indicate the 50% chance level; dashed lines indicate the 76% and 24% threshold levels (with d' = ± 1). The interpolated virtual main electrodes with 50% responses are shown for each subject.

Fig. 5.4 indicate 76% and 24% responses respectively (i.e., d' = ±1), which were used as the threshold to determine if the spanned and standard pTP stimuli were discriminable. For S1 and S2, $pTP_{(6,8,9),\alpha=0.5}$ created an intermediate pitch or spectral channel discriminable from those of both $pTP_{(7,8,9),\alpha=0.5}$ and $TP_{(8,9,10),\alpha=0.5}$. S4 could not discriminate the pitch of $pTP_{(6,8,9),\alpha=0.5}$ from either that of $pTP_{(7,8,9),\alpha=0.5}$ or that of $TP_{(8,9,10),\alpha=0.5}$. For the other subjects, the perceived pitch of $pTP_{(6,8,9),\alpha=0.5}$ was discriminable from that of $pTP_{(7,8,9),\alpha=0.5}$, but not from that of $pTP_{(8,9,10),\alpha=0.5}$. Also, $pTP_{(7,8,10),\alpha=0.5}$ created an intermediate pitch or spectral channel discriminable from those of both $pTP_{(6,7,8),\alpha=0.5}$ and $pTP_{(7,8,9),\alpha=0.5}$ for S1 and S3L, but not for the other subjects.

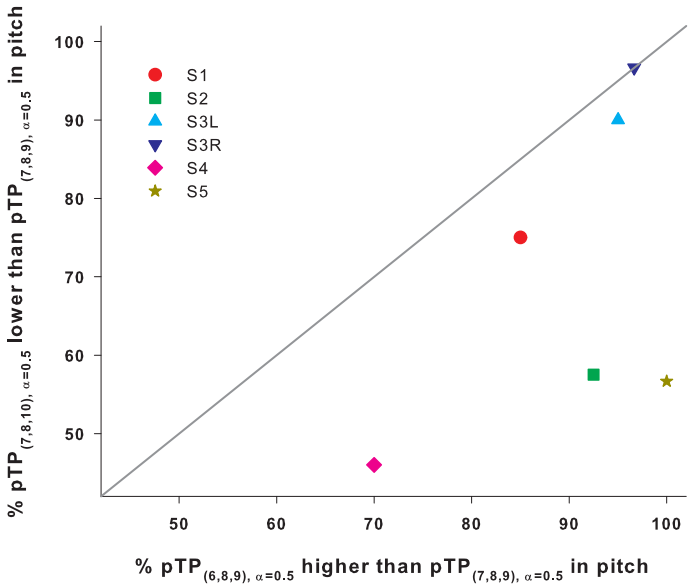

Fig. 5.5. Pitch-ranking results of $pTP_{(7,8,10),\alpha=0.5}$ vs. $pTP_{(7,8,9),\alpha=0.5}$ compared to the pitch-ranking results of $pTP_{(6,8,9),\alpha=0.5}$ vs. $pTP_{(7,8,9),\alpha=0.5}$. The diagonal line indicates equal response percentages.

Compared to the standard $pTP_{(7,8,9),\alpha=0.5}$, apically spanned $pTP_{(6,8,9),\alpha=0.5}$ elicited a higher pitch, while basally spanned $pTP_{(7,8,10),\alpha=0.5}$ elicited a lower pitch. Using $pTP_{(7,8,9),\alpha=0.5}$ as the common reference, the degree of pitch shift caused by apical or basal spanning can be quantified and compared. Fig. 5.5 shows the percentage that

$\text{pTP}_{(7,8,10),\alpha=0.5}$ was judged as lower in pitch than $\text{pTP}_{(7,8,9),\alpha=0.5}$, compared to the percentage that $\text{pTP}_{(6,8,9),\alpha=0.5}$ was judged as higher in pitch than $\text{pTP}_{(7,8,9),\alpha=0.5}$. An equal amount of pitch shift for apical and basal spanning is indicated by the diagonal line. All data points lie below the diagonal line, suggesting that $\text{pTP}_{(6,8,9),\alpha=0.5}$ elicited more salient pitch changes than $\text{pTP}_{(7,8,10),\alpha=0.5}$. A paired t-test showed that the difference in the response percentages was significant between $\text{pTP}_{(6,8,9),\alpha=0.5}$ and $\text{pTP}_{(7,8,10),\alpha=0.5}$ ($t_5 = 2.76, p = 0.04$). Note that pitch ranking of standard pTP stimuli was not better between $\text{pTP}_{(7,8,9),\alpha=0.5}$ and $\text{pTP}_{8,9,10),\alpha=0.5}$ [which surrounded $\text{pTP}_{(6,8,9),\alpha=0.5}$ in pitch] than between $\text{pTP}_{6,7,8),\alpha=0.5}$ and $\text{pTP}_{(7,8,9),\alpha=0.5}$ [which surrounded $\text{pTP}_{(7,8,10),\alpha=0.5}$ in pitch] (paired t-test: $t_5 = 1.40, p = 0.22$). Although the same amount of centroid shift in the opposite direction was predicted for apical or basal spanning in the simplified model, $\text{pTP}_{(7,8,10),\alpha=0.5}$ may not be as effective as $\text{pTP}_{(6,8,9),\alpha=0.5}$ in shifting the centroid of neural excitation in a real cochlea. Previous CI studies (e.g., [73] [74] [48] [54]) have shown that current was prone to flow from the apex to the base of a cochlea, possibly because the current pathway towards the base has a lower impedance. For $\text{pTP}_{(7,8,10),\alpha=0.5}$, the favored current flow to the base may make less reduction of basal current spread and a smaller apical shift of excitation centroid.

5.3 Experiment 2: Asymmetric Electrode Spanning with Current Steering

This experiment tested whether combining asymmetric electrode spanning with current steering can replace a standard pTP channel [e.g., $\text{pTP}_{(7,8,9),\alpha=0.5}$] when either of its return electrodes (e.g., EL7 or EL9) is defective. Results of Experiment 1 showed that simply spanning the defective return electrode [e.g., $\text{pTP}_{(6,8,9),\alpha=0.5}$ or $\text{pTP}_{(7,8,10),\alpha=0.5}$] sometimes elicited a pitch discriminable from that of the missing standard pTP channel [e.g., $\text{pTP}_{(7,8,9),\alpha=0.5}$] but not from that of the neighboring available standard pTP channel [e.g., $\text{pTP}_{8,9,10),\alpha=0.5}$ or $\text{pTP}_{6,7,8),\alpha=0.5}$]. To create a

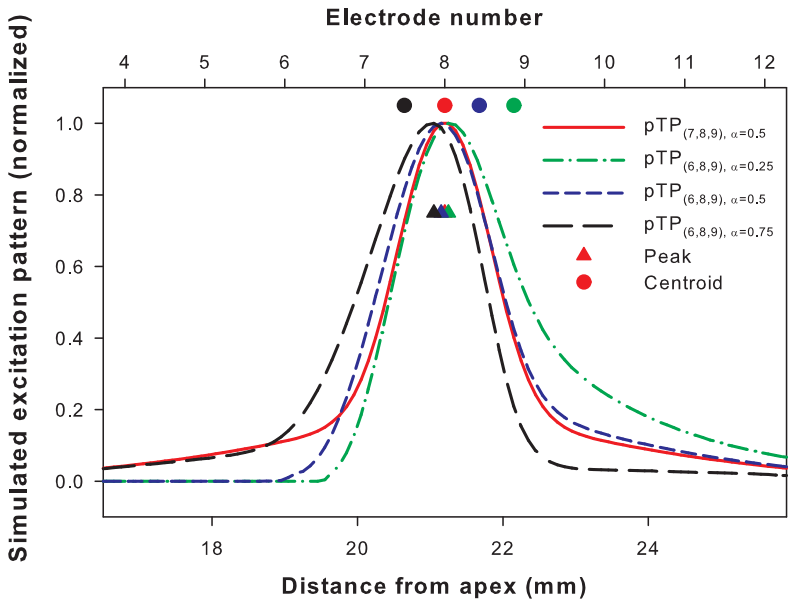

Fig. 5.6. Simulated neural excitation patterns for $pTP_{(7,8,9),\alpha=0.5}$ and $pTP_{(6,8,9)}$ with $\alpha = 0.25$, 0.5, and 0.75. See the caption of Fig. 5.2 for more details.

channel that can replace $pTP_{(7,8,9),\alpha=0.5}$, current steering may be applied to asymmetrically spanned pTP stimuli so that the excitation centroid is shifted back onto EL8 and the discriminability from the neighboring available standard pTP channels is improved. The neural excitation patterns of $pTP_{6,8,9}$ with different steering coefficient α were simulated using the computational model ([30]) and shown in Fig. 5.6. In line with the results of current steering in standard pTP mode (Chapter 3), the excitation centroids (circles) of $pTP_{6,8,9}$ shifted towards the apex as α increased or when more current was returned to the basal return electrode. The excitation peaks (triangles) had much smaller apical shifts than the centroids did. Based on the modeling results, an α between 0.5 (blue curve and circle) and 0.75 (black curve and circle) for $pTP_{6,8,9}$ was expected to shift the centroid back onto EL8 and thus elicit a pitch similar to that of $pTP_{(7,8,9),\alpha=0.5}$ (red curve and circle). The model also predicted that for $pTP_{7,8,10}$ (not shown in Fig. 5.6), an α between 0.25 and 0.5 may shift the centroid back onto EL8 and thus elicit a pitch similar to that of $pTP_{(7,8,9),\alpha=0.5}$.

Since a number of assumptions were simplified to make the model computationally tractable, these model predictions had inherent uncertainties and were tested in the following experiment.

5.3.1 Methods

Based on the modeling results, $\text{pTP}_{6,8,9}$ and $\text{pTP}_{7,8,10}$ with different steering coefficient α from 0.25 to 0.75 in steps of 0.125 were first matched in loudness and then compared in pitch to $\text{pTP}_{(7,8,9),\alpha=0.5}$ at MCL, using methods similar to those in Experiment 1. The same σ_{max} for $\text{pTP}_{(7,8,9),\alpha=0.5}$ was used for $\text{pTP}_{6,8,9}$ and $\text{pTP}_{7,8,10}$ with different α. The other stimulation parameters were the same as those in Experiment 1. In each trial of the pitch-ranking task, the standard pTP stimulus and a randomly chosen target stimulus (i.e., an apically or basally spanned pTP stimulus with a randomly chosen α) were presented in random order. Subjects were asked to judge which stimulus was higher in pitch. The percentages that the targets were chosen were recorded. Each target stimulus was tested ten times in a run. If the results of two runs differed by more than 30% for any stimulus pair, an additional run was tested.

5.3.2 Results

Fig. 5.7 shows the current level at MCL as a function of the steering coefficient α for apically or basally spanned pTP stimuli (left and right panels, respectively). One-way RM ANOVAs showed a significant effect of α on the MCL level for $\text{pTP}_{6,8,9}$ ($F_{4,20} = 4.79, p = 0.007$) but not for $\text{pTP}_{7,8,10}$ ($F_{4,20} = 1.01, p = 0.43$). Post-hoc Bonferroni t-tests showed that the MCL level for $\text{pTP}_{6,8,9}$ was only significantly higher with $\alpha = 0.75$ than with $\alpha = 0.25 (p = 0.006)$. This differed from the loudness-balance results with current steering in standard pTP mode. Chapter 3 found that the MCL level for $\text{pTP}_{7,8,9}$ was significantly higher with $\alpha = 0.5$ than with α around 0 or 1, presumably because the excitation pattern was more focused for pTP mode ($\alpha = 0.5$)

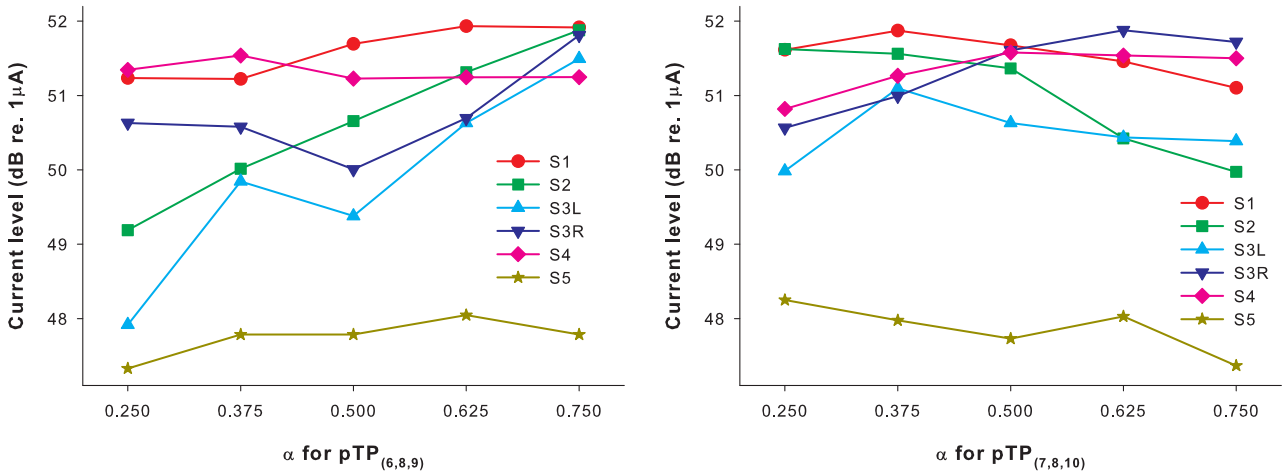

Fig. 5.7. Loudness-balanced most comfortable levels (in dB re 1μA) as a function of the steering coefficient α for the apically spanned $\text{pTP}_{(6,8,9)}$ (left panel) and basally spanned $\text{pTP}_{(7,8,10)}$ (right panel).

than for pBP mode ($\alpha = 0$ or 1). It is not surprising that apical or basal spanning in pTP mode may have changed the relative degree of current focusing and thus the equal-loudness current requirements with different α.

Fig. 5.8 shows the pitch-ranking results between the standard stimulus $\text{pTP}_{(7,8,9),\alpha=0.5}$ and the target stimuli [i.e., $\text{pTP}_{6,8,9}$ or $\text{pTP}_{7,8,10}$ with different α]. The percentages that the target stimuli were judged as higher in pitch than the standard pTP stimulus are plotted as a function of α for $\text{pTP}_{6,8,9}$ (left panel) and $\text{pTP}_{7,8,10}$ (right panel). For all subjects, the psychometric functions for $\text{pTP}_{6,8,9}$ plateaued with α from 0.25 to 0.5 and decreased with α from 0.5 to 0.75. For all subjects except S5, the psychometric functions for $\text{pTP}_{7,8,10}$ monotonically decreased with α from 0.25 to 0.5 and leveled off with α from 0.5 to 0.75. One-way RM ANOVAs found a significant effect of α on the response percentages for both $\text{pTP}_{6,8,9}$ ($F_{4,20} = 31.88, p < 0.001$) and $\text{pTP}_{7,8,10}$ ($F_{4,20} = 16.98, p < 0.001$). These results suggest that asymmetrically spanned pTP stimuli with increasing α elicited lower pitches. Different subjects were

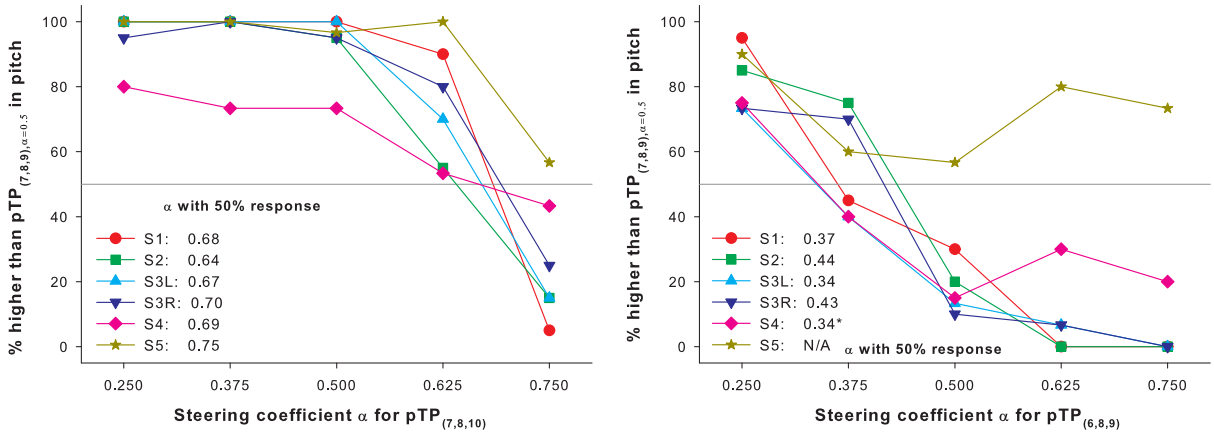

Fig. 5.8. Percentages that $\text{pTP}_{(6,8,9),\alpha=0.25,\ldots,0.75}$ (left panel) and $\text{pTP}_{(7,8,10),\alpha=0.25,\ldots,0.75}$ (right panel) were judged as higher in pitch than $\text{pTP}_{(7,8,9),\alpha=0.5}$. The interpolated α values with 50% responses (gray lines) for $\text{pTP}_{(6,8,9)}$ and $\text{pTP}_{(7,8,10)}$ are shown for each subject.

not equally sensitive to current steering in spanned pTP modes. For example, S4 and S5 performed the worst among subjects. Again, the σ_{max} value was not significantly correlated with the slope of psychometric function in each panel of Fig. 5.8.

All the psychometric functions in Fig. 5.8 were fitted with the sigmoid function in Equation 5.1 to find the α values for $\text{pTP}_{6,8,9}$ and $\text{pTP}_{7,8,10}$ that may elicit a similar pitch as $\text{pTP}_{(7,8,9),\alpha=0.5}$. The interpolated α values with 50% responses on the best-fit sigmoid functions for $\text{pTP}_{6,8,9}$ and $\text{pTP}_{7,8,10}$ are shown for each subject in Fig. 5.8. Due to pitch reversals, the functions of S4 and S5 for $\text{pTP}_{7,8,10}$ were not successfully fitted with the sigmoid function. Instead, the α value with 50% responses for S4 was estimated by a linear interpolation between $\alpha = 0.25$ and 0.375. The interpolated α values with 50% responses for $\text{pTP}_{6,8,9}$ ranged from 0.64 to 0.75 with a mean of 0.69 across subjects, while those for $\text{pTP}_{7,8,10}$ ranged from 0.34 to 0.44 with a mean of 0.38. These α values were within the ranges estimated by the computational model.

5.4 Experiment 3: Symmetric Electrode Spanning with Current Focusing

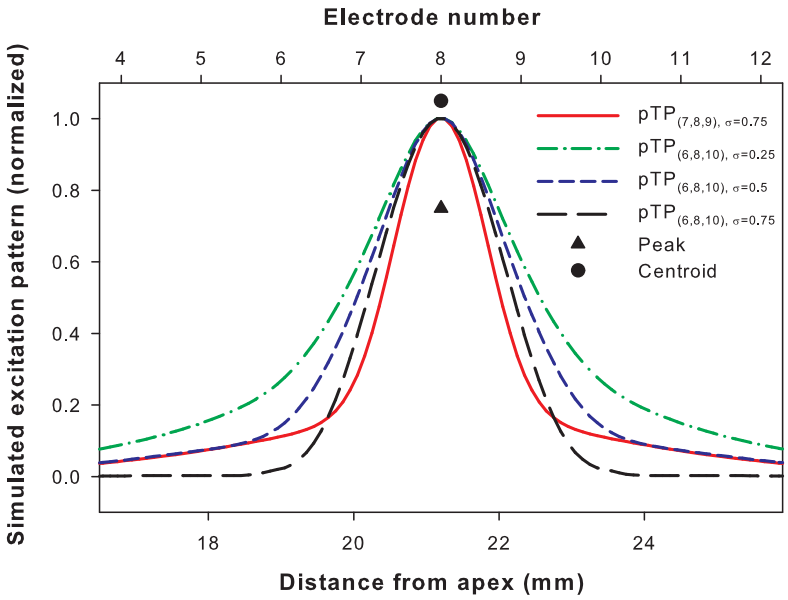

Fig. 5.9. Simulated neural excitation patterns for $\text{pTP}_{(7,8,9),\sigma=0.75}$ and $\text{pTP}_{(6,8,10)}$ with $\sigma = 0.25$, 0.5, and 0.75. The steering coefficient α is fixed at 0.5 for all the simulations. See the caption of Fig. 5.2 for more details.

Another approach to handling defective return electrodes [e.g., EL7 and/or EL9 for $\text{pTP}_{(7,8,9),\alpha=0.5}$] was to symmetrically span both return electrodes [e.g., $\text{pTP}_{(6,8,10),\alpha=0.5}$]. The simulated excitation patterns in Fig. 5.9 showed that with the same compensation coefficient σ (0.75), $\text{pTP}_{(6,8,10),\alpha=0.5}$ had the same excitation centroids (circles) and peaks (triangles) as $\text{pTP}_{(7,8,9),\alpha=0.5}$ (all on EL8). However, the excitation pattern of $\text{pTP}_{(6,8,10),\alpha=0.5}$ (black curve) was broader around EL8 but more reduced around EL6 and EL10 than that of $\text{pTP}_{(7,8,9),\alpha=0.5}$ (red curve). It is unclear whether and how such changes in excitation pattern predicted by the simplified model may affect pitch perception. Also, results of Experiment 1 suggest that apical and basal spanning may not have perfectly symmetric effects on the excitation centroid. When they both occur in symmetric electrode spanning, the pitch may change. To find a symmetrically spanned pTP channel that is similar to $\text{pTP}_{7,8,9}$ in pitch, we proposed

to adjust the compensation coefficient σ while maintaining the steering coefficient α at 0.5 for $\text{pTP}_{6,8,10}$. This may vary the degree of focusing for $\text{pTP}_{6,8,10}$ while keeping the excitation centroid and peak on EL8 (e.g., blue curve for $\sigma = 0.5$ and green curve for $\sigma = 0.25$ in Fig. 5.9). Previous studies [31] [75] [20] have shown that more focused stimuli may have a purer, cleaner, or higher sound quality with a more salient pitch. The following experiment thus tested pitch ranking between $\text{pTP}_{6,8,10}$ with various σ and $\text{pTP}_{7,8,9}$ with its highest possible σ_{max} (as determined in Experiment 1) to see which σ for $\text{pTP}_{6,8,10}$ may elicit a similar pitch as $\text{pTP}_{7,8,9}$.

5.4.1 Methods

The steering coefficient α was fixed at 0.5 for all the stimuli in this experiment. The highest compensation coefficient σ_{max} that supported full loudness growth for the symmetrically spanned $\text{pTP}_{6,8,10}$ was determined using the binary search algorithm (Chapter 3) and was found to be slightly higher than the σ_{max} for the standard $\text{pTP}_{7,8,9}$ in all subjects. The tested σ for $\text{pTP}_{6,8,10}$ ranged from 0 to the subject- and mode-specific σ_{max}. The standard $\text{pTP}_{7,8,9}$ used its own σ_{max} as determined in Experiment 1. The symmetrically spanned $\text{pTP}_{6,8,10}$ with different σ were first matched in loudness and then compared in pitch to the standard $\text{pTP}_{7,8,9}$ at MCL, using methods similar to those in the previous experiments.

5.4.2 Results

The loudness-balanced MCL levels for $\text{pTP}_{6,8,10}$ are plotted as a function of σ for each subject in Fig. 5.10. A linear mixed model was used to fit the MCL levels in dB with subject as the random factor and σ as the fixed factor. There was a significant effect of σ ($t_4 9 = 35.14, p < 0.01$) and the coefficient for σ was 14.41. Monotonically increasing equal-loudness contours across σ have also been found for standard pTP mode [31] [20]. A higher σ in standard or symmetrically spanned pTP mode may

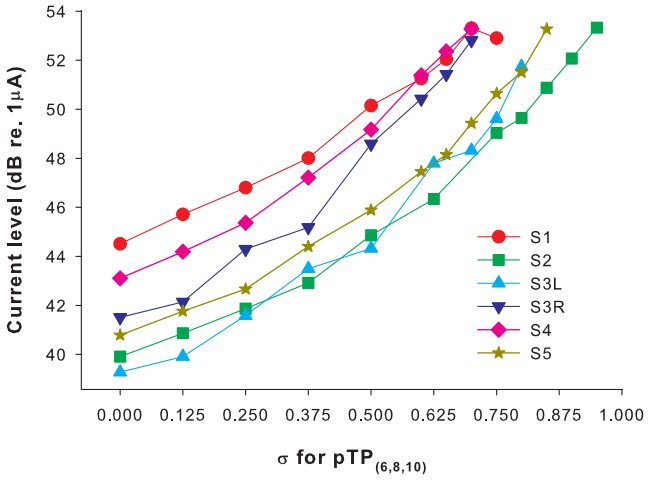

Fig. 5.10. Loudness-balanced most comfortable levels (in dB re 1μA) as a function of the compensation coefficient σ for the symmetrically spanned $\text{pTP}_{(6,8,10)}$.

narrow the spread of excitation and thus require more current to maintain equal loudness.

Fig. 5.11 shows the percentages that $\text{pTP}_{6,8,10}$ with various σ were judged as higher in pitch than $\text{pTP}_{7,8,9}$ with its own σ_{max}. For all subjects except S4, the response percentages generally increased from $\leq$ 50% to $\sim$ 100% when the σ for $\text{pTP}_{6,8,10}$ increased from 0 (i.e., MP mode; the left most data point of each plot) to the subject- and mode-specific σ_{max} (i.e., the right most data point of each plot). A linear mixed model was used to fit the percentages with subject as the random factor and σ as the fixed factor. There was a significant effect of σ ($t_4 9 = 9.68, p < 0.01$) and the coefficient for σ was 99.64. This suggests that most subjects perceived higher pitches with increasing σ for $\text{pTP}_{6,8,10}$. Consistent with the results of Litvak [31] and Landsberger [20], MP mode (i.e., $\sigma = 0$; the left most data point of each plot) was generally lower in pitch than standard $\text{pTP}_{7,8,9}$ with its own σ_{max}.

The psychometric functions in Fig. 5.11 were fitted with the sigmoid function in Equation 5.1 to find the interpolated σ values with 50% responses for $\text{pTP}_{6,8,10}$,

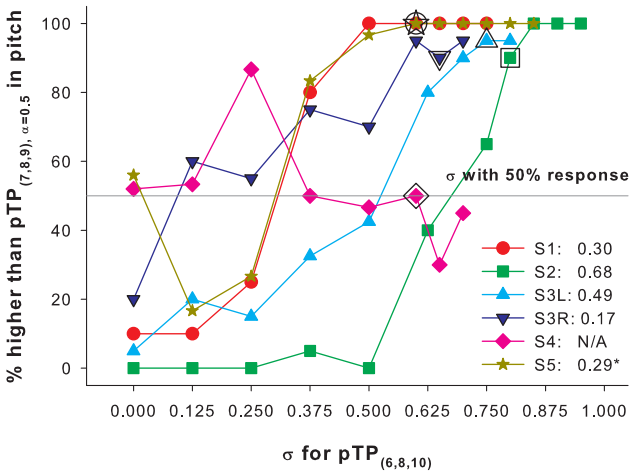

Fig. 5.11. Percentages that $\text{pTP}_{(6,8,10)}$ with various σ were judged as higher in pitch than $\text{pTP}_{(7,8,9)}$ with its own σ_max. The pitch-ranking results of $\text{pTP}_{(7,8,9)}$ vs. $\text{pTP}_{(6,8,10)}$ with the same σ [i.e., the σ_max for $\text{pTP}_{(7,8,9)}$] are enclosed by black borders and were mostly higher than the 50% chance level (gray line). The interpolated σ values with 50% responses for $\text{pTP}_{(6,8,10)}$ are shown for each subject.

which may elicit a pitch similar to that of $\text{pTP}_{7,8,9}$. The fitting was successful for all subjects except S4, who may have damaged auditory nerve fibers from NF2 tumor removal [76]. The data point of $\text{pTP}_{6,8,10}$ with $\sigma = 0$ was removed for S5 to have more accurate function fitting. The interpolated σ values with 50% responses for $\text{pTP}_{6,8,10}$ were always smaller than the σ_{max} for $\text{pTP}_{7,8,9}$ and ranged from 0.17 to 0.68 across subjects.

5.5 Discussion

5.5.1 Asymmetric Electrode Spanning

The relative pitches of asymmetrically spanned pTP stimuli [i.e., $\text{pTP}_{(6,8,9),\alpha=0.5}$ and $\text{pTP}_{(7,8,10),\alpha=0.5}$] were in good agreement with the shifted centroids of their simulated excitation patterns in the computational model. These results, together with

those of pTP-mode current steering (Chapter 3, 4), suggest that place-pitch perception with CIs is more likely determined by the centroid than by the peak of excitation. This point has also been made by examining the pitch perception results [24] and forward-masking patterns [54] of phantom electrode stimuli. In pTP mode with asymmetric electrode spanning, the electric fields of non-adjacent return and main electrodes may still be fused together to elicit a single pitch percept, as predicted by the computational model. In fact, no subject reported hearing multiple pitches with either the apically or basally spanned pTP stimulus. Asymmetric electrode spanning was predicted to reduce the spread of excitation in regions further away from the main electrode on the side of electrode spanning. Such predicted changes in excitation patterns can explain the perceived pitch shifts in the pitch-ranking tests, but should be verified in the future using measures such as psychophysical forward-masking patterns.

The pitch shifts of basal electrode spanning in pTP mode were largely in the same direction as those in pBP mode [24], although the latter were more variable across subjects and electrodes (i.e., pitch decreased or was the same in only 12 out of 20 cases). The smaller number of subjects and electrodes tested in this study may partially explain why the effects of pTP-mode electrode spanning were more consistent across cases. Also, the return current within the cochlea was divided into halves and sent to two (instead of one) electrodes in pTP mode, which may have reduced the perceptual salience of side lobes around return electrodes (a possible cause of pitch reversals in pBP mode [24]). Another possibility is that pTP mode had two side lobes, which may have more evenly balanced the shift of excitation centroid caused by basal electrode spanning. It is not possible to directly compare the degree of pitch shifts caused by basal electrode spanning in pTP or pBP mode, due to the differences in study design.

Subjects showed variable sensitivity to the pitch changes caused by apically or basally spanned pTP stimuli, maybe due to different neural survival and electrode-neuron distances. For example, S4 may have the poorest neural survival among

subjects because of her NF2 tumor removal. S4 did have the shallowest psychometric functions in Fig. 5.4, suggesting that she was the least sensitive to the pitch changes caused by either apical or basal spanning. Neither the age at testing nor duration of CI use seemed to affect the pitch-ranking results of asymmetric electrode spanning. For example, the oldest S1 and the youngest S2 performed similarly. Also, S3 had similar performance in both ears, even though her right ear was implanted five years later than her left ear. The inter-subject variability in pitch sensitivity to asymmetric electrode spanning was also not due to the used σ_{max} values, as indicated by the lack of correlation between the σ_{max} value and slope of psychometric function in each panel of Fig. 5.4.

It is possible that subjects with better pitch discrimination of main electrodes in standard pTP mode would be more sensitive to the pitch changes caused by asymmetric electrode spanning in pTP mode, because both measures may be commonly affected by factors such as subjects neural survival. For example, the best performers S1 and S2 in standard pTP-mode electrode discrimination also had the steepest psychometric functions for apical spanning pitch discrimination (top panel of Fig. 5.4). On the other hand, the poorest performers S4 and S5 in standard pTP-mode electrode discrimination had the shallowest functions for basal spanning pitch discrimination (bottom panel of Fig. 5.4). However, across subjects, there was no correlation between the electrode discrimination ability and function slope in each panel of Fig. 5.4. In another analysis using $\text{pTP}_{(7,8,9),\alpha=0.5}$ as the reference stimulus, the overall sensitivity to both apical and basal spanning was quantified by adding the perceptual distance (i.e., d' value) between $\text{pTP}_{(6,8,9),\alpha=0.5}$ and $\text{pTP}_{(7,8,9),\alpha=0.5}$ to that between $\text{pTP}_{(7,8,9),\alpha=0.5}$ and $\text{pTP}_{(7,8,10),\alpha=0.5}$ in Fig. 5.4. Because the pitches of the two asymmetrically spanned pTP stimuli were generally between those of the standard pTP stimuli on main electrodes EL7 and EL9, the relevant electrode discrimination ability was quantified as the cumulative d' from $\text{pTP}_{(6,7,8),\alpha=0.5}$ to $\text{pTP}_{(7,8,9),\alpha=0.5}$ and then to $\text{pTP}_{(8,9,10),\alpha=0.5}$ in Fig. 5.3. Again, there was no significant correlation ($r = -0.28, p = 0.59$) between the electrode discrimination ability and sensitivity

to spanning. The excitation pattern seemed to have major changes only around the non-adjacent return electrode in asymmetric spanning (Fig. 5.2), while the whole pattern shifted from one electrode to the next in electrode discrimination. The two tasks may thus require different degree of place-pitch sensitivity and involve responses from different neuron populations. Consequently, a CI users electrode discrimination ability in standard pTP mode cannot predict his/her sensitivity to pTP-mode electrode spanning.

5.5.2 Asymmetric Electrode Spanning with Current Steering

Pitch lowering with increasing steering coefficient α has also been found between pairs of standard pTP stimuli with an α interval of 0.1 (Chapter 3). However, the degree of pitch changes with α cannot be compared between spanned and standard pTP modes, due to the different designs of pitch-ranking tests in the two studies. Nevertheless, current steering seemed to have a similar effect on pitch perception (at least in terms of the direction of pitch changes) in both spanned and standard pTP modes. Although one of the return electrodes was not adjacent to the main electrode in asymmetrically spanned pTP modes, varying the distributions of return current was still able to shift the excitation centroid and change the perceived pitch, as suggested by the modeling results. In clinical fittings, the exact pitch-matched α values for $\text{pTP}_{(6,8,9)}$ and $\text{pTP}_{(7,8,10)}$ cannot be determined when the target channel $\text{pTP}_{(7,8,9),\alpha=0.5}$ does not have a well-defined pitch percept and is not testable due to the defective return electrode. Based on the results of Experiment 2, clinicians may simply use $\text{pTP}_{(6,8,9)}$ with α around 0.69 to replace $\text{pTP}_{(7,8,9),\alpha=0.5}$ if EL7 is defective and check whether the channel used for replacement is well discriminable from the next available channel $\text{pTP}_{(8,9,10),\alpha=0.5}$. If EL9 is defective, $\text{pTP}_{(7,8,10)}$ with α around 0.38 may be used to replace $\text{pTP}_{(7,8,9),\alpha=0.5}$ as long as the channel used for replacement is well discriminable from the previous available channel $\text{pTP}_{(6,7,8),\alpha=0.5}$.

5.5.3 Symmetric Electrode Spanning with Current Focusing

Litvak [31] reported that some CI users perceived symmetrically spanned pTP stimuli [e.g., $pTP_{(4,8,12)}$ with various compensation coefficient σ] as higher in pitch than MP stimuli. In a test of the sound quality with current focusing, Landsberger [20] found that for CI users who showed narrower forward-masking patterns from MP to standard pTP stimuli, a higher σ usually produced a purer, cleaner, or higher sound. Compared to MP stimuli, focused pTP stimuli may also enhance pitch strength [75]. Based on these results, the higher degree of current focusing with increasing σ for $pTP_{(6,8,10)}$ may have produced a purer, cleaner, or higher sound with a more salient pitch, which may be confounded with a pitch increase. On the other hand, although the model predicted the excitation centroid of $pTP_{(6,8,10)}$ to be on EL8 (Fig. 5.9), the actual current spread and neural excitation may be stronger on the basal side than on the apical side, due to the lower basal impedance. This would also lead to higher pitch percepts with increasing σ for $pTP_{(6,8,10)}$.

When $pTP_{(6,8,10)}$ and $pTP_{7,8,9}$ had the same σ value [i.e., the σ_{max} for $pTP_{(7,8,9)}$ as indicated by the symbols with black borders in Fig. 5.11], $pTP_{(6,8,10)}$ was higher in pitch than $pTP_{(7,8,9)}$ for all subjects except S4. Based on the modeling results (Fig. 5.9), the spread of excitation for $pTP_{(6,8,10)}$ may be broader around EL8 but more reduced around EL6 and EL10, compared to that of $pTP_{(7,8,9)}$ with the same σ. It is possible that the reduction of neural activity around EL6 and EL10 for $pTP_{(6,8,10)}$ may have been more notable than the increase of neural activity around EL8, leading to an overall more focused excitation pattern and thus a higher-pitched sound. Another possibility is that when both return electrodes were spanned in $pTP_{(6,8,10)}$, apical spanning may have been more effective than basal spanning in shifting the neural excitation centroid (Fig. 5.5, Experiment 1). The excitation centroid of $pTP_{(6,8,10)}$ may thus have an overall basal shift caused by the more effective apical spanning and elicit a pitch higher than that of $pTP_{(7,8,9)}$ with the same σ. These two possible explanations call for direct measurements of the neural excitation

patterns for $pTP_{(7,8,9)}$ and $pTP_{(6,8,10)}$ with the same σ. Preliminary data from Padilla [77] suggest that with the same σ (0.75), $pTP_{(7,8,9)}$ may have a narrower excitation pattern than $pTP_{(6,8,10)}$.

In clinical fittings, the exact pitch-matched σ values for $pTP_{(6,8,10)}$ again cannot be determined when the target channel $pTP_{(7,8,9)}$ does not have a well-defined pitch percept and is not testable due to the defective return electrode. Based on the data of Experiment 3, the missing target channel may be replaced by a symmetrically spanned pTP channel with a smaller σ value as long as the channel used for replacement is well discriminable from the neighboring available standard pTP channels.

5.6 Conclusions

This study investigated pitch perception of standard, asymmetrically spanned, and symmetrically spanned pTP stimuli on the same main electrode EL8 in five female CI users and in a computational model. The following conclusions can be made:

1. Compared to standard $pTP_{(7,8,9),\alpha=0.5}$, apically spanned $pTP_{(6,8,9),\alpha=0.5}$ generally elicited a higher pitch between those of $pTP_{(7,8,9),\alpha=0.5}$ and $pTP_{(8,9,10),\alpha=0.5}$, while basally spanned $pTP_{(7,8,10),\alpha=0.5}$ elicited a lower pitch between those of $pTP_{(6,7,8),\alpha=0.5}$ and $pTP_{(7,8,9),\alpha=0.5}$. The pitch increase caused by apical spanning was more salient than the pitch decrease caused by basal spanning.

2. Current steering in apically or basally spanned pTP mode had a similar effect on pitch perception as that in standard pTP mode. Pitch decreased when the steering coefficient α (i.e., the ratio of current returned to the basal electrode) increased. Apically spanned $pTP_{(6,8,9)}$ with α around 0.69 or basally spanned $pTP_{(7,8,10)}$ with α around 0.38 may elicit a similar pitch as $pTP_{(7,8,9),\alpha=0.5}$ and can be used to replace the standard pTP channel when either of its return electrodes is defective.

3. For symmetrically spanned $\text{pTP}_{(6,8,10),\alpha=0.5}$, higher pitches were perceived as the compensation coefficient σ (i.e., the ratio of current returned to the two intra-cochlear electrodes) increased, possibly due to the narrower excitation patterns. With the same σ, $\text{pTP}_{(6,8,10),\alpha=0.5}$ was higher in pitch than $\text{pTP}_{(7,8,9),\alpha=0.5}$. A smaller σ was thus required for $\text{pTP}_{(6,8,10),\alpha=0.5}$ to elicit a similar pitch as $\text{pTP}_{(7,8,9),\alpha=0.5}$ or to replace the standard pTP channel when either of its return electrodes is defective.

6. EXCITATION PATTERNS OF STANDARD AND SPANNED PARTIAL TRIPOLAR COCHLEAR IMPLANT STIMULATION

6.1 Introduction

In Chapter 5, symmetrically spanned $pTP_{(6,8,10)}$ was higher in pitch than the standard $pTP_{(7,8,9)}$ when the same σ was used, even though modeling results showed both had the same excitation centroid located on EL8. One hypothesis was that the excitation pattern generated by $pTP_{(6,8,10)}$ was more restricted and may have produced a cleaner or higher sound [20]. Alternatively, since the pitch increase caused by apical spanning was more salient than the pitch decrease caused by basal spanning (Chapter 5), applying apical and basal spanning simultaneously as in $pTP_{(6,8,10)}$ may have generated an overall higher pitch. Therefore, this chapter tested both hypotheses by investigating whether $pTP_{(6,8,10)}$ generated a more focused excitation pattern than $pTP_{(7,8,9)}$, or whether the centroid of excitation was more basal for $pTP_{(6,8,10)}$ than for $pTP_{(7,8,9)}$. The excitation pattern of each stimulation mode was measured at the physical (i.e., intra-cochlear electrical potential distribution), neural (i.e., spatial profile of evoked compound action potential), and perceptual levels (i.e., psychophysical forward masking pattern) with EFI, ECAP, and PFM method, respectively.

6.2 Method

Subject demographic details can be found in Table 4.1. The stimuli and procedure used to measure EFI, ECAP, and PFM patterns are also described in detail in Chapter 4.

For each excitation pattern, the excitation peak, centroid, and width between standard and symmetrically spanned pTP stimuli were analyzed by separate paired t-tests or Wilcoxon signed rank test when normality test fails. To investigate how the excitation patterns of both pTP stimuli varied at the physical, neural, and perceptual levels, the pattern features (peak, centroid, and width) were analyzed by separate two-way RM ANOVAs with the stimulation mode and measurement level as the two factors, followed by the Holm-Sidak post-hoc t-tests.

6.3 Results

6.3.1 EFI Patterns

Fig. 6.1 shows the normalized potential distribution as a function of recording electrode for standard [i.e., $\text{pTP}_{(7,8,9)}$; black circle] and symmetrically spanned [i.e., $\text{pTP}_{(6,8,10)}$; green diamond] pTP stimulation for each subject. Compared to the original un-normalized electrical potentials for $\text{pTP}_{(7,8,9)}$ stimulation, the original potentials for $\text{pTP}_{(6,8,10)}$ stimulation were larger on EL8 (by 0–10 mV) but smaller from EL1–6 and EL10–16 (by 0–10 mV), especially for subjects using larger σ (S2, S3L, and S3R). This relative change in the potential distribution was preserved in the normalized EFI patterns. The EFI patterns of the MP and standard pTP stimuli had a single sharp peak on EL8. The centroid of the EFI pattern (as indicated by the circles near the x-axis) was also around EL8 and not significantly different for both pTP stimuli (Wilcoxon signed rank test: $Z = -0.41, p = 0.81$). Although the EFI pattern of $\text{pTP}_{(6,8,10)}$ was smaller beyond the activated electrodes than that of $\text{pTP}_{(7,8,9)}$, the width at 75% peak amplitude of the EFI pattern was not significantly different between $\text{pTP}_{(7,8,9)}$ and $\text{pTP}_{(6,8,10)}$ stimulation (Wilcoxon signed rank test: $Z = 0.41, p = 0.81$).

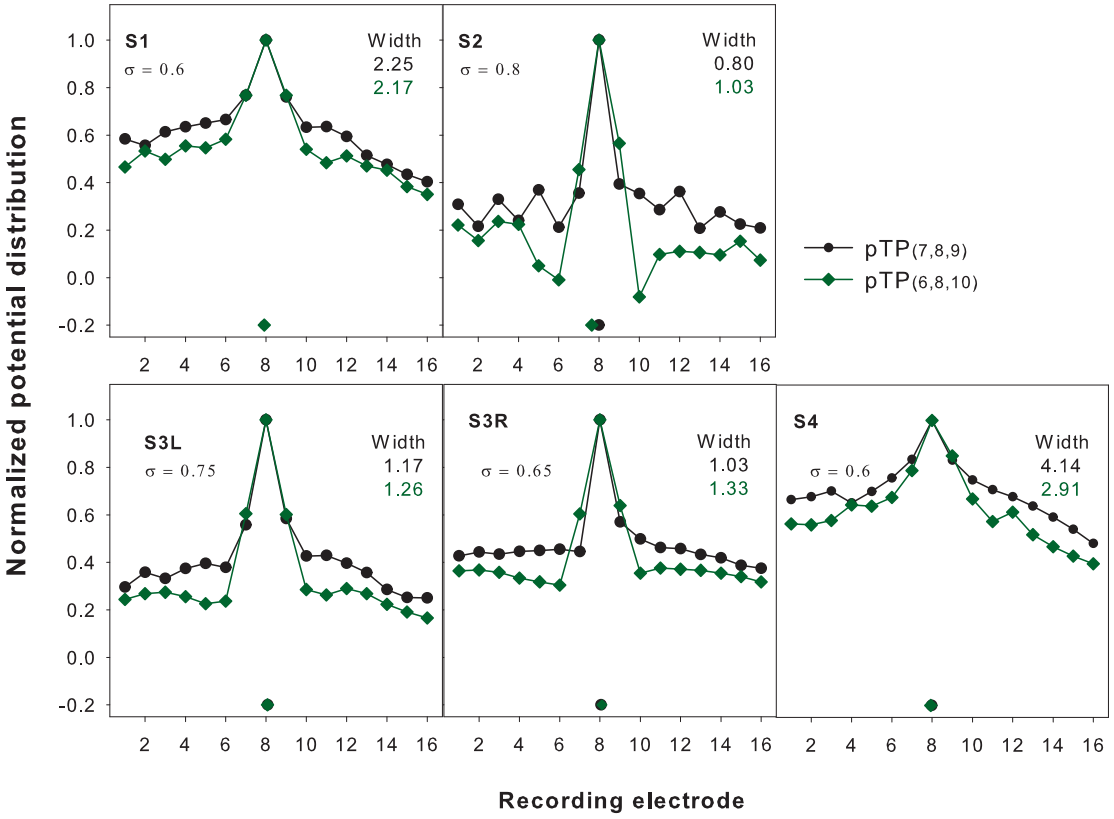

Fig. 6.1. The normalized EFI patterns as a function of recording electrode for for standard [i.e., $pTP_{(7,8,9)}$; black circle] and symmetrically spanned [i.e., $pTP_{(6,8,10)}$; green diamond] pTP stimulation.

6.3.2 ECAP Patterns

Fig. 6.2 shows the normalized ECAP amplitude as a function of masker electrode for standard [i.e., $pTP_{(7,8,9)}$; black circle] and symmetrically spanned [i.e., $pTP_{(6,8,10)}$; green diamond] pTP stimulation for each subject. There was no clear pattern as to whether $pTP_{(6,8,10)}$ or $pTP_{(7,8,9)}$ generated an overall larger original unnormalized ECAP amplitude. The normalized ECAP pattern for either pTP stimulus was generally irregular and exhibiting multiple peaks. Only subject S3L clearly showed a shift in the peak of ECAP pattern for $pTP_{(7,8,9)}$ (EL8) and $pTP_{(6,8,10)}$ (EL9). There

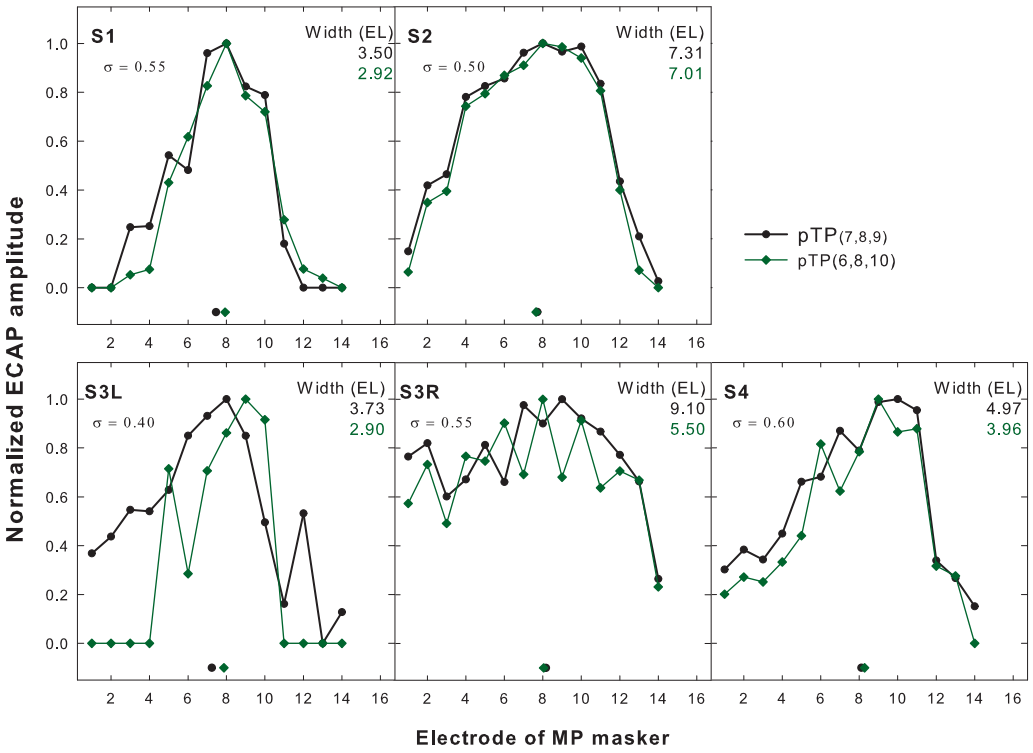

Fig. 6.2. The normalized ECAP patterns as a function of masker electrode for for standard [i.e., $\text{pTP}_{(7,8,9)}$; black circle] and symmetrically spanned [i.e., $\text{pTP}_{(6,8,10)}$; green diamond] pTP stimulation.

seemed to be a trend that, as symmetric spanning was applied, the normalized ECAP amplitudes slightly decreased on the apical side of EL8 but remained similar on the basal side of EL8. However, paired t-tests did not reveal significant difference in peak of ECAP pattern ($t_4 = 0.20, p = 0.85$), nor in centroid of ECAP pattern ($t_4 = -1.48, p = 0.21$) for $\text{pTP}_{(7,8,9)}$ and $\text{pTP}_{(6,8,10)}$ stimulation. Although the width of ECAP pattern was smaller for $\text{pTP}_{(6,8,10)}$ than for $\text{pTP}_{(7,8,9)}$ across subjects, the difference in width just was only approaching significance level (Wilcoxon signed rank test: $Z = -2.02, p = 0.06$).

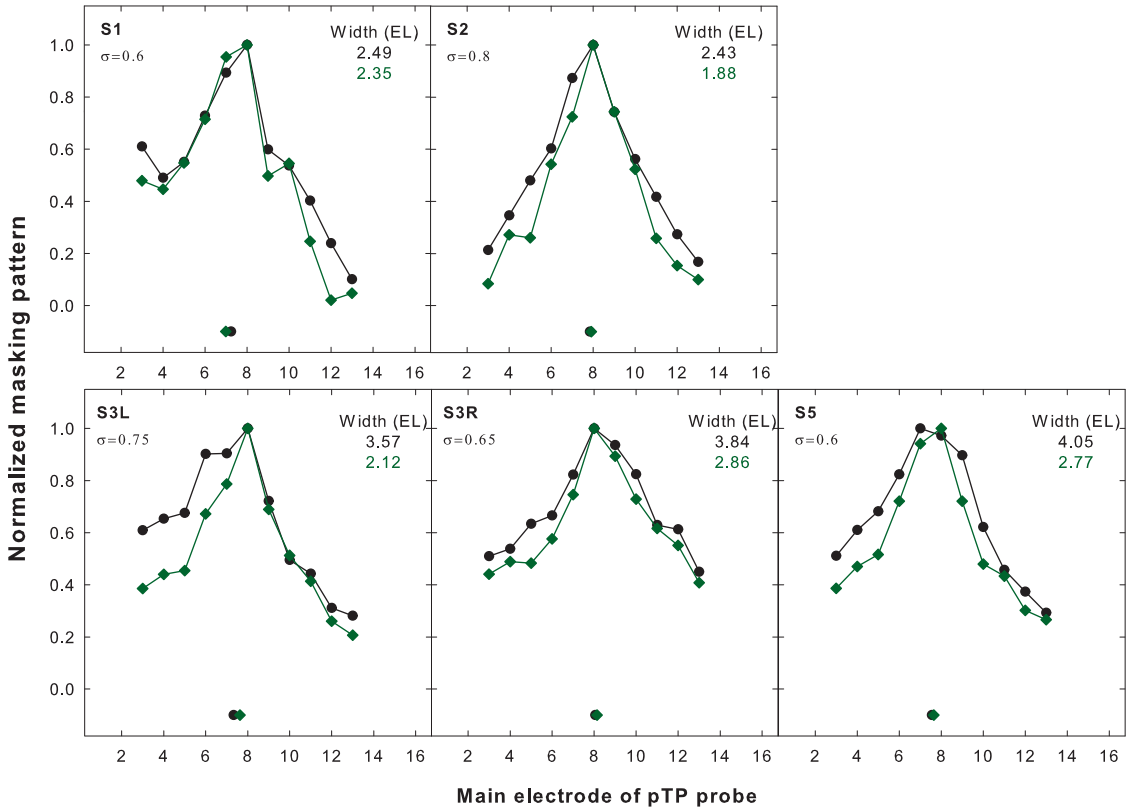

Fig. 6.3. The normalized threshold shift of pTP probe (calculated as the dB difference between the masked and unmasked probe thresholds) with the forward masker $pTP_{(7,8,9)}$ (black circles) or $pTP_{(6,8,10)}$ (green diamonds) as a function of probe electrode

6.3.3 PFM Patterns

Fig. 6.3 shows the normalized threshold shift of pTP probe (calculated as the dB difference between the masked and unmasked probe thresholds) with the forward masker $pTP_{(7,8,9)}$ (black circles) or $pTP_{(6,8,10)}$ (green diamonds) as a function of probe electrode for each subject. The normalized PFM patterns of both pTP stimuli generally exhibited a single peak at the main electrode EL8 and decreased monotonically towards the apex and base when the probe moved away from the masker. No significant difference was found in the peak of ECAP pattern (Wilcoxon signed rank test:

$Z = -1.00, p = 1.00$), nor in centroid of ECAP pattern ($t_4 = -0.67, p = 0.54$) for $\text{pTP}_{(7,8,9)}$ and $\text{pTP}_{(6,8,10)}$ stimulation. It can be observed that across subject, PFM pattern of $\text{pTP}_{(6,8,10)}$ was consistently sharper and narrower than that of $\text{pTP}_{(7,8,9)}$. Paired t-test indeed shows the width of PFM pattern was significantly narrower ($t_4 = 3.674, p = 0.02$) for $\text{pTP}_{(6,8,10)}$ (2.40 EL) than for $\text{pTP}_{(7,8,9)}$ (3.28 EL).

6.3.4 Comparisons across measurement levels

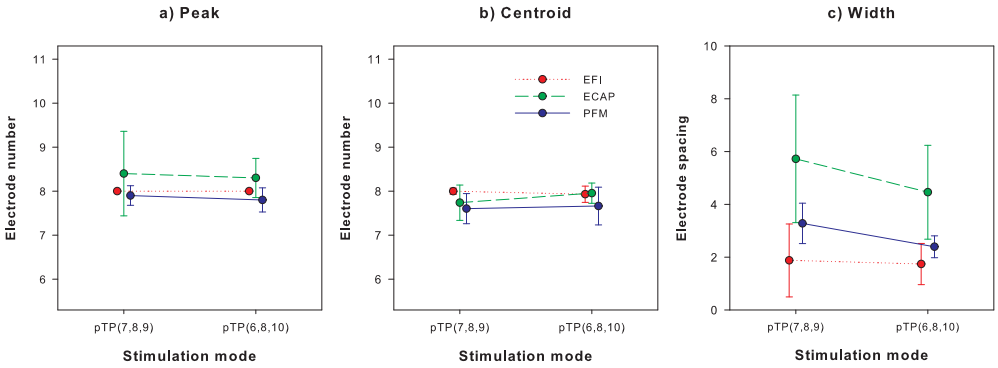

Fig. 6.4. The (a)peak, (b)centroid, and (c)width of excitation measured by EFI, ECAP, or PFM method as functions of pTP stimulation modes

The peak, centroid, and width of excitation measured by EFI, ECAP, or PFM method are shown as functions of pTP stimulation modes in Fig. 6.4. The excitation peak and centroid are expressed in the location of electrode contact, while the width of excitation is expressed in the unit of electrode spacing. Excitation patterns measured by EFI, ECAP, and PFM method shows similar peak and centroid location for $\text{pTP}_{(7,8,9)}$ and $\text{pTP}_{(6,8,10)}$ in Fig. 6.4ab. A two-way RM ANOVA on the location of excitation peak did not show any significant effect of stimulation mode ($F_{1,8} = 0.17, p = 0.70$), measurement level ($F_{2,8} = 2.98, p = 0.11$), and their interaction ($F_{2,8} = 0.04, p = 0.97$). Similarly, no significant effect was found for stimulation mode ($F_{1,8} = 1.01, p = 0.37$), measurement level ($F_{2,8} = 2.43, p = 0.15$), nor their interaction ($F_{2,8} = 2.02, p = 0.20$) on the centroid of excitation.

The width of excitation was smaller for $\text{pTP}_{(6,8,10)}$ than $\text{pTP}_{(7,8,9)}$ across measurement levels in Fig. 6.4. A two-way RM ANOVA on the width of excitation showed significant effects of stimulation mode ($F_{1,8} = 9.90, p = 0.04$) and measurement level($F_{2,8} = 6.80, p = 0.02$), but not their interaction ($F_{2,8} = 2.08, p = 0.19$). Pair-wise comparison using Holm-Sidak method showed width was not significantly different between ECAP and PFM patterns ($p = 0.08$) or between PFM and EFI patterns (p=0.29), but ECAP patterns were significantly wider than EFI patterns ($p = 0.02$). This is most likely due to the smaller σ (i.e., less focused stimulation) used in ECAP method. On average, symmetrically spanned $\text{pTP}_{(6,8,10)}$ can narrow the excitation pattern by 0.76 electrode spacing as compare to standard $\text{pTP}_{(7,8,9)}$.

6.4 Conclusion

This study investigated the excitation pattern changes with standard and symmetrically spanned pTP stimuli at the physical (measured with EFI), neural (measured with ECAP), and perceptual levels (measured with PFM). Across all measurement levels, applying symmetrical spanning to pTP stimulation narrowed the width of excitation but did not change the excitation peak or centroid. The results suggest that it was the narrowing of excitation pattern, rather than a shift of the excitation, that caused an increase in pitch for symmetric spanning in pTP mode.

7. SUMMARY AND FUTURE WORK

The large spread of excitation is a major cause of poor spectral resolution for CI users. The standard pTP stimulation has been shown to reduce current spread and improve spatial selectivity, by returning an equally distributed fraction ($0.5 \times \sigma$) of current to two flanking electrodes and the rest to an extra-cochlear ground. Processing strategy in pTP mode showed improved speech recognition in noise relative to the matched MP strategy, but not for the clinical MP strategy [2]. Therefore, it is worthwhile to further explore the potential benefit of pTP stimulation, which may consequently lead to improved coding of spectral fine structures for future processing strategies. In this study, pTP mode was combined with current steering (i.e., steered pTP mode) in order to create additional spectral channels, or combined with electrode spanning (i.e., spanned pTP mode) in order to provide focused stimulation even with defective electrodes. The loudness, pitch, and spread of excitation patterns were investigated with steered and spanned pTP mode and results are summarized below.

7.1 Current Steering with pTP Stimulation

Chapter 3 tested the efficacy of incorporating current steering into pTP mode to add spectral channels. Different proportions of current [$\alpha \times \sigma$ and $(1 - \alpha) \times \sigma$] were returned to the basal and apical flanking electrodes respectively to shape the electric field. Loudness and pitch perception with α from 0 to 1 in steps of 0.1 was simulated with a computational model of CI stimulation and tested on the apical, middle, and basal electrodes of six CI subjects. The highest σ allowing for full loudness growth within the implant compliance limit was chosen for each main electrode. Pitch ranking was measured between pairs of loudness-balanced steered pTP stimuli with an α interval of 0.1 at the most comfortable level. Results demonstrated that steered

pTP stimuli with α around 0.5 required more current to achieve equal loudness than those with α around 0 or 1. Subjects usually perceived decreasing pitches as α increased from 0 to 1, somewhat consistent with the apical shift of the center of gravity of excitation pattern in the model. Pitch discrimination was not better with α around 0.5 than with α around 0 or 1, except for some subjects and electrodes. For three subjects with better pitch discrimination, about half of the pitch ranges of two adjacent main electrodes overlapped with each other in steered pTP mode. In other words, the lowest pitch on main EL8 (i.e., $\mathrm{pTP}_{EL8,\alpha=1}$) was comparable to the elicited pitch of standard pTP stimulation on EL7 (i.e., $\mathrm{pTP}_{EL7,\alpha=0.5}$), while the highest pitch on main EL7 (i.e., $\mathrm{pTP}_{EL7,\alpha=0}$) was comparable to the pitch of standard pTP stimulation on EL8 (i.e., $\mathrm{pTP}_{EL8,\alpha=0.5}$).

To further study the mechanism behind the pitch change elicited by steered pTP mode, the excitation pattern of the highest (i.e., $\mathrm{pTP}_{EL8,\alpha=0}$), intermediate(i.e., $\mathrm{pTP}_{EL8,\alpha=0.5}$), and lowest (i.e., $\mathrm{pTP}_{EL8,\alpha=1}$) pitched stimulus was measured at the physical (i.e., intra-cochlear electrical potential distribution; EFI pattern), neural (i.e., spatial profile of evoked compound action potential; ECAP pattern), and perceptual levels (i.e., psychophysical forward masking pattern; PFM pattern). Spatial interaction, characterized by the width of excitation, was largest at neural level and least at the physical level, most likely because less focused steered pTP stimuli were used in ECAP pattern measurement due to its method limitation. Within measurements at the same level, the width of excitation did not vary significantly for steered pTP stimulus with different α. As α increased (i.e., pitch decreased), the centroid of excitation pattern was shifted apically at physical and perceptual levels, and the peak of excitation pattern was also shifted apically but only at the perceptual level. It is likely the information regarding the centroid of excitation was preserved across auditory pathway and had a positive effect on determining the peak of excitation pattern in the higher processing level. These results suggest the pitch elicited by steered pTP stimulation may be related to the centroid of excitation patterns.

7.2 Electrode Spanning with pTP Stimulation

In chapter 5, the perceptual effects of electrode spanning (i.e., the use of nonadjacent return electrodes) in pTP mode were tested on a main electrode EL8 in five CI users. The motivation was that standard pTP mode on EL8 [i.e., $\mathrm{pTP}_{(7,8,9),\alpha=0.5}$] was not possible when EL7 or EL9 was defective, and spanning the defective electrode [i.e., $\mathrm{pTP}_{(6,8,9),\alpha=0.5}$ or $\mathrm{pTP}_{(7,8,10),\alpha=0.5}$] may be an alternative way to provide focused stimulation. Experiment 1 tested whether asymmetric spanning with α=0.5 created channels that were distinguishable from the nearby standard pTP stimuli. It was found that in general, apical spanning [i.e., $\mathrm{pTP}_{(6,8,9),\alpha=0.5}$; returning current to EL6 rather than EL7] elicited a pitch between those of standard pTP stimuli on main electrodes EL8and EL9, while basal spanning [i.e., $\mathrm{pTP}_{(7,8,10),\alpha=0.5}$; returning current to EL10 rather than EL9] elicited a pitch between those of standard pTP stimuli on main electrodes EL7 and EL8. The pitch increase caused by apical spanning was more salient than the pitch decrease caused by basal spanning. To replace the standard pTP channel on the main electrode EL8 when EL7 or EL9 is defective, experiment 2 tested asymmetrically spanned pTP stimuli with various α, and experiment 3 tested symmetrically spanned pTP stimuli with various σ. The results showed that pitch increased with decreasing α in asymmetric spanning, or with increasing σ in symmetric spanning. Apical spanning with α around 0.69 and basal spanning with α around 0.38 may both elicit a similar pitch as the standard pTP stimulus. With the same σ, the symmetrically spanned pTP stimulus was higher in pitch than the standard pTP stimulus. A smaller σ was thus required for symmetric spanning to match the pitch of the standard pTP stimulus. Further studies on the excitation patterns suggest symmetrically spanned pTP mode can narrow the excitation pattern at physical, neural, and perceptual levels. These results suggest electrode spanning is useful for adding spectral channels and handling defective electrodes with CIs.

7.3 Future Work

The benefits of current focusing and steering to speech and music perception will be evaluated in CI users. The proposed experimental pTP mode will be programmed to a research processor with the Bionic Ear Programming System (BEPS+). Subjects will be fitted with several experimental mode (i.e., MP, MP-mode steering, pTP, and steered pTP mode) and perform tests in sentence recognition in noise, pitch contour identification, basic frequency discrimination, etc. Experimental programs (e.g., MP, pTP, steered pTP mode) will be created by Bionic Ear Programming System (BEPS+) and written onto a research processor. For each subject, the experimental programs will be matched in the number of main electrodes, filter banks (input frequency range: 306-8054 Hz), stimulation rate (140 μs/phase), and loudness. Then, the programs will be tested in random order for pitch ranking with harmonic complex tones [78], spectral ripple discrimination [79], vocal emotion recognition [80], melodic contour identification [81], hearing in noise test (HINT; [82]). It is also interesting to see whether speech perception benefits with pTP-mode current steering may be predicted by psychophysically measured pitch ranking abilities and/or excitation pattern shifts.

REFERENCES

REFERENCES

[1] "Cochlear implants," https://www.nidcd.nih.gov/health/hearing/pages/coch.aspx, accessed: 2014-09-18.

[2] A. G. Srinivasan, M. Padilla, R. V. Shannon, and D. M. Landsberger, "Improving speech perception in noise with current focusing in cochlear implant users," *Hearing research*, vol. 299, pp. 29–36, 2013.

[3] J. A. Bierer and K. F. Faulkner, "Identifying cochlear implant channels with poor electrode-neuron interface: partial tripolar, single-channel thresholds and psychophysical tuning curves," *Ear and hearing*, vol. 31, no. 2, p. 247, 2010.

[4] J. A. Bierer, K. F. Faulkner, and K. L. Tremblay, "Identifying cochlear implant channels with poor electrode-neuron interface: electrically-evoked auditory brainstem responses measured with the partial tripolar configuration," *Ear and hearing*, vol. 32, no. 4, p. 436, 2011.

[5] C.-C. Wu and X. Luo, "Current steering with partial tripolar stimulation mode in cochlear implants," *Journal of the Association for Research in Otolaryngology*, vol. 14, no. 2, pp. 213–231, 2013.

[6] C. Wu and X. Luo, "Electrode spanning with partial tripolar stimulation mode in cochlear implants." *Journal of the Association for Research in Otolaryngology: JARO*, 2014.

[7] M. C. Liberman and M. E. Oliver, "Morphometry of intracellularly labeled neurons of the auditory nerve: correlations with functional properties," *Journal of Comparative Neurology*, vol. 223, no. 2, pp. 163–176, 1984.

[8] W. Yost, *Fundamentals of Hearing: An Introduction*. Academic Press, 2007. [Online]. Available: http://books.google.com/books?id=q1hoIKeBi90C

[9] "Cochlear implant system," http://kidshealth.org/parent/general/eyes/cochlear.html, accessed: 2014-10-14.

[10] B. S. Wilson, C. C. Finley, D. T. Lawson, R. D. Wolford, D. K. Eddington, and W. M. Rabinowitz, "Better speech recognition with cochlear implants," *Nature*, vol. 352, no. 6332, pp. 236–238, 1991.

[11] P. C. Loizou, "Mimicking the human ear," *Signal Processing Magazine, IEEE*, vol. 15, no. 5, pp. 101–130, 1998.

[12] K. E. Fishman, R. V. Shannon, and W. H. Slattery, "Speech recognition as a function of the number of electrodes used in the speak cochlear implant speech processor," *Journal of Speech, Language, and Hearing Research*, vol. 40, no. 5, pp. 1201–1215, 1997.

[13] L. M. Friesen, R. V. Shannon, D. Baskent, and X. Wang, "Speech recognition in noise as a function of the number of spectral channels: comparison of acoustic hearing and cochlear implants," *The Journal of the Acoustical Society of America*, vol. 110, no. 2, pp. 1150–1163, 2001.

[14] R. V. Shannon, Q.-J. Fu, and J. Galvin 3rd, "The number of spectral channels required for speech recognition depends on the difficulty of the listening situation." *Acta oto-laryngologica. Supplementum*, no. 552, pp. 50–54, 2004.

[15] A. Kral, R. Hartmann, D. Mortazavi, and R. Klinke, "Spatial resolution of cochlear implants: the electrical field and excitation of auditory afferents," *Hearing research*, vol. 121, no. 1, pp. 11–28, 1998.

[16] J. A. Bierer and J. C. Middlebrooks, "Auditory cortical images of cochlear-implant stimuli: dependence on electrode configuration," *Journal of Neurophysiology*, vol. 87, no. 1, pp. 478–492, 2002.

[17] ——, "Cortical responses to cochlear implant stimulation: channel interactions," *Journal of the Association for Research in Otolaryngology*, vol. 5, no. 1, pp. 32–48, 2004.

[18] R. L. Snyder, J. A. Bierer, and J. C. Middlebrooks, "Topographic spread of inferior colliculus activation in response to acoustic and intracochlear electric stimulation," *Journal of the Association for Research in Otolaryngology*, vol. 5, no. 3, pp. 305–322, 2004.

[19] J. A. Bierer, "Threshold and channel interaction in cochlear implant users: Evaluation of the tripolar electrode configurationa)," *The Journal of the Acoustical Society of America*, vol. 121, no. 3, pp. 1642–1653, 2007.

[20] D. M. Landsberger, M. Padilla, and A. G. Srinivasan, "Reducing current spread using current focusing in cochlear implant users," *Hearing research*, vol. 284, no. 1, pp. 16–24, 2012.

[21] G. S. Donaldson, H. A. Kreft, and L. Litvak, "Place-pitch discrimination of single-versus dual-electrode stimuli by cochlear implant usersa)," *The Journal of the Acoustical Society of America*, vol. 118, no. 2, pp. 623–626, 2005.

[22] J. B. Firszt, L. K. Holden, R. M. Reeder, and M. W. Skinner, "Speech recognition in cochlear implant recipients: comparison of standard hires and hires 120 sound processing," *Otology & neurotology: official publication of the American Otological Society, American Neurotology Society [and] European Academy of Otology and Neurotology*, vol. 30, no. 2, p. 146, 2009.

[23] C. K. Berenstein, L. H. Mens, J. J. Mulder, and F. J. Vanpoucke, "Current steering and current focusing in cochlear implants: comparison of monopolar, tripolar, and virtual channel electrode configurations," *Ear and hearing*, vol. 29, no. 2, pp. 250–260, 2008.

[24] A. A. Saoji and L. M. Litvak, "Use of phantom electrode technique to extend the range of pitches available through a cochlear implant," *Ear and hearing*, vol. 31, no. 5, pp. 693–701, 2010.

[25] J. Snel-Bongers, J. J. Briaire, F. J. Vanpoucke, and J. H. Frijns, "Influence of widening electrode separation on current steering performance," *Ear and hearing*, vol. 32, no. 2, pp. 221–229, 2011.

[26] A. A. Saoji, L. M. Litvak, and M. L. Hughes, "Excitation patterns of simultaneous and sequential dual-electrode stimulation in cochlear implant recipients," *Ear and hearing*, vol. 30, no. 5, pp. 559–567, 2009.

[27] J. Snel-Bongers, J. J. Briaire, F. J. Vanpoucke, and J. H. Frijns, "Spread of excitation and channel interaction in single-and dual-electrode cochlear implant stimulation," *Ear and hearing*, vol. 33, no. 3, pp. 367–376, 2012.

[28] J. H. Frijns, J. Snel-Bongers, D. Vellinga, E. Schrage, F. J. Vanpoucke, and J. J. Briaire, "Restoring speech perception with cochlear implants by spanning defective electrode contacts," *Acta oto-laryngologica*, vol. 133, no. 4, pp. 394–399, 2013.

[29] M. K. Qin and A. J. Oxenham, "Effects of envelope-vocoder processing on f0 discrimination and concurrent-vowel identification," *Ear and hearing*, vol. 26, no. 5, pp. 451–460, 2005.

[30] J. H. Goldwyn, S. M. Bierer, and J. A. Bierer, "Modeling the electrode–neuron interface of cochlear implants: effects of neural survival, electrode placement, and the partial tripolar configuration," *Hearing research*, vol. 268, no. 1, pp. 93–104, 2010.

[31] L. M. Litvak, A. J. Spahr, and G. Emadi, "Loudness growth observed under partially tripolar stimulation: model and data from cochlear implant listeners," *The Journal of the Acoustical Society of America*, vol. 122, no. 2, pp. 967–981, 2007.

[32] B. H. Bonham and L. M. Litvak, "Current focusing and steering: modeling, physiology, and psychophysics," *Hearing research*, vol. 242, no. 1, pp. 141–153, 2008.

[33] J. B. Nadol, J. Shiao, B. J. Burgess, D. R. Ketten, D. K. Eddington, B. J. Gantz, I. Kos, P. Montandon, N. J. Coker, J. T. Roland *et al.*, "Histopathology of cochlear implants in humans," *Annals of Otology Rhinology and Laryngology*, vol. 110, no. 9, pp. 883–891, 2001.

[34] C. C. Finley and M. W. Skinner, "Role of electrode placement as a contributor to variability in cochlear implant outcomes," *Otology & neurotology: official publication of the American Otological Society, American Neurotology Society [and] European Academy of Otology and Neurotology*, vol. 29, no. 7, p. 920, 2008.

[35] F. Rattay, "The basic mechanism for the electrical stimulation of the nervous system," *Neuroscience*, vol. 89, no. 2, pp. 335–346, 1999.

[36] C. A. Miller, P. J. Abbas, B. K. Robinson, J. T. Rubinstein, and A. J. Matsuoka, "Electrically evoked single-fiber action potentials from cat: responses to monopolar, monophasic stimulation," *Hearing research*, vol. 130, no. 1, pp. 197–218, 1999.

[37] T. H. Cormen, C. E. Leiserson, R. L. Rivest, and C. Stein, "Introduction to algorithms. 2009," *Possíveis Questionamentos*, 2009.

[38] W. Jesteadt, "An adaptive procedure for subjective judgments," *Attention, Perception, & Psychophysics*, vol. 28, no. 1, pp. 85–88, 1980.

[39] M. J. Hacker and R. Ratcliff, "A revised table of dfor m-alternative forced choice," *Attention, Perception, & Psychophysics*, vol. 26, no. 2, pp. 168–170, 1979.

[40] B. J. Kwon and C. van den Honert, "Dual-electrode pitch discrimination with sequential interleaved stimulation by cochlear implant users," *The Journal of the Acoustical Society of America*, vol. 120, no. 1, pp. EL1–EL6, 2006.

[41] L. H. Mens and C. K. Berenstein, "Speech perception with mono-and quadrupolar electrode configurations: a crossover study," *Otology & Neurotology*, vol. 26, no. 5, pp. 957–964, 2005.

[42] D. M. Landsberger and A. G. Srinivasan, "Virtual channel discrimination is improved by current focusing in cochlear implant recipients," *Hearing research*, vol. 254, no. 1, pp. 34–41, 2009.

[43] M. Chatterjee and R. V. Shannon, "Forward masked excitation patterns in multielectrode electrical stimulation," *The Journal of the Acoustical Society of America*, vol. 103, no. 5, pp. 2565–2572, 1998.

[44] B. J. Kwon and C. van den Honert, "Effect of electrode configuration on psychophysical forward masking in cochlear implant listenersa)," *The Journal of the Acoustical Society of America*, vol. 119, no. 5, pp. 2994–3002, 2006.

[45] A. G. Srinivasan, D. M. Landsberger, and R. V. Shannon, "Current focusing sharpens local peaks of excitation in cochlear implant stimulation," *Hearing research*, vol. 270, no. 1, pp. 89–100, 2010.

[46] L. T. Cohen, L. M. Richardson, E. Saunders, and R. S. Cowan, "Spatial spread of neural excitation in cochlear implant recipients: comparison of improved ecap method and psychophysical forward masking," *Hearing research*, vol. 179, no. 1, pp. 72–87, 2003.

[47] M. L. Hughes and L. J. Stille, "Psychophysical versus physiological spatial forward masking and the relation to speech perception in cochlear implants," *Ear and hearing*, vol. 29, no. 3, p. 435, 2008.

[48] Q. Tang, R. Benítez, and F.-G. Zeng, "Spatial channel interactions in cochlear implants," *Journal of neural engineering*, vol. 8, no. 4, p. 046029, 2011.

[49] C. K. Berenstein, F. J. Vanpoucke, J. J. Mulder, and L. H. Mens, "Electrical field imaging as a means to predict the loudness of monopolar and tripolar stimuli in cochlear implant patients," *Hearing research*, vol. 270, no. 1, pp. 28–38, 2010.

[50] J. A. Undurraga, R. P. Carlyon, O. Macherey, J. Wouters, and A. Van Wieringen, "Spread of excitation varies for different electrical pulse shapes and stimulation modes in cochlear implants," *Hearing research*, vol. 290, no. 1, pp. 21–36, 2012.

[51] Z. Zhu, Q. Tang, F.-G. Zeng, T. Guan, and D. Ye, "Cochlear-implant spatial selectivity with monopolar, bipolar and tripolar stimulation," *Hearing research*, vol. 283, no. 1, pp. 45–58, 2012.

[52] L. T. Cohen, P. Busby, and G. M. Clark, "Cochlear implant place psychophysics," *Audiology and Neurotology*, vol. 1, no. 5, pp. 278–292, 1996.

[53] C. Boëx, M.-I. Kós, and M. Pelizzone, "Forward masking in different cochlear implant systems," *The Journal of the Acoustical Society of America*, vol. 114, no. 4, pp. 2058–2065, 2003.

[54] A. A. Saoji, D. M. Landsberger, M. Padilla, and L. M. Litvak, "Masking patterns for monopolar and phantom electrode stimulation in cochlear implants," *Hearing research*, vol. 298, pp. 109–116, 2013.

[55] C. A. Fielden, K. Kluk, and C. M. McKay, "Place specificity of monopolar and tripolar stimuli in cochlear implants: The influence of residual maskinga)," *The Journal of the Acoustical Society of America*, vol. 133, no. 6, pp. 4109–4123, 2013.

[56] J. Laneau, J. Wouters, and M. Moonen, "Relative contributions of temporal and place pitch cues to fundamental frequency discrimination in cochlear implantees," *Journal of the Acoustical Society of America*, vol. 116, no. 6, pp. 3606–3619, 2004.

[57] C. J. Brown, P. J. Abbas, and B. Gantz, "Electrically evoked whole-nerve action potentials: Data from human cochlear implant users," *The Journal of the Acoustical Society of America*, vol. 88, no. 3, pp. 1385–1391, 1990.

[58] P. J. Abbas, M. L. Hughes, C. J. Brown, C. A. Miller, and H. South, "Channel interaction in cochlear implant users evaluated using the electrically evoked compound action potential," *Audiology and Neurotology*, vol. 9, no. 4, pp. 203–213, 2004.

[59] P. J. Abbas, C. J. Brown, J. K. Shallop, J. B. Firszt, M. L. Hughes, S. H. Hong, and S. J. Staller, "Summary of results using the nucleus ci24m implant to record the electrically evoked compound action potential," *Ear and Hearing*, vol. 20, no. 1, pp. 45–59, 1999.

[60] W. K. Lai and N. Dillier, "A simple two-component model of the electrically evoked compound action potential in the human cochlea," *Audiology and Neurotology*, vol. 5, no. 6, pp. 333–345, 2000.

[61] A. Morsnowski, B. Charasse, L. Collet, M. Killian, and J. Müller-Deile, "Measuring the refractoriness of the electrically stimulated auditory nerve," *Audiology and Neurotology*, vol. 11, no. 6, pp. 389–402, 2006.

[62] S. B. C. Dynes, "Discharge characteristics of auditory nerve fibers for pulsatile electrical stimuli," Ph.D. dissertation, Massachusetts Institute of Technology, 1996.

[63] J. A. Undurraga, R. P. Carlyon, J. Wouters, and A. Van Wieringen, "Evaluating the noise in electrically evoked compound action potential measurements in cochlear implants," *Biomedical Engineering, IEEE Transactions on*, vol. 59, no. 7, pp. 1912–1923, 2012.

[64] M. Chatterjee, J. J. Galvin III, Q.-J. Fu, and R. V. Shannon, "Effects of stimulation mode, level and location on forward-masked excitation patterns in cochlear implant patients," *Journal of the Association for Research in Otolaryngology*, vol. 7, no. 1, pp. 15–25, 2006.

[65] E. R. Lee, D. R. Friedland, and C. L. Runge, "Recovery from forward masking in elderly cochlear implant users," *Otology & Neurotology*, vol. 33, no. 3, pp. 355–363, 2012.

[66] C. A. Miller, P. J. Abbas, K. V. Nourski, N. Hu, and B. K. Robinson, "Electrode configuration influences action potential initiation site and ensemble stochastic response properties," *Hearing research*, vol. 175, no. 1, pp. 200–214, 2003.

[67] J. B. Nadol, "Patterns of neural degeneration in the human cochlea and auditory nerve: implications for cochlear implantation," *Otolaryngology–Head and Neck Surgery*, vol. 117, no. 3, pp. 220–228, 1997.

[68] J. G. Dingemanse, J. H. Frijns, and J. J. Briaire, "Psychophysical assessment of spatial spread of excitation in electrical hearing with single and dual electrode contact maskers," *Ear and hearing*, vol. 27, no. 6, pp. 645–657, 2006.

[69] R. D. Patterson, "Auditory filter shapes derived with noise stimuli," *The Journal of the Acoustical Society of America*, vol. 59, no. 3, pp. 640–654, 1976.

[70] A. G. Srinivasan, R. V. Shannon, and D. M. Landsberger, "Improving virtual channel discrimination in a multi-channel context," *Hearing research*, vol. 286, no. 1, pp. 19–29, 2012.

[71] M. L. Hughes, C. J. Brown, and P. J. Abbas, "Sensitivity and specificity of averaged electrode voltage measures in cochlear implant recipients," *Ear and hearing*, vol. 25, no. 5, pp. 431–446, 2004.

[72] O. Macherey, R. P. Carlyon, A. Van Wieringen, J. M. Deeks, and J. Wouters, "Higher sensitivity of human auditory nerve fibers to positive electrical currents," *Journal of the Association for Research in Otolaryngology*, vol. 9, no. 2, pp. 241–251, 2008.

[73] C. Jolly, F. Spelman, and B. Clopton, "Quadrupolar stimulation for cochlear prostheses: modeling and experimental data," *Biomedical Engineering, IEEE Transactions on*, vol. 43, no. 8, pp. 857–865, 1996.

[74] F. J. Vanpoucke, A. J. Zarowski, and S. A. Peeters, "Identification of the impedance model of an implanted cochlear prosthesis from intracochlear potential measurements," *Biomedical Engineering, IEEE Transactions on*, vol. 51, no. 12, pp. 2174–2183, 2004.

[75] M. Marzalek, M. Dorman, A. Spahr, and L. Litvak, "Effects of multi-electrode stimulation on tone perception: Modeling and outcomes," in *Conference on Implantable Auditory Prosthesis, Tahoe, CA*, 2007.

[76] V. Colletti, R. Shannon, M. Carner, S. Veronese, and L. Colletti, "Outcomes in nontumor adults fitted with the auditory brainstem implant: 10 years' experience," *Otology & Neurotology*, vol. 30, no. 5, pp. 614–618, 2009.

[77] M. Padilla and D. Landsberger, "Spread of excitation using a new stimulation mode: the virtual tripole," in *Conference on Implantable Auditory Prosthesis, Tahoe, CA*, 2013.

[78] X. Luo, Y. Chang, C. Lin, and R. Y. Chang, "Contribution of bimodal hearing to lexical tone normalization in mandarin-speaking cochlear implant users," *Hearing research*, vol. 312, pp. 1–8, 2014.

[79] J. M. Aronoff and D. M. Landsberger, "The development of a modified spectral ripple test," *The Journal of the Acoustical Society of America*, vol. 134, no. 2, pp. EL217–EL222, 2013.

[80] X. Luo, Q.-J. Fu, and J. J. Galvin, "Vocal emotion recognition by normal-hearing listeners and cochlear implant users," *Trends in Amplification*, vol. 11, no. 4, pp. 301–315, 2007.

[81] J. J. Galvin III, Q.-J. Fu, and G. Nogaki, "Melodic contour identification by cochlear implant listeners," *Ear and hearing*, vol. 28, no. 3, p. 302, 2007.

[82] M. Nilsson, S. D. Soli, and J. A. Sullivan, "Development of the hearing in noise test for the measurement of speech reception thresholds in quiet and in noise," *The Journal of the Acoustical Society of America*, vol. 95, no. 2, pp. 1085–1099, 1994.

VITA

VITA

Ching-Chih Wu

wu94@purdue.edu

EDUCATION

Doctor of Philosophy

Electrical and Computer Engineering

Purdue University, December 2014

Master of Science

Electrical and Computer Engineering

Purdue University, December 2009

Bachelor of Science

Computer Science

National Chiao-Tung University

WORK EXPERIENCE

Research Assistant, Purdue University, August 2009 – August 2014

- Studied pitch perception with steered and spanned partial tripolar (pTP) modes in cochlear implants.
- Developed and conducted psychophysical pitch ranking tests using implant research interface
- Analyzed psychophysical data using ANOVA and generalized linear model in SAS and R
- Simulated neural excitation patterns of steered and spanned pTP modes using a computational model

- Measured spread of excitation of steered and spanned pTP modes at physical, neurophysiological, and perceptual levels using the EFI, ECAP, and psychophysical forward masking, respectively

Graduate Assistant, Purdue University, February 2008 – May 2009

- Created graphical user interface using Psyscope to implement experiments used in a multi-center (Purdue University and House Ear Institute) audio-vision comprehension study
- Wrote scoring programs using excel VBA to efficiently count the number of correct keywords in sentence recognition tests (300 sentences) for more than 30 human subjects
- Used Perl to run batch commands on more than 3000 .wav files
- Provided technical assistance and consultation to researchers at both research centers